Proteomic Analysis of Nanoparticles-Mediated Soybean Response under Flooding Stress

January 2016

Ghazala MUSTAFA

Proteomic Analysis of Nanoparticles-Mediated Soybean Response under Flooding Stress

A Dissertation Submitted to

the Graduate School of Life and Environmental Sciences,

the University of Tsukuba

in Partial Fulfillment of the Requirements

for the Degree of Doctor of Philosophy in Biotechnology

(Doctoral Program in Life Sciences and Bioengineering)

Ghazala MUSTAFA

Abbreviations

Ag	Silver
Al_2O_3	Aluminum oxide
CHAPS	3-[(3-Cholamidopropyl)dimethylammonio]-1-propanesulfonate
LC	Liquid chromatography
MS	Mass spectrometry
MLP	Major latex proteins
NPs	Nanoparticles
qRT-PCR	Quantitative reverse transcription polymerase chain reaction
RuBisCO	Ribulose-1,5-bisphosphate carboxylase/oxygenase
ROS	Reactive oxygen species
ZnO	Zinc oxide

TABLE OF CONTENTS

INTRODUCTION

Changing climatic conditions alter the plant's physiological state and stimulate the different biological pathways in order to combat unfavorable stress conditions (Gorrnall et al., 2010). Climatic trends around the world are fairly rapid in the past few decades that are responsible for the imbalance in the environment. Climate change is potentially the greatest threat to biodiversity (Eigenbrod et al., 2015). The industrial revolution has resulted in elevated levels of carbon dioxide and other greenhouse gases that induce global warming and change precipitation patterns (Hao et al., 2010). Increasing climatological extremes lead to catastrophic loss of crop productivity (Bita and Gerats, 2013). In these changing conditions, plants are under the effects of various abiotic stresses like drought (Manavalan et al., 2009), salinity (Parvaiz and Satyawati 2008), cold (Beck et al., 2004; Beck et al., 2007), and high temperature (Bita and Gerats, 2013). These climatic conditions could result in the alterations in plant system.

Global warming is associated with increased abiotic stressors and leads to reduced crop growth and productivity (Hashiguchi et al., 2010). In particular, flooding constitutes a major abiotic constraint for crop productivity worldwide (Jackson and Colmer, 2005). Approximately 16% of the world's crop producing area has been affected by the flooding or waterlogging (Boyer, 1982). Flooding has devastating effects on crop growth and ultimately causes a reduction in crop production (Normile, 2008). Flooding reduces gas exchange between the atmosphere and the plant tissue because gas such as oxygen diffusion is 10,000 times slower in water than in air (Armstrong, 1979). Flooding leads to change in soil chemical characteristics including soil pH and redox potential (Dat et al., 2004). The elevated level of water in soil limits oxygen availability causing hypoxic conditions, and as a result, plant root directly undergoes anoxia (Sauter, 2013). The respiration of plant root, which leads to substantial reduction in energy status, is inhibited by oxygen deficiency (Ashraf, 2012). This flooding-induced oxygen deprivation is the primary signal triggering the response as well as the main limiting factor for normal plant development (Saglio et al., 1988). In addition, energy production *via* mitochondrial oxidative phosphorylation is limited and toxic end-products *via* anaerobic metabolism are accumulated, resulting in growth inhibition and

death in most crop species under flooding (Bailey-Serres and Voesenek, 2008). Plants experiencing flooding stress undergo various morphological and anatomical alterations in the root system that need to be explored.

Growth and development of various plant species is impeded by the flooding in soil, which could lead to the plant death (Subbaiah and Sachs, 2003). Root respiration rate has been reduced. Apart from alcoholic fermentation, several fermentative bypasses occur, which ameliorate the poisoning through the increased accumulation of metabolic inetrmediates (Liao and Lin, 2001). Photosynthetic ability has also been reduced in flooding sensitive crops. Under flooding stress, the most prominent factor is the oxygen and carbon dioxide limitation due to extremely low diffusion rates in the flood water. Reduction in the root respiration acts as an early response to anoxic conditions (Carpenter and Mitchell, 1980). Proteomic analysis was used to understand the molecular mechanisms in crop plants affected by flooding stress. Proteomic studies identified a variety of flooding-induced proteins providing insight into flooding-responsive mechanisms in plants. Proteomic studies on the plants under flooding stress revealed differentially identified proteins. In wheat, the flooding stress decreased the proteins related to glycolytic pathways and cell wall structure; while, it increased the proteins related to disease/defense (Kong et al., 2010). In tomato, the proteins related to secondary metabolism, programmed cell death, and disease/defense were increased under flooding stress (Ahsan et al., 2007). Flooding is responsible to cause alterations in the plant metabolic system which results in reduced growth.

Soybean is an important legume crop due to its high protein contents and as a source of vegetable oil. The soybean production and consumption is gradually increasing worldwide (Figure 1). Soybean is susceptible to flooding stress (Hou et al., 1991), a major problem that affects its growth and yield around the world. This crop is particularly affected at its germination stage and early vegetative stages, and the grain yield is markedly affected by flooding (Githiri et al., 2006). Early exposure of soybean plants to flooding stress causes severe damage due to rapid imbibition of water by the cotyledons and destruction of the root systems (Nakayama et al., 2004). Flooding stress leads to a shift to alternative pathways of energy generation. The shortage of oxygen under flooding stress results in a shift from aerobic to anaerobic respiration. A low

diffusion rate of oxygen under flooding stress is a limiting factor for plant survival, and most plants die under limited oxygen supply (Voesenek et al., 2006). In soybean, flooding mainly impairs plant growth not only by impairing root elongation due to the loss of root tips in waterlogged soil, but also by reducing hypocotyl pigmentation (Russel et al., 1990; Hashiguchi et al., 2009), which leads to low intracellular oxygen levels and the synthesis of proteins related to anaerobic metabolic pathways (Huang et al., 2005). Plant response to the unfavourable envionmetal conditions depends on the activation of the molecular mechanisms involving stress perception, signal transduction, changes in gene and protein levels and post-translational modifications of the stress responsive proteins (Hossain et al., 2013). In soybean, the flooding tolerance mechanism has been summarized recently (Komatsu et al., 2015). The flooding tolerance mechanism in soybean is regulated by protein changes in the glycolysis, hormonal signaling, transcriptional control, glucose degradation/sucrose accumulation, alcohol fermentation, mitochondrial impairment, cell wall loosening, and suppression of reactive oxygen species (ROS).

As flooding-responsive mechanisms are regulated by phytohormones, Oh and colleagues (2014) examined the effect of gibberellic acid on soybean under flooding conditions and found the changed abundance of proteins related to secondary metabolism, cell cycle, and protein degradation/synthesis. Komatsu et al. (2009) reported that the genes associated with alcohol fermentation and ethylene biosynthesis are up-regulated in soybean seedlings under flooding stress. Komatsu et al. (2013a) reported that abscisic acid is involved in the enhancement of flooding tolerance of soybean through the control of energy conservation processes. By examining the abundance levels of flooding stress indicator proteins, Nanjo et al. (2014) demonstrated that flooding tolerance in soybean is regulated by multiple mechanisms involving various cellular factors.

Advances in nanotechnology have led to the development of breakthrough applications in various fields, including biotechnology, electronics, drug development, cosmetics, and biosensors, and have large commercial potential (Nel et al., 2006). Nanoparticles (NPs) are the materials with the characteristic size range from 1 to 100 nm (Nowack and Bucheli, 2007). The characteristics of these materials lie between the

molecule and the bulk material. Division of bulk materials into smaller and smaller units gives them unique physical and chemical properties (Jefferson, 2000). The NPs have characteristic size that lies between the individual atoms and molecules and they have different physiochemical activities. This decrease in size could be responsible for the material interactions that leads to their toxicological effects (Oberdörster et al., 2005). From millions of years ago these nano-sized particles are present on the earth. Nanomaterials have characteristic properties due to their small size, chemical composition, surface structures, solubility, shape, and aggregation. NPs are produced from bulk materials on a large scale (Brunner et al., 2006), and their possible entry into terrestrial and aquatic ecosystems has been predicted (Owen and Handy, 2007). The effect of these NPs on the molecular mechanisms in plants and animals is of great concern.

The NPs are gaining huge commercial interest due to their breakthrough applications in different fields like biotechnology, electronics, drug industry, cosmetics, and biosensors (Nel et al., 2006). They are extensively being used in differnet products due to their tremendous characteristics. In the last decade, NPs has gained much attention due to their usage and the improving ability to synthesize these NPs (Guzmán et al., 2006). Due to increased production, the environment and humans are on the exposure to these NPs. As a result, much attention has been paid to studying the impacts of these NPs on the environment and the biological systems of plants and animals during the last decade. The NPs are used in agricultural products on large scale. Aslani et al. (2014) summarized the use of engineered NPs in agriculture (Figure 2). An essential aspect of understanding the toxicity of these NPs is to elaborate the interaction of these NPs with the plants, which are the primary producers in the ecosystem (Ma et al., 2010). Rico et al. (2011) reviewed the interaction of NPs with edible plants and its implications within the food chain. The uptake, translocation, and ultimate accumulation of NPs depends on the plant species and the size, type, chemical composition, functionalization, and stability of NPs (Figure 3).

The NPs like titanium oxide, zinc oxide (ZnO), cerium oxide, and silver (Ag) had been deposited on the surface of cell as well as in the organelles that resulted in the oxidative stress to the cell through the induction of oxidative stress signaling (Buzea et

al., 2007). NPs had been reported to form new large size pores in the cell walls for the internal compartmentalization of large size NPs (Navarro et al., 2008). In *Cucurbita pepo*, the effect of Ag, copper, ZnO, and silicon NPs indicated that the seed germination was unaffected by these NPs and their counterpart bulk materials; however, copper NPs reduced root length compared to the control and plants treated with the bulk copper powder (Stampoulis et al., 2009). Metal NPs caused differnatial growth effects on plants; however, the molecular mechanisms altered under NPs stress needs investigations. NPs follow different entry routes for their accumulation in plants. Copper oxide NPs significantly reduced the root and shoot development in mung bean by the production of excess ROS and lipid peroxidation at the low concentrations (Nair et al., 2014). In spinach, the titanium oxide NPs promoted the spectral responses, primary electron separation, electron transfer, and light energy conservation of D1/D2/Cyt b559 complex (Su et al., 2009). In *Lemna gibba*, the toxicity of nickel oxide NPs was related to the deterioration of the photochemical activities of photosynthesis and oxidative stress induction (Oukarroum et al., 2015). On the other hand, the barley plants exposed to gold NPs were able to regenerate; while, the root growth was permanently decreased (Feichtmeier et al., 2015). Different NPs are causing differential growth effects depending on the plant species and growth phase.

The Ag is naturally present in the environment but reducing its size to less than 100 nm changed its physiochemical and biochemical properties that are quite differnet from the bulk Ag (Winjhoven et al., 2009). Ag NPs are among the most extensively used nanomaterials due to its unique antimicrobial properties. The worldwide production of Ag NPs is increasing with the count of tons per year (Nowack et al., 2011). In the environment, the Ag NPs undergo different transformations indicating its variable fate in the environment and within the biological systems (Sanford et al., 2010; Luoma, 2008). In the environment, the Ag NPs interact with biological systmes and cause differential effects. The main toxicity mechanism is characterized by the surface oxidation, release of Ag ions, and interaction with biomolecules within the organisms (Sanford et al., 2010; Reidy et al., 2013; Sharma, 2013). This increasing production results in increasing interaction of Ag with the crops.

The widespread use of Ag and its compounds from ancient times were attributed to

their potent antimicrobial property against a wide range of pathogenic microorganisms (Russel and Hugo, 1994). There is also a growing demand of synthetic Ag NPs as an antiseptic in health care and water treatment facilities (Duran et al., 2007), and as a major ingredient of several commercial agricultural products (Benn and Westerhoff, 2008). This indiscriminate release of Ag NPs with varied physical and surface properties into the environment poses a serious threat to the ecological system including plant. Several studies have been conducted to evaluate the toxicity of Ag NPs on animal (van der Zande et al., 2012), algae (Miao et al., 2009), bacteria (Choi and Hu, 2008), fish (Asharani et al., 2008), and human (Kim et al., 2009). However, research focusing on the impact of Ag NPs on higher plant is limited. The Ag NPs cause differential growth effects on different plant species (Table 1). The Ag NPs alter the physiochemical properties and metabolic pathways of plant, although the underlying mechanisms and specific pathways involved remain unclear.

Aluminum oxide (Al_2O_3) NPs are increasingly being used as an energetic material (Novrotsky, 2003) and as a component of agricultural products, such as pesticides and fertilizers (Vernikov et al., 2009, Stadler et al., 2011). Although various studies have indicated that NPs pose a threat to human health and the environment (Dietz and Herth, 2011), Al_2O_3 NPs are reported to have no cytotoxic effects on mammalian cells (Radziun et al., 2011). However, the current knowledge of the phytotoxic status of Al_2O_3 NPs is limited, and further studies are therefore warranted. Although Al_2O_3 NPs had positive effects on the root elongation of radish, rape, ryegrass, and lettuce (Lin and Xing, 2007), the root elongation of corn, cucumber, soybean, cabbage, and carrot was impaired by the exposure to Al_2O_3 NPs (Yang and Watts, 2005). In addition, Al_2O_3 NPs negatively affect the growth and development of tobacco (Burklew et al., 2012) and wheat (Riahi-Madvar et al., 2012). Notably, however, the antioxidant enzyme systems of wheat reduced the harmful effects of Al_2O_3 NPs through the scavenging of ROS (Riahi-Madvar et al., 2012). Based on these findings, further studies aimed at determining the mode of action of Al_2O_3 NPs on plants are needed, particularly for higher plants.

Studies on phytotoxicity indicated the effects of different NPs on the soybean plant. Nair and Chung, (2014) reported that the copper oxide NPs reduced the shoot growth,

weight, and total chlorophyll content in soybean. However, the hydrogen peroxide, peroxidase, and lignin contents were increased. The copper oxide exposure enhanced the lignification of root cells, which leads to the changes in root developmental process in soybean seedlings (Nair and Chung, 2014). In another study, the mixture of titanium oxide and silicon oxide increased the nitrate reductase activity, water and fertilizer absorbance and utilization. Along with this, the antioxidant system was stimulated, which improved the soybean resistance to adversities (Lu et al., 2002). Yin et al., (2015) reported that the exposure to $NaYF_4$-upconversion NPs promoted the growth; however, at higher concentrations the soyben experienced concentration-dependent growth inhibition. Copper oxide NPs have also been demonstrated to enhance the lignification of root, which affects the root development in soybean seedlings (Nair and Chung, 2014). Considering the phytotoxic status, the molecular mechanisms of soybean affected by the NPs need to be investigated. Different anthropogenic activities are responsible for changing the Earth's terrestrial and aquatic biosphere (Stott et al., 2010). Naturally, the plants are subjected to multiple stresses and these competing stresses might have synergistic or antagonistsic interactions with each other. For example, the cold stress has antagonistic effect on osmotic stress by inducing the dehydration-responsive gene *RD29A* (Xiong et al., 1999). The study of these multiple stresses that result from the human activities could be important to understand the molecular mechanisms that are regulated under multiple perturbations.

Because of the increasing use of NPs in agricultural products (Vernikov et al., 2009), and very less information about the molecular mechanisms affected with these NPs (Table 2), the effect of these NPs in plants needs to be explored at the molecular level. In this study, proteomic technique was used to identify the NPs-responsive proteins in soybean. Firstly, to gain insight into soybean response towards NPs, the morphological analysis was performed. Secondly, to gain insights into the soybean response towards Ag NPs under floodeing stress, a gel-free proteomic technique was used. Thirdly, to gain insights into the soybean response towards Al_2O_3 NPs under flooding stress, a gel-free proteomic technique was used. Based on the results of first three experiments, further analysis was carried out to get better undertsnading of the effects of varying sizes of Ag and Al_2O_3 NPs on proteins of soybean under flooding

stress. For this purpose, temporal proteomic experiment under varying sizes of Ag and Al_2O_3 NPs was performed.

Table 1. List of publications on Ag and Al NPs toxicity in plants[a].

Metal NPs	Plant species	Treatment	Major findings	References
Ag	*Arabidopsis*	1, 2.5, 10, 20 mg/L	1) Under the Ag NPs and Ag+ exposure, the up-regulated genes were primarily associated with the response to metals and oxidative stress; while, down-regulated genes were associated with the response to pathogens and hormonal stimuli. 2) Three highly up-regulated genes specifically in the presence of Ag NPs were related to thalianol biosynthetic pathway, which is involved in the plant defence system.	Kaveh et al., 2013
	Arabidopsis	0, 2, 100 μM	1) Ag NPs induced ROS accumulation and root growth promotion. 2) Ag NPs activated gene expression involved in cellular events including cell proliferation, metabolism, and hormone signaling pathways.	Syu et al., 2014
	Lemna minor	0, 5, 10, 20, 40, 80, 160 μg/L	1) Initially 20 and 100nm Ag NPs inhibited the plant growth at low concentrations which become more acute with a longer exposure time. 2) There was a linear dose-response relationship after 14 days exposure.	Gubbins et al., 2011
	Lolium multiflorum	0, 1, 5, 10, 20, 40 mg/L	1) Ag NPs toxicity was influenced by total nanoparticle surface area with smaller NPs (6 nm) affected the growth more strongly then the similar concentrations of the larger NPs (25 nm). 2) X-ray spectro microscopy documented Ag speciation within exposed roots and suggested that Ag is oxidized within the plant tissues.	Yin et al., 2011
	Potato	0, 1, 1.5, 2 ppm	1) Leaf surface was increased; while, stem length and root length were decreased. 2) Ag NPs caused decrease in the number of isolated protoplasts and the viability of isolated protoplast.	Ehsanpour and Nejati, 2013
	Ricinus commuins	0, 100, 200, 500, 1000, 2000, 4000 mg/L	1) Ag NPs had no significant effects on seedling growth even at higher concentrations. 2) Ag NPs enhanced enzymatic activity of ROS enzymes and phenolic content in castor seedlings.	Yasur and Rani, 2013
	Thymus kotschyanus	20, 40, 60, 80, 100 ppm	1) Moderate levels of Ag NPs had the highest positive effects on survival rate, diameter of canopy area, days to flowering, yield and essential oil amount; however, the 100 ppm had the minimal positive	Aghajani et al., 2013

			impact. 2) One component of essential oil α-terpinyl acetate was increased in 60 ppm Ag NPs. 3) Ag NPs can be used to change the stages of plant growth and the amount of secondary metabolites.	
Al	*Nicotiana tabacum*	0.1, 0.5, 1% Al_2O_3	1) Al_2O_3 NPs have a negative effect on the growth and development of tobacco seedlings. 2) miRNAs play important role in the ability of plants to mediate the plant responses to NPs stress.	Burklew et al., 2012
	Wheat	50, 200, 500, 1000 mg/L	1) Root growth is affected by the NPs; however, the seed germination, root length, and dry biomass were unaffated. 2) The oxidative damage was introduced as a way of inducing toxicity in plants through uptake of NPs.	Riahi-Madvar et al., 2012
	Allium cepa	0.01, 0.1, 1, 10, 100 μg/mL	1) The biouptake of Al_2O_3 in particulate form led to the ROS generation, which in turn probably contributed to the induction of chromosomal aberrations.	Rajeshwari et al., 2015

a) List of publications consist of last ten years data.

Table 2. List of publications on proteomic analyses in plants under NPs stress.

Metal NPs	Plant species	Organ	Treatment	Proteomic methodology	Major findings	Reference
Ag, Al_2O_3, ZnO	Soybean	Root, leaf	500 ppm Al_2O_3 500 ppm ZnO, and 50 ppm Ag	nanoLC-MS/MS	1) The commonly identified proteins under Al_2O_3, ZnO, and Ag NPs were related to secondary metabolism, cell organization, and hormone metabolism. 2) High abundance of proteins involved in oxidation reduction, stress signaling, hormonal pathways related to growth and development were the principal key for the optimum growth of soybean under Al_2O_3 NPs.	Hossain et al., 2015
Ag	Wheat	Shoot, root	1, 10 mg/L Ag	2-DE IEF/SDS-PAGE, LC–ESI–MS/MS	1) The abundance of proteins related to primary metabolism and cell defense were altered under the 10 mg/L Ag NPs.	Vannini et al., 2014
	Rice cv.IR651	Root	30, 60 µg/mL Ag	2-DE, nanoLC/FT-ICR MS	1) Increased abundance of proteins related to oxidative stress response pathway, Ca^{2+} regulation and signaling, transcription, protein degradation, cell wall, cell division, and apoptosis.	Mirzajani et al., 2014
	Eruca sativa	Root	0.1-100 mg/L Ag or $AgNO_3$	2-DE, nanoLC-nESI-MS/MS	1) Alteration of proteins related to the ER and vacuole indicating these two organelles as targets of the Ag NPs action. 2) Effects of Ag NPs are not simply due to the release of Ag ions.	Vannini et al., 2013

2-DE, two-dimensional gel electrophoresis; MS, mass spectrometry; LC, liquid chromatography; FT, fourier transform; ICR, ion cyclotron resonance; ESI, electrospray ionization;

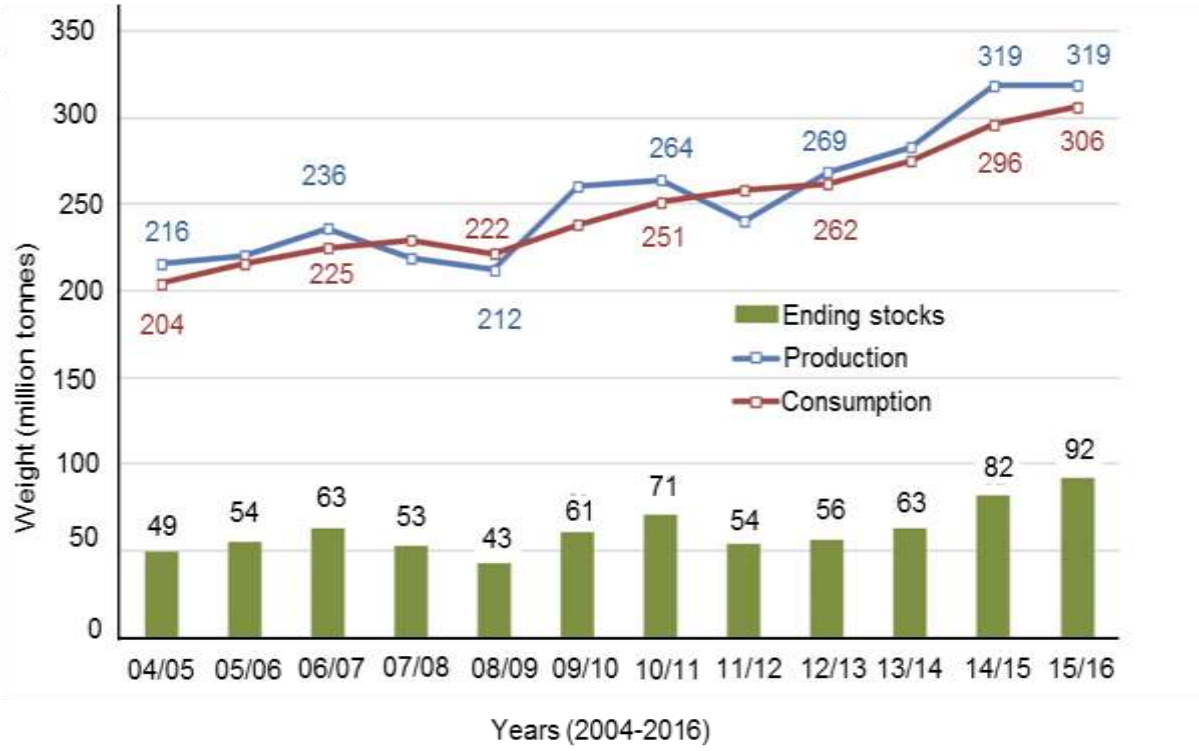

Source: US Department of Agriculture, Area Median Income, 2015 (http://www.ufop.de/english/news/chart-of-the-week/archive-chart-of-the-week/)

Figure 1. Production and consumption data of soybean in the world during the last decade. Soybean production and consumption are increased in the last ten years. The harvest of soybean in USA in 2015 is estimated at 105.7 x10^6 tonnes, down only around 2.3 x10^6 tonnes from the previous year. At 319 million tonnes, the world's 2015/2016 soybean production could again be extremely large, reaching the previous year's record level. The data for 2015-2016 is estimated.

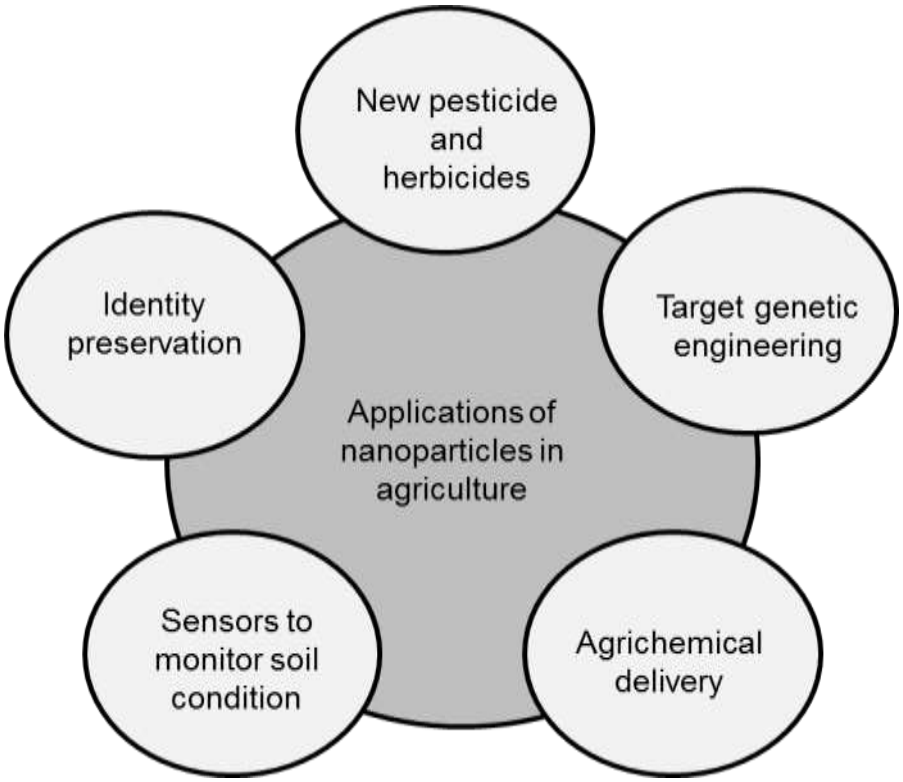

(Modification from Aslani et al., 2014)

Figure 2. Applications of NPs in agriculture. Different types of NPs are using in agricultural products like herbicides, pesticides, in the agrochemical delivery, and genetic engineering.

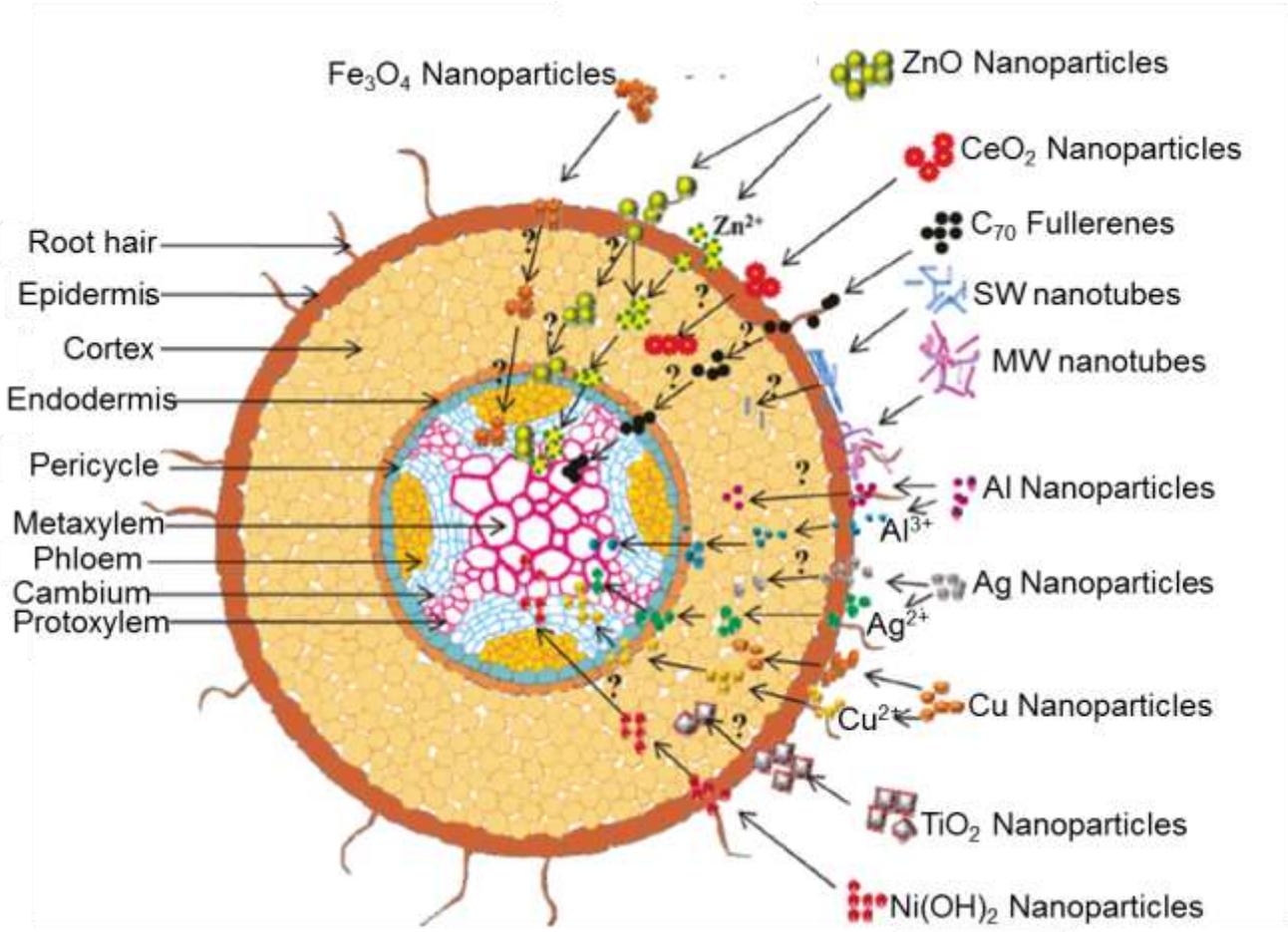

(Modification from Rico et al., 2011)

Figure 3. The uptake, translocation, and biotransformation pathway of NPs in the plants. Different NPs are translocated thorugh various systems in different plant species. Abbreviations: MW, multiwalled; SW, single walled.

CHAPTER 1
MORPHOLOGICAL ANALYSIS OF THE EFFECT OF NANOPARTICLES ON THE SOYBEAN UNDER FLOODING STRESS

1.1. Introduction

Plant is an essential part of the ecosystem as being the primary producer. Studies on the influence of NPs on the plant growth indicated that the NPs mainly influence the seed germination (Aslani et al., 2014). The toxicological studies reported that the certain types of NPs could be toxic in the free form circulating in the living system. The different types of NPs affect the entry routes, behavior, and capability of plants (Aslani et al., 2014). Toxic impacts of NPs on plants are due to their physical and chemical properties, surface area, size, and shape. Both positive and negative impacts of these NPs on plants were studied (Yang and Watts, 2005). Positive impacts include the seed germination, growth of plant seedlings, protection of chloroplast from aging, increase of electron transfer, biomass accumulation, activity of ribulose-1, 5-bisphosphate carboxylase/oxygenase (RuBisCO), increase of chlorophyll content, and increase in shoot and root length.

In the comparative analysis of the effects of various types of NPs on *Arabidopsis*, Al_2O_3 NPs were less toxic than ZnO, iron oxide, and silicon oxide NPs (Lee et al., 2010). The Ag NPs negatively affect the growth of *Cucurbita pepo* (Stampoulis et al., 2009) and root tip extension of *Allium cepa* (Kumari et al., 2009). In *Spirodela polyrrhiza*, exposure to Ag NPs inhibits seed germination, root, and shoot growth (Jiang et al., 2012). Although Ag NPs are often detrimental to plant growth, several studies have demonstrated the growth-stimulatory effects of Ag NPs. For example, exposure to Ag NPs enhances the root extension of *Brassica juncea* (Sharma et al., 2012) and stimulates the plant growth of *Eruca sativa* (Vannini et al., 2013). Ag NPs also enhanced the growth of various wetland plant (Yin et al., 2012) and increased the shoot and root lengths of *Phaseolus vulgaris* and maize (Salama, 2012). The Al_2O_3 NPs caused positive effects on the root elongation of radish, rape, ryegrass, and lettuce (Lin and Xing, 2007); however, the root elongation of corn, cucumber, soybean, cabbage, and carrot was impaired by exposure to Al_2O_3 NPs (Yang and Watts, 2005). In addition, Al_2O_3 NPs negatively affected the growth and development of tobacco (Burklew et al., 2012) and wheat (Riahi-Madvar et al., 2012). Riahi-Madvar et al. (2012) indicated that the root growth of *Triticum aestivum* was affected by the different concentrations of the Al_2O_3 NPs; however, NPs did not affect the seed germination, shoot length, and dry

biomass compared to the untreated plants. On the other hand, seed germination was not affected in the case of ZnO NPs (Lopez-Moreno et al., 2010). The toxicological status of Al_2O_3, ZnO, and Ag NPs on soybean plant needs to be explored.

Because of the variable growth effects of NPs on different plant sepcies and their possible interaction within the environment, the toxicological status of these NPs on soybean plant is a point of concern. In this Chapter, the effects of Al_2O_3, ZnO, and Ag NPs on the seedling growth of soybean under flooding stress were evaluated. Based on this experiment, the suitable size and concentration of NPs will be selected for further proteomic analysis. For this purpose, morphological parameters were used to assess the effects of NPs on soybean seedlings under flooding stress.

1.2. Materials and methods

1.2.1. Plant material and treatments

Soybean (*Glycine max* L.) cultivar Enrei was used as the plant material in this study. Seeds were sterilized in 3 % sodium hypochlorite solution and allowed to germinate on silica sand. Seedlings were maintained at 25°C in a growth chamber illuminated with white fluorescent light (160 μmol m^{-2} s^{-1}, 16-h light period/day). To expose plants to flooding stress, 2-day-old soybeans were transferred to glass tubes (38 mm ID x 130 mm) containing 120 mL reverse osmosis water. After covering the mouth of the tubes with plastic caps allowing air flow, the tubes were kept in the dark for treatment period in the growth chamber at 25°C (Nanjo et al., 2013). Control seedlings were maintained in sand under the same growth conditions.

To study the effects of differnet NPs on the morphology of soybean, Al_2O_3, ZnO, and Ag NPs were used. Concentrations of 5, 50, and 500 ppm Al_2O_3 (30-60 nm particle size, Sigma-Aldrich, St Louis, MO, USA), 5, 50, and 500 ppm ZnO (<50 nm particle size, Sigma-Aldrich), and 0.5, 5, and 50 ppm Ag (15 nm particle size, US Research Nanomaterials, Houston, TX, USA) were used. Two-day-old soybeans were treated for 0, 2, 3, and 4 days and fresh weight and length of root including hypocotyl were measured (Figure 4).

To study the size dependent effects of Ag NPs on morphology of soybean plants under flooding stress, Ag NPs of different sizes (2, 15, and 50-80 nm; US Research

Nanomaterials) and concentrations (0.2, 2, and 20 ppm) were screened. In addition, 2 ppm Ag NO_3 (Sigma-Aldrich) was used as a negative control. To study the effects of Al_2O_3 NPs on the morphology of soybean plants under flooding stress, Al_2O_3 NPs of different sizes (5, 30-60, and 135 nm; US Research Nanomaterials) and concentrations (5, 50, and 500 ppm) were screened. Two-day-old soybeans were transferred to glass tubes containing 120 mL water supplemented with different concentrations of Ag and Al_2O_3 NPs and particle sizes. Fresh weights of untreated, flooded, and NPs-treated flooded soybean seedlings were measured on 0, 2, 3, and 4 days of treatment (Figure 4).

1.2.2. Statistical analysis

The statistical significance of comparisons between multiple groups was evaluated with Tukey's multiple Range test and comparison between two groups was evaluated by Student's *t* test. A *p* value of <0.05 was considered as statistically significant. All calculations were performed using SPSS software (version 12.0J; IBM Corp. Armonk, NY, USA).

1.3. Results

1.3.1. Effects of Al_2O_3, ZnO, and Ag NPs on soybean growth under flooding stress

To investigate the effects of NPs on soybean under flooding stress, morphological changes were first analyzed. Two-day-old soybeans were flooded without or with 5, 50, and 500 ppm Al_2O_3, 5, 50, and 500 ppm ZnO, and 0.5, 5, and 50 ppm Ag NPs. The fresh weight of plant and length of root including hypocotyl were measured on 0, 2, 3, and 4 days of treatments (Figure 5, left panels). The fresh weight of plants was increased by exposure to 50 ppm Al_2O_3 NPs compared to flooding-treated plants, but decreased by treatment with 5 and 500 ppm Al_2O_3 NPs (Figure 5, upper left). For soybean treated with ZnO NPs, the fresh weight of plants was lower with 50 ppm ZnO NPs compared to the flooding stress throughout the treatment period. In contrast, for soybean treated with 5 and 500 ppm ZnO NPs, the fresh weight of plants was lower than the flooding and flooding with 50 ppm ZnO NPs stress throughout the treatment period (Figure 5, upper left). Upon exposure to 5 ppm Ag NPs, the fresh weight of plants increased compared to the flooding-treated plants in the first 3 days of the

treatment period. In contrast, the plants treated with 50 ppm Ag NPs displayed the lowest fresh weight throughout the treatment period. Exposure to 0.5 ppm Ag NPs also reduced the fresh weight of plant compared to flooding-treated soybean (Figure 5, lower left).

The length of root including hypocotyl of soybean treated with 50 ppm Al_2O_3 NPs was increased compared to the flooding-treated plants (Figure 5, upper right). In contrast, the length of root including hypocotyl was initially increased after one day of treatment with 5 and 500 ppm Al_2O_3 NPs, and subsequently decreased with continued stress exposure. Under treatment with 50 ppm ZnO NPs, the length of root including hypocotyl was increased after two days of stress, but then decreased during the remainder of the 4-day treatment period. In contrast, the length of root including hypocotyl of soybean treated with 5 and 500 ppm ZnO NPs was decreased compared to the flooding-treated plants during the treatment period (Figure 5, middle right). For Ag NPs, the length of root including hypocotyl of soybean treated with 5 ppm Ag NPs progressively increased during the treatment period compared to the flooding-treated plants (Figure 5, lower right). However, soybean exposed to 0.5 ppm Ag NPs had the shortest length throughout the 4-day treatment period, whereas the length of root including hypocotyl of soybean treated with 50 ppm Ag NPs was similar to that of flooding-treated soybean. As both the fresh weight of plant and length of root including hypocotyl of soybean treated with 50 ppm Al_2O_3 NPs were higher compared to other two examined concentrations, proteomic analysis was performed using flooding-stressed soybean exposed to 50 ppm Al_2O_3 NPs.

1.3.2. Effects of varying sizes of Ag NPs on the growth of soybean seedlings under flooding stress

To investigate the effects of Ag NPs on the morphological changes induced in soybean by flooding stress, 2-day-old soybeans were flooded without or with 2 ppm Ag NPs, with sizes of 2, 15, or 50-80 nm. Soybean plants treated with flooding and 2 ppm Ag NO_3 were used as a negative control. The fresh weight of plants were measured on 0, 1, 2, 3, and 4 days of treatment (Figure 4). The weight of seedlings treated with 15 nm Ag NPs was significantly greater than that of the seedlings treated with flooding and

seedlings treated with flooding and 2 or 50-80 nm Ag NPs or Ag NO_3 throughout the treatment period (Figure 6). The weight of seedlings treated with 2 nm Ag NPs remained the lowest among all treatment conditions during the 4-day treatment period, while the weights of seedlings treated with 50-80 nm Ag NPs and Ag NO_3 were lower than those of the flooded and 15 nm Ag NPs-treated seedlings.

To examine the effect of different concentrations of 15 nm Ag NPs on the morphological changes induced in soybean under flooding stress, 2-day-old soybeans were flooded without or with 15 nm Ag NPs at concentrations of 0.2, 2, and 20 ppm. The fresh weight of plants were measured on 0, 1, 2, 3, and 4 days of treatment (Figure 4). The weight of seedlings treated with 15 nm Ag NPs at 2 ppm was significantly higher throughout the treatment period compared to the seedlings treated with flooding and the higher and lower concentrations of 15 nm Ag NPs (Figure 7). The seedlings treated with 0.2 ppm Ag NPs had the lowest weights among the examined treatments, while the weight of seedlings treated with 20 ppm Ag NPs was similar to that of seedlings treated only with flooding (Figure 7).

1.3.3. Effects of varying sizes of Al_2O_3 NPs on growth of soybean seedlings under flooding stress

To investigate the effects of Al_2O_3 NPs on the morphological changes induced in soybean by flooding stress, 2-day-old soybeans were flooded without or with 50 ppm Al_2O_3 NPs, with sizes of 5, 30-60, and 135 nm. The plant fresh weight were measured on 0, 1, 2, 3, and 4 days of treatments (Figure 4). The fresh weight of plant treated with 30-60 nm was significantly greater then the flooding and other Al_2O_3 NPs treated seedlings throughout the treatment period. The fresh weight of plant treated with 135 nm Al_2O_3 NPs was almost equal to the flooding treated seedlings. On the other hand, the fresh weight of plant treated with 5 nm Al_2O_3 NPs was lowest among all the treatements (Figure 8). The length of root including hypocotyl was significantly greater with the 30-60 nm Al_2O_3 NPs compared to the flooding and other Al_2O_3 NPs treated soybean. On the other hand, the length of root including hypocotyl of soybean treated with 5 and 135 nm Al_2O_3 NPs was in between the 30-60 nm Al_2O_3 NPs and flooding treated soybean (Figure 8).

To examine the effect of different concentrations of 30-60 nm Al_2O_3 NPs on the morphological changes induced in soybean by flooding stress, 2-day-old soybeans were flooded without or with 30-60 nm Al_2O_3 NPs at concentrations of 5, 50, and 500 ppm.The fresh weight of plant and length of root including hypocotyl were increased by the exposure to 50 ppm Al_2O_3 NPs compared to flooding-treated plants, and decreased by the treatment with 5 and 500 ppm Al_2O_3 NPs (Figure 9).

1.4. Discussion

1.4.1. The effects of Ag NPs on soybean growth under flooding stress

The present study analyzed the effects of Ag NPs on the morphology of soybean under flooding stress. The weight of soybean seedlings exhibited the highest increase upon exposure to 15 nm Ag NPs compared to other examined particle sizes. The 15 nm Ag NPs were found to be the most effective for increasing the growth of flooding-treated seedlings at 2 ppm concentration. These results indicate that a relatively low concentration of 15 nm Ag NPs has enhancing effects on soybean under flooded conditions. Yin et al. (2012) reported that the application of 20 nm Ag NPs increased the germination rate of various wetland plants. In the present study, 20 ppm Ag NPs was found to be lethal for soybean; whereas, the low concentration (2 ppm) showed positive effects: the results that are inconsistent with the previous findings. Salama (2012) reported that low concentrations (20 and 40 ppm) of Ag NPs have stimulatory effects on the growth of *P. vulgaris* and maize, whereas higher concentrations (100 ppm) had inhibitory effects. Aghajani et al. (2013) showed that moderate concentrations of Ag NPs effectively enhanced the growth of *Thymus kotschyanus*, whereas higher concentrations had negative effects. In the present study, low Ag NPs concentrations enhanced the seedling growth of soybean under flooding stress. These results of the effect of Ag NPs on the soybean plant under flooding stress are inconsistent with the previous studies indicating that the higher concentrations of Ag NPs are lethal for the plant growth; however, low or moderate concentrations are beneficial in enhancing the plant growth.

1.4.2. The effects of Al_2O_3 NPs on soybean growth under flooding stress

In soybean, ZnO and cerium oxide NPs impart differential effects on plant growth, but do not affect seed germination (López-Moreno et al., 2010). Hossain et al. (2015) compared the phytotoxicity of three NPs and reported that the Al_2O_3 NPs treated soybeans maintained normal seedling growth like control; however, the ZnO and Ag NPs negatively affect the growth of soybean. In contrast, Al_2O_3 NPs at higher concentrations inhibit root growth in corn, cucumber, soybean, cabbage, and carrot (Yang and Watts, 2005). However, Lin and Xing (2007) reported that Al_2O_3 NPs did not have toxic effects on the root elongation of radish, rape, ryegrass, lettuce, and cucumber, but did inhibit root elongation in corn. In the present study, among the various sizes of Al_2O_3 NPs the 30-60 nm enhanced the soybean growth under flooding stress compared to smaller and larger sizes. On the other hand, a moderate exposure to 30-60 nm Al_2O_3 NPs had enhancing effects on soybean growth under flooding stress. However, lower (5 ppm) and higher (500 ppm) concentrations of Al_2O_3 NPs did not positively affect soybean growth under flooding stress. Because the treatment with 50 ppm Al_2O_3 NPs enhanced soybean growth under flooding stress conditions, this concentration was used for the proteomic analysis.

1.5. Conclusion

NPs caused various growth effects on different plant species (Yang and Watt, 2005). The present morphological study highlights the effects of Ag, ZnO, and Al_2O_3 NPs on soybean exposed to flooding stress. The major findings are as follows: (i) among the differnet kinds of NPs, Al_2O_3 and Ag NPs had growth stimulatory effects compared to ZnO NPs; (ii) among the various sizes of Ag NPs, 15 nm size enhanced the soybean growth under flooding stress; (iii) 2 ppm of 15 nm Ag NPs treatment has a protective role against flooding as evident from enhanced seedling growth; (iv) among the Al_2O_3 NPs 30-60 nm particles increased the soybean growth under flooding stress; and (v) exposure to 50 ppm of 30-60 nm Al_2O_3 NPs increased the fresh weight of plants and the length of root including hypocotyl. Taken together, these results suggest that the Ag and Al_2O_3 NPs facilitate the soybean growth under flooding stress and root was most affected organ. Based on these results, 2 ppm of 15 nm Ag NPs and 50 ppm of 30-60 nm Al_2O_3 NPs were used for the proteomic analysis.

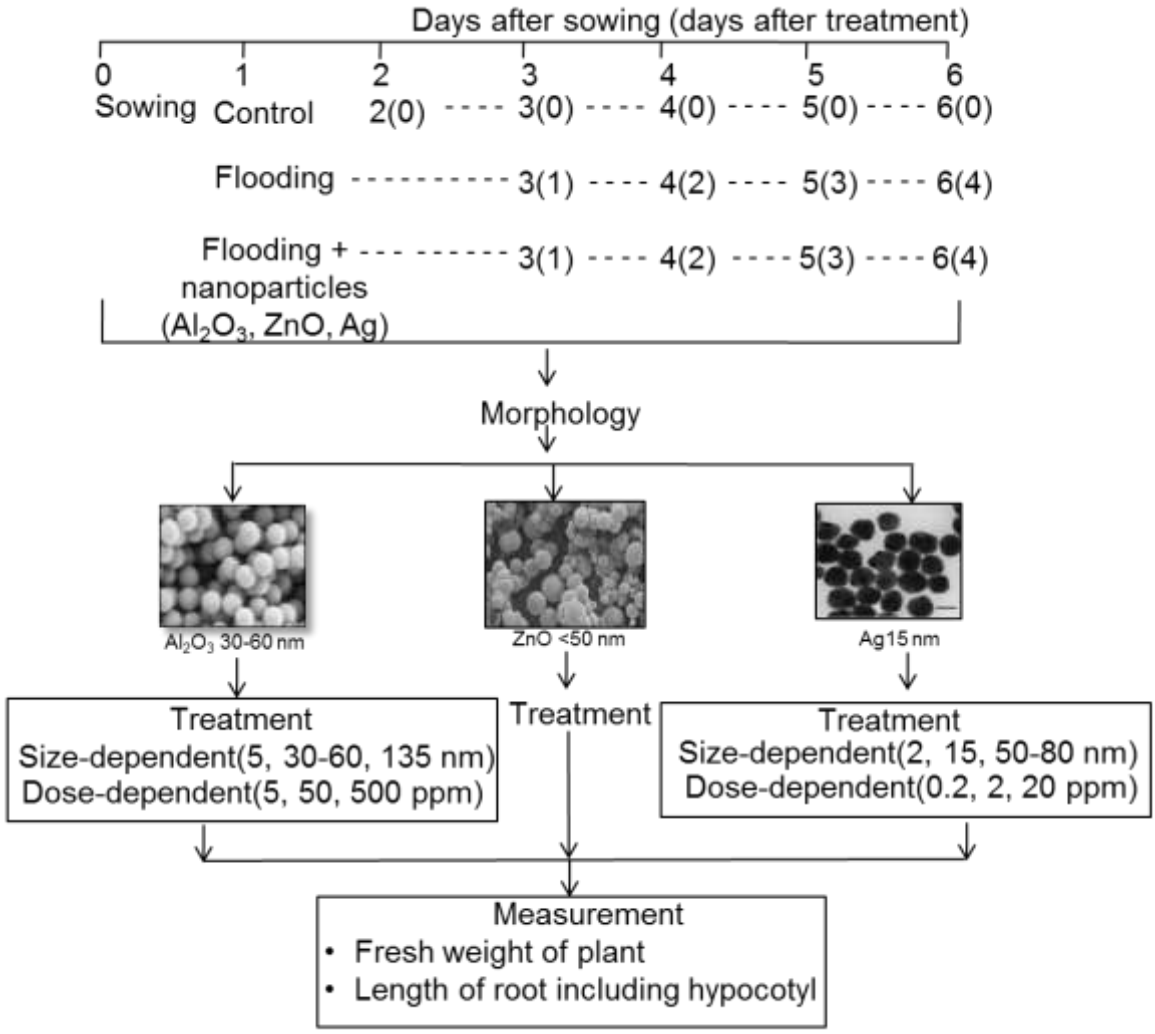

Figure 4. Experimental design to study the effects of NPs on soybean under flooding stress. Two-day-old soybeans were flooded without or with Al_2O_3, ZnO, or Ag NPs for 0, 1, 2, 3, and 4 days. Untreated plant served as control. The fresh weight of plant and length of root including hypocotyl were measured at the indicated treatment points.

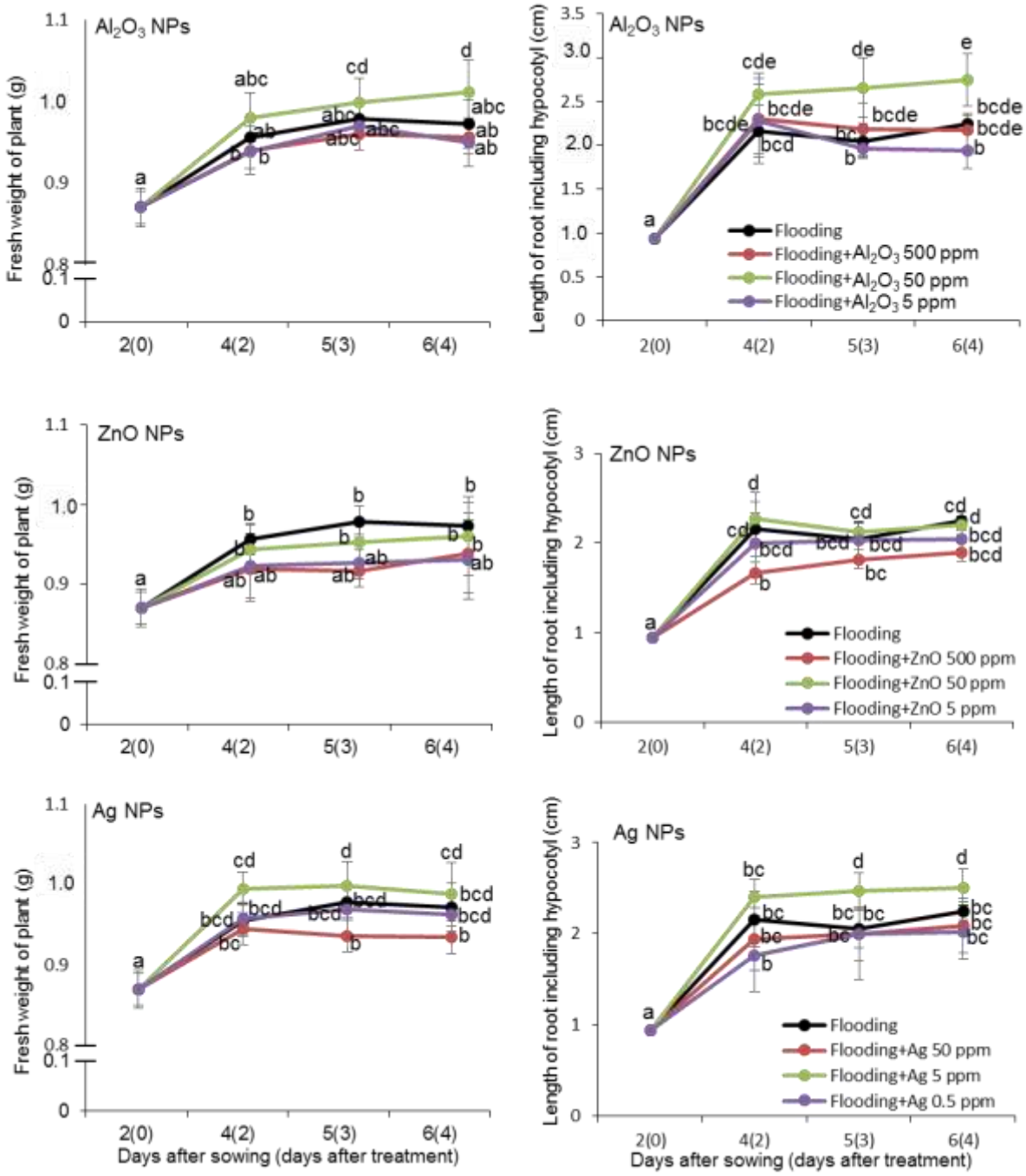

Figure 5. Effects of varying concentrations of Al_2O_3, ZnO, and Ag NPs on the growth of soybean seedlings under flooding stress. Two-day-old soybeans were flooded without or with Al_2O_3 (5, 50, and 500 ppm), ZnO (5, 50, and 500 ppm), or Ag NPs (0.5, 5, and 50 ppm) for 0, 2, 3, and 4 days. After the treatments, the fresh weight of plant and length of root including hypocotyl were measured. The data are presented as the mean ± S.D. from six independent biological replicates (n=6). Mean values in each point with different letters are significantly different at the 5% level according to Tukey's Multiple Range test.

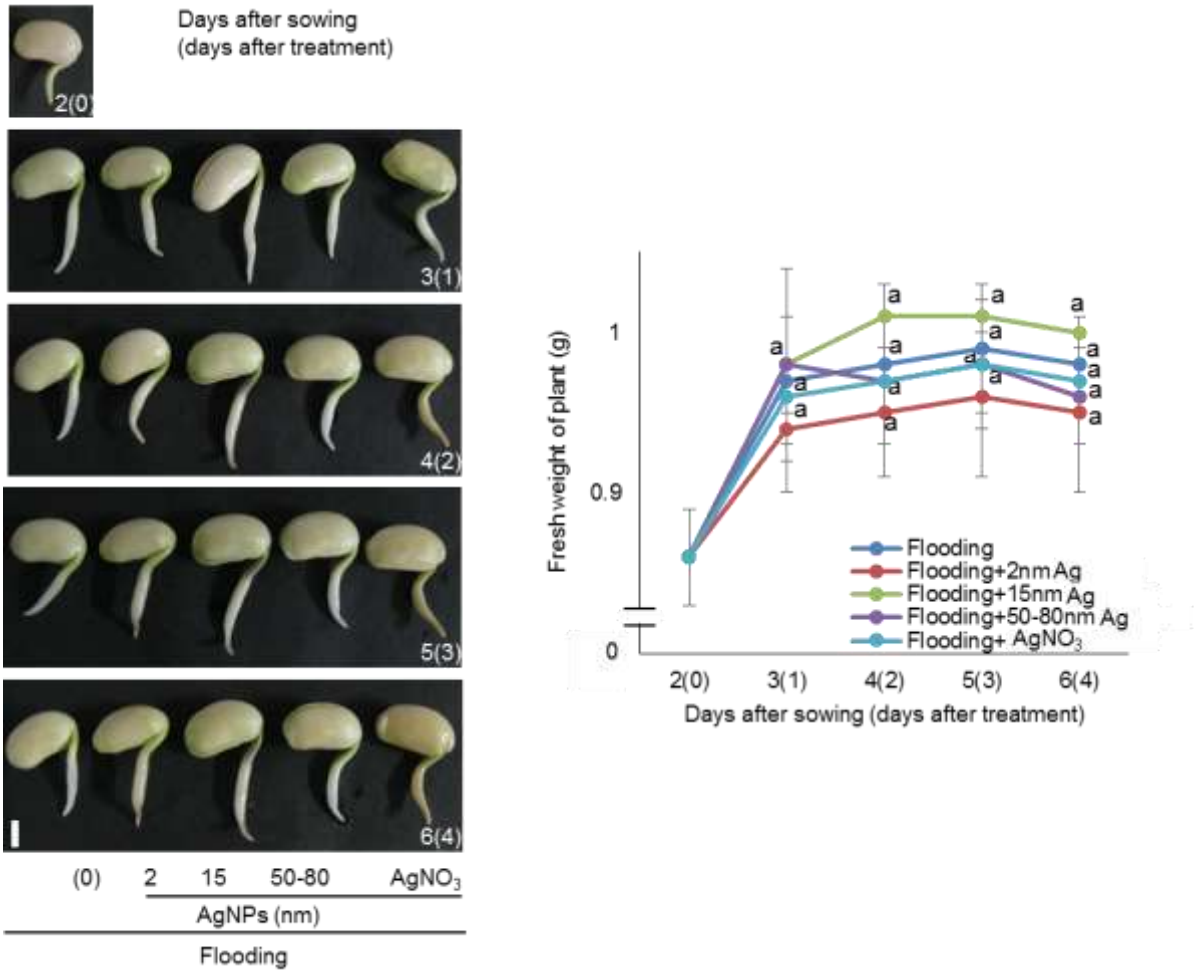

Figure 6. Size-dependent effects of Ag NPs on the growth of soybean exposed to flooding stress. Two-day-old soybeans were flooded without (dark blue) or with 2 ppm of 2 nm (red), 15 nm (green), 50-80 nm (purple) Ag NPs particles, or Ag NO_3 (light blue). Photographs show soybean seedlings at 0, 1, 2, 3, and 4 days of flooding and Ag NPs treatments. Bar indicates 1 cm. The fresh weight of plant was measured at the indicated time points. The data are presented as the mean ± S.D. from three independent biological replicates (n=3). Statistical analysis is same as described in Figure 5.

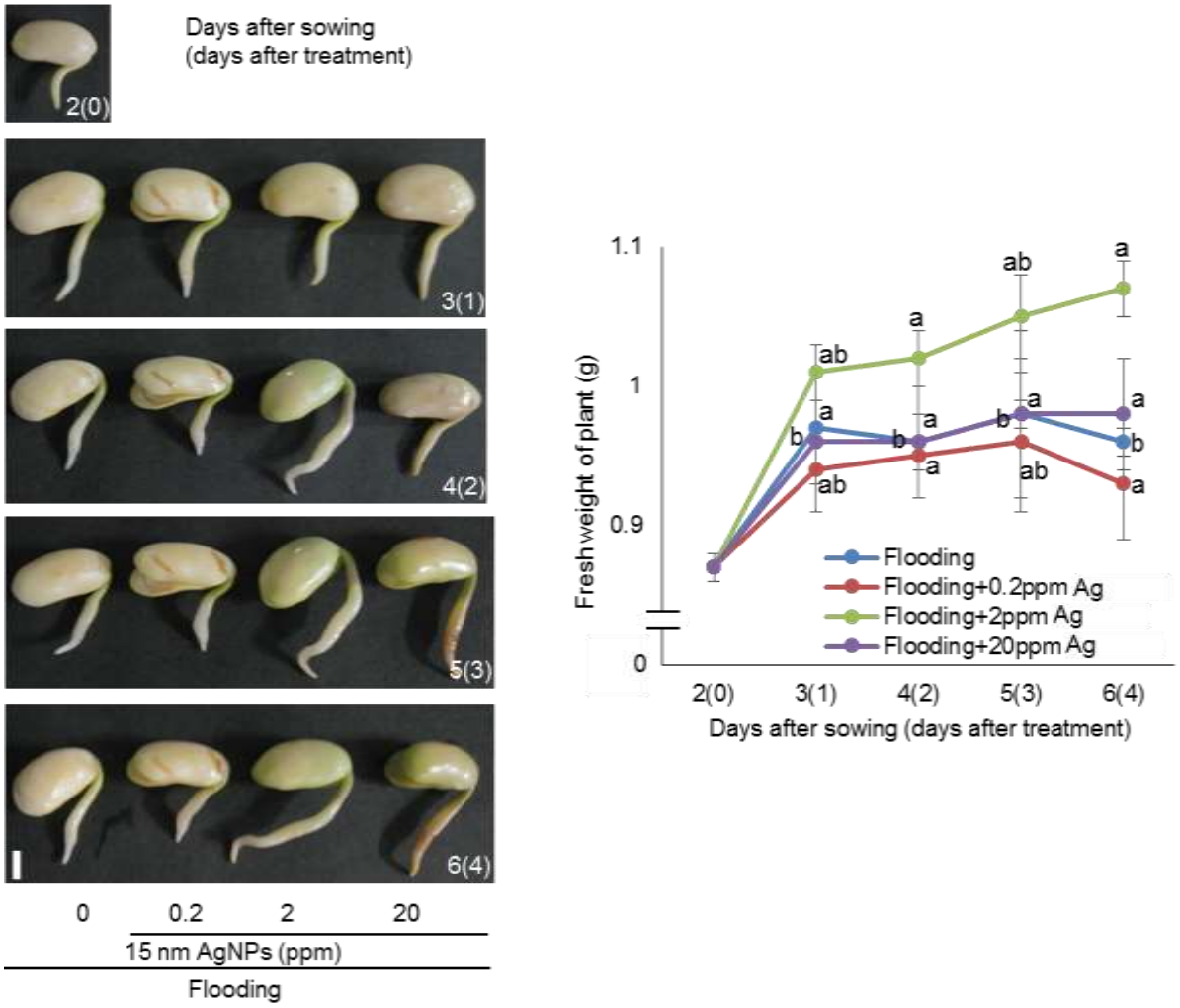

Figure 7. Dose-dependent effects of 15 nm Ag NPs on the growth of soybean under flooding conditions. Two-day-old soybeans were flooded without (dark blue) or with 15 nm Ag NPs at concentrations of 0.2 ppm (red), 2 ppm (green), and 20 ppm (purple). Photographs show soybean seedlings at 0, 1, 2, 3, and 4 days of flooding and Ag NPs treatments. Bar indicates 1 cm. The fresh weight of plant was measured at the indicated time points. The data are presented as the mean ± S.D. from three independent biological replicates (n=3). Statistical analysis is same as described in Figure 5.

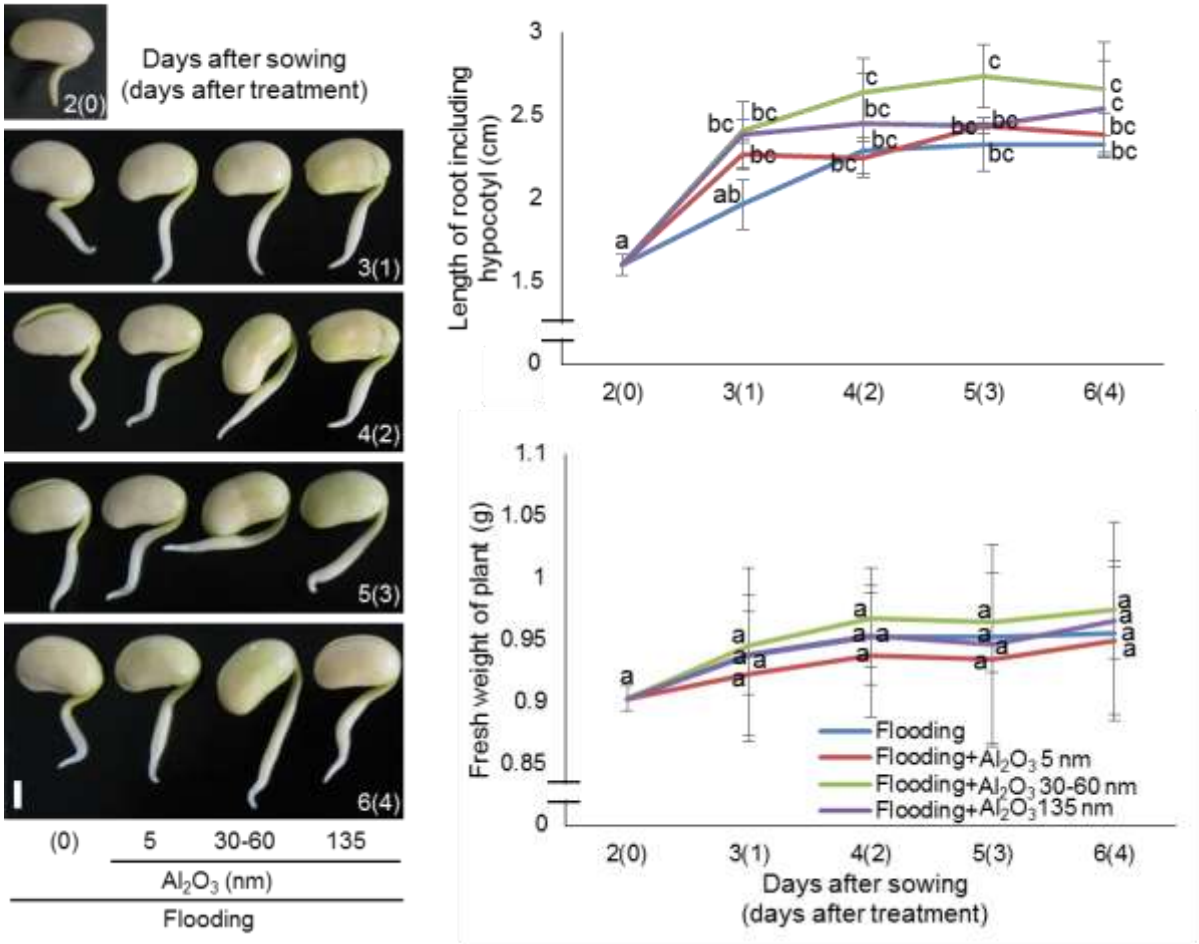

Figure 8. Size-dependent effects of Al_2O_3 NPs on the growth of soybean exposed to flooding stress. Two-day-old soybeans were flooded without (dark blue) or with 50 ppm of 5 nm (red), 30-60 nm (green), and 135 nm (purple) Al_2O_3 NPs. Photographs show soybean seedlings at 0, 1, 2, 3, and 4 days of flooding and Al_2O_3 NPs treatments. Bar indicates 1 cm. Fresh weight of plant and length of root including hypocotyl were measured at the indicated time points. The data are presented as the mean ± S.D. from three independent biological replicates (n=3). Statistical analysis is same as described in Figure 5.

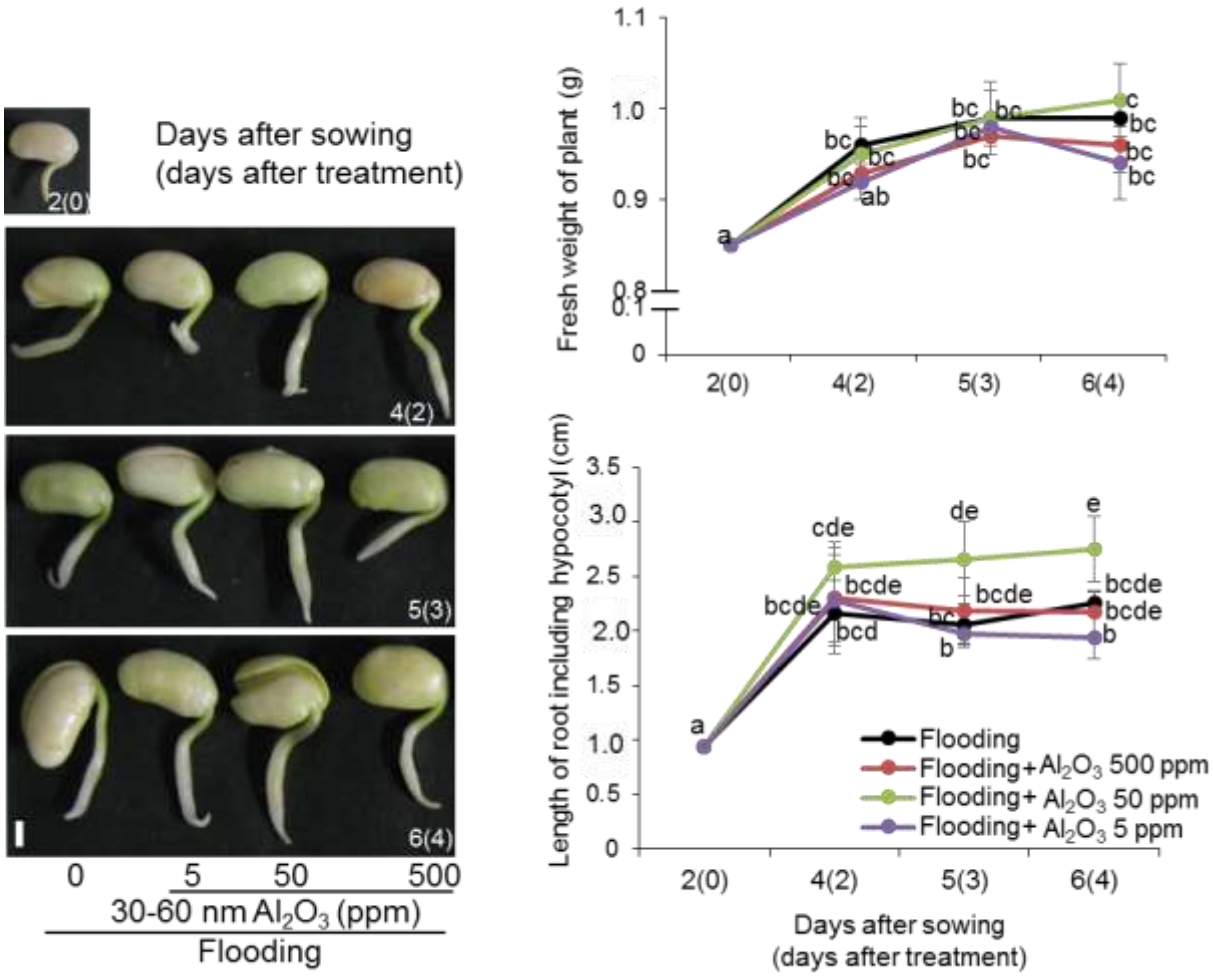

Figure 9. Dose-dependent effects of 30-60 nm Al_2O_3 NPs on the growth of soybean under flooding conditions. Two-day-old soybeans were flooded without (black) or with 30-60 nm Al_2O_3 NPs at concentrations of 500 ppm (red), 50 ppm (green), and 5 ppm (purple). Photographs show soybean seedlings at 0, 2, 3, and 4 days of flooding and Al_2O_3 NPs treatments. Bar indicates 1 cm. Fresh weight of plant and length of root including hypocotyl were measured at the indicated time points. The data are presented as the mean ± S.D. from three independent biological replicates (n=3). Statistical analysis is same as described in Figure 5.

CHAPTER 2

CHARACTERIZATION OF SOYBEAN PROTEINS AFFECTED BY SILVER NANOPARTICLES UNDER FLOODING STRESS

2.1. Introduction

The Ag is a valuable element as being used in the industrial application and also in the jewelery and the related items. The Ag ions are recognized as bioactive molecules (Santoro et al., 2007). Due to its unique properties, Ag is being used from ancient times as an important antimicrobial agent. The Ag could easily be oxidized with the oxygen and produce the Ag ions that are known toxic ions (McShan et al., 2014). These Ag ions stimulate the production of ROS and ultimately caused the oxidative DNA damage, activation of antioxidant enzymes, and depletion of antioxidant molecules (McShan et al., 2014). The antimicrobial characteristics of Ag are attributed to their ability to generate ROS in the bacteria and de-activation of the microbial enzymes (Matsumura et al., 2003). The Ag is present in the earth crust as a rare element; however, the tremendously increasing use in the industrial products makes it a major point of concern due to the toxicological effects.

The Ag NPs are reported to promote the growth of flooding-stressed *Crocus sativus* roots by blocking ethylene signaling (Rezvani et al., 2012). In *Arabidopsis*, Ag NPs induce the accumulation of ROS and promote root growth, and also function as ethylene perception inhibitors (Syu et al., 2014). Gene expression profiling of *Arabidopsis* treated with Ag NPs has indicated that genes associated with response to metal, oxidative stress, and the thalianol biosynthetic pathway are up-regulated; whereas, genes associated with the ethylene signaling pathway are down-regulated (Kaveh et al., 2013). In *P. vulgaris* and maize, increasing concentrations of Ag NPs lead to corresponding increase in chlorophyll, carbohydrate, and protein levels (Salama, 2012). Proteomic analysis of the Ag NPs toxicity on rice revealed the accumulation of protein precursors, which are indicative of dispersal of electron motive force (Mirzajani et al., 2014). The exposure to Ag NPs results in differential changes in the levels of proteins related to oxidative stress tolerance, calcium regulation/signaling, transcription/degradation, cell wall, cell division, and apoptosis in rice (Mirzajani et al., 2014). In *E. sativa*, the Ag NPs changed the proteins related to redox regulation and sulfur metabolism that play important role in maintaining the cellular homeostasis. The Ag NPs also altered the proteins related to the endoplasmic reticulum and vacuoles in *E. sativa* indicating these two organelles as a primary target for the NPs (Vannini et al.,

2013). However, the effect of Ag NPs on the proteomic profiles of soybean under flooding stress has yet to be determined.

Because of the increasing use of Ag NPs in agricultural products, the biological effects of these particles in plants, particularly soybean, which is cultivated worldwide and is highly susceptible to flooding, warrant intensive investigation. Although Rezvani et al. (2012) reported that Ag NPs treatment had positive effects by preventing the ethylene action in *C. sativus* under flooding stress. Only few studies have examined the effects of Ag NPs on animal (van der Zande et al., 2012), bacteria (Choi and Hu, 2008), and algae (Miao et al., 2009). However, the research focusing on the molecular mechanisms affected by Ag NPs is very limited. This experiment is carried out to understand the molecular processes being altered by the application of Ag NPs on soybean under flooding stress. Because the 2 ppm of 15 nm Ag NPs promoted the soybean growth under flooding stress (Chapter 1), this concentration and size of Ag NPs were used for this proteomic study. In order to understand the cellular processes affected by the Ag NPs in soybean under flooding stress, protein profiles of root including hypocotyl and cotyledons of soybean exposed to flooding stress were evaluated using a gel-free proteomic technique.

2.2. Materials and methods

2.2.1. Plant material and treatments

Soybean was used as the plant material in this study. Plant growth conditions are described in 1.2.1 in Chapter 1. To study the effects of Ag NPs on soybean plants under flooding stress, 15 nm Ag NPs at 2 ppm were used for the proteomic and mRNA expression analyses. For proteomic analysis, root including hypocotyl and cotyledons were collected on 0, 2, and 4 days of treatment; whereas, root including hypocotyl was harvested on 0, 1, and 2 days of treatment for quantitative reverse transcription-polymerase chain reaction (qRT-PCR) analysis (Figure 10). Three independent experiments were performed as biological replicates for all experiments.

2.2.2. Protein extraction, purification, and digestion

A portion (300 mg) of each collected sample was ground in liquid nitrogen with a

mortar and pestle. The resulting powder was transferred to a solution containing 10% trichloroacetic acid and 0.07% 2-mercaptoethanol in acetone, the resulting suspension was vortexed, sonicated for 10 min, and then incubated for 60 min at -20°C. After the suspension was centrifuged at 9,000 ×*g* for 20 min at 4°C, the supernatant was discarded, and the pellet obtained was washed twice with 0.07% 2-mercaptoethanol in acetone. The final pellet was dried using a Speed-Vac concentrator (Savant Instruments, Hicksville, NY, USA) and then re-suspended by vortexing for 60 min at 25°C in lysis buffer consisting of 8 M urea, 2 M thiourea, 5% CHAPS, and 2 mM tributylphosphine. The suspension was centrifuged at 20,000 ×*g* for 20 min at 25°C and the resulting supernatant was collected as protein extract. Protein concentration was determined using the Bradford method (Bradford, 1976) with bovine serum albumin as the standard.

For mass spectrometry (MS) analysis, proteins (150 µg) were purified by phase separation using standard procedures (Komatsu et al., 2013a). Briefly, 600 µL methanol was added to 150 µL of each protein sample, and the resulting solution was thoroughly mixed before 150 µL chloroform was added. After further mixing by vortexing, 450 µL water was added into the samples to induce phase separation, and then centrifuged at 20,000 ×*g* for 10 min. The upper aqueous layer was discarded and 450 µL methanol was added to the organic phase. After the samples were further centrifuged at 20,000 ×*g* for 10 min, the resulting supernatants were discarded, and the pellets were dried at 25ºC. The dried pellets were re-suspended in 50 mM ammonium bicarbonate, and proteins in the samples were reduced by treatment with 50 mM dithiothreitol for 30 min at 56ºC, and then alkylated with 50 mM iodoacetamide for 30 min at 37ºC in the dark. Alkylated proteins were digested with trypsin (Wako, Osaka, Japan) at 1:100 enzyme/protein concentration at 37ºC for 16 h. The resulting tryptic peptides were acidified to pH < 3 with 10 µL of 20% formic acid, desalted with a C18-pipette tip (Nikkyo Technos, Tokyo, Japan), and examined by liquid chromatography (LC) MS.

2.2.3. Mass spectrometry analysis

Using an Ultimate 3,000 nanoLC system (Dionex, Germering, Germany), peptides in 0.1% formic acid were loaded onto a C18 PepMap trap column (300 µm ID

x 5 mm, Dionex). The peptides were eluted from the trap column with a linear acetonitrile gradient (8-30% in 120 min) in 0.1% formic acid at a flow rate of 200 nL/min. The peptides eluted from the trap column were separated and sprayed onto a C18 Tip column (75 µm 1D x 120 mm, nanoLC capillary column; Nikkyo Technos) with a spray voltage of 1.5 kV. The eluted peptides were analyzed on a nanospray LTQ XL Orbitrap MS (Thermo Fisher Scientific, San Jose, CA, USA) operated in data-dependent acquisition mode with the installed Xcalibur software (version 2.1, Thermo Fisher Scientific). Full-scan mass spectra were acquired in the Orbitrap MS over 400-1,500 *m/z* with a resolution of 30,000. A lock mass function was used to obtain high mass accuracy (Olsen et al., 2005). As the lock mass, the ions $C_{24}H_{39}O_4^+$ (*m/z* 391.28429), $C_{14}H_{46}NO_7Si_7^+$ (*m/z* 536.16536), and $C_{16}H_{52}NO_8Si_8^+$ (*m/z* 610.18416) were used. The top 10 most intense ions were selected for collision-induced fragmentation in the linear ion trap at a normalized collision energy of 35%. Dynamic exclusion was employed within 90 sec (Zhang et al., 2009) to prevent repetitive selection of peptides. The acquired MS spectra were used for protein identification. The mass spectrometry proteomic data have been deposited with the ProteomeXchange Consortium (http://proteomecentral.proteomexchange.org) via the PRIDE partner repository (Vizcaíno et al., 2013) with the data set identifier: PXD001579.

2.2.4. Protein identification of acquired mass spectrometry data

Identification of proteins was performed using the Mascot search engine (version 2.4.1) (Matrix Science, London, UK) and Proteome Discoverer software (version 1.4.0.288; Thermo Fisher Scientific) against a soybean peptide database (54,175 sequences) (Phytozome, version 9.0, http://www.phytozome.net/soybean) (Schmutz et al., 2010). In the Mascot search, carbamidomethylation of cysteine was set as a fixed modification and oxidation of methionine was set as a variable modification. Trypsin was specified as the proteolytic enzyme and one missed cleavage was allowed. Peptide mass tolerance was set at 5 ppm, fragment mass tolerance was set at 0.8 Da, and peptide charge was set at +2, +3, and +4. An automatic decoy database search was also performed. Mascot results were filtered with Mascot Percolator to improve the accuracy and sensitivity of the peptide identification (Brosch et al., 2009). False discovery rates

for peptide identification of all searches were less than 1.0%. Peptides with a percolator ion score of more than 13 ($p < 0.05$) were used for protein identification. The Mascot results generated msf files that were analyzed using SIEVE software (version 2.1.0, Thermo Fisher Scientific).

2.2.5. Differential analysis of the identified proteins

The relative abundances of peptides and proteins were compared between the control and treated groups using the commercial label-free quantification package SIEVE software. To compare protein content between control and treated groups, extracted ion chromatograms (XIC) were generated based on a comparison approach using SIEVE software. For the analysis, the chromatographic peaks detected by MS were aligned, and the peptide peaks were detected as frames using the following settings: frame time width (5 min), frame *m/z* width (10 ppm), and produce frames on all parent ions scanned by MS/MS. Chromatographic peak area of each sample within a single frame was compared, and the ratios between two sample groups in each frame were determined. The frames detected in the MS/MS scan were matched to the imported Mascot search results. The ratio of peptides between control and treated groups was determined from the variance-weighted average of the ratios in frames, which matched the peptides in the MS/MS spectrum. The ratios of peptides were further integrated to determine the ratio of the corresponding protein. In the differential analysis of protein abundance, total ion current was used for normalization. The minimum requirement for the identification of a protein was a minimum of two matched peptides. Significant changes in the abundance of proteins between the control and treated groups were analyzed ($p < 0.05$). The identified peptides in the total protein fraction were used to calculate protein abundance.

2.2.6. Functional analysis of identified proteins

Protein functions were categorized using MapMan bin codes software (http://mapman.gabipd.org/) (Usadel et al., 2005).

2.2.7. Cluster analysis of protein abundance

Protein abundance ratios at different time points of flooding stress for soybeans supplemented with Ag NPs were used for cluster analysis by the hierarchical clustering method (a centroid linkage method based on a Euclidean distance metric).

2.2.8. RNA extraction and quantitative reverse transcription polymerase chain reaction analysis

A portion (100 mg) of each collected sample was ground into powder in liquid nitrogen with a sterilized mortar and pestle. Total RNA was extracted from the powdered tissue using an RNeasy Plant Mini kit (Qiagen, Valencia, CA, USA). RNA was reverse-transcribed using an iScript cDNA Synthesis kit (Bio-Rad, Hercules, CA, USA) according to the manufacturer's instructions. qRT-PCR was performed in a 10 μL reaction using SsoAdvanced SYBR Green Universal Supermix (Bio-Rad) and a MyiQ single-color real-time PCR detection system (Bio-Rad). The PCR conditions were as follows: 95ºC for 210 sec, followed by 45 cycles of 95ºC for 30 sec, 60ºC for 30 sec, and 72ºC for 30 sec. Gene expression was normalized using 18S rRNA as an internal control. Three biological replicates were used for each gene in each treatment and each biological replicate was technically duplicated to reduce the error rate. The primers were designed using the Primer3 web interface (http://frodo.wi.mit.edu). The specificity of primers was checked by BLASTN searches against the Phytozome-*G.max* database with the designed primer sequences as queries and by melting curve analysis. The primers used are listed in Supplemental Table 1.

2.2.9. Statistical analysis

Statistical analysis is described in 1.2.2 in Chapter 1.

2.3. Results

2.3.1. Protein identification in Ag NPs-treated soybean using gel-free proteomics

To better understand the effects of Ag NPs on soybean under flooding stress, a gel-free proteomic technique was used. The soybean plant exposed to 15 nm Ag NPs at 2 ppm showed the increased fesh weight of plant compared to the flooding stress. The results of the Chapter 1 indicated that the low concentrations of Ag NPs has growth

enhancing effects under the flooding stress. In the differential analysis of total proteins, the accumulation levels of 484 proteins with more than 2-fold change, which included 125 increased and 359 decreased proteins, were significantly changed in 4-day-old soybean roots compared to 2-day-old roots under control conditions (Figure 11). In 4-day-old soybean roots exposed to 2 days of flooding stress, 460 proteins with more than 2-fold change, which included 416 increased and 42 decreased proteins, were differentially changed compared to 2-day-old soybean roots (Figure 11). In response to Ag NPs treatment under flooding stress, the abundances of 620 proteins with more than 2-fold change, which consisted of 41 increased and 577 decreased proteins, were differentially changed (Figure 11). In the Ag NPs-treated roots, the levels of eukaryotic aspartyl protease family protein and expansin-like B1 increased by 10 fold, whereas the levels of 90 other proteins decreased by 10 fold.

To determine the functional role of these identified proteins, functional categorization was performed using MapMan bin codes. The analysis revealed that the majority of the differentially changed proteins in the roots of 4-day-old soybeans compared to 2-day-old soybeans were related to protein synthesis/degradation (169 proteins), photosynthesis (36 proteins), stress (27 proteins), hormone metabolism (26 proteins), and development (24 proteins) (Figure 11). In roots exposed to 2 days of flooding stress, the changed proteins compared to 2-day-old untreated soybeans were predominantly related to protein synthesis/degradation (180 proteins), cell wall (23 proteins), transport (21 proteins), and stress (13 proteins). Functional categorization of the changed proteins identified in 4-day-old soybean treated with Ag NPs and flooding stress for 2 days was performed. The majority of proteins were related to protein synthesis/degradation (191 proteins), stress (32 proteins), hormone metabolism (20 proteins), amino acid metabolism (32 proteins), signaling (36 proteins), and cell metabolism (30 proteins) (Figure 11). These results indicated that Ag NPs predominantly affected proteins related to stress, signaling, and cell metabolism in the roots of soybean. Out of the 32 stress-related proteins affected by Ag NPs treatment, 6 were increased and 26 were decreased in abundance (Figure 11). A similar trend was observed for the 13 stress-related proteins differentially changed in response to flooding stress, as 2 were increased and 11 were decreased. The combination of flooding and Ag

NPs treatment also appeared to affect more proteins than flooding stress alone, as 36 signaling- and 30 cell metabolism-related proteins were differentially changed by flooding and Ag NPs treatment compared to only 16 and 10 proteins, respectively, by flooding stress (Figure 11).

2.3.2. Time-dependent analysis of root proteins during exposure to Ag NPs

A gel-free proteomic approach was used to examine the temporal effects of Ag NPs on proteins in the roots of flooding-stressed soybean. In the differential analysis, 107 root proteins were commonly changed after 2, 4, and 6 days of control, flooding, and flooding with Ag NPs treatment (Table 3). Functional categorization of these commonly changed proteins revealed that the majority of proteins were related to protein synthesis/degradation/folding (62 proteins), although proteins involved in development (7 proteins) and fermentation (6 proteins) were detected (Table 3). The abundance of 1,274 proteins was significantly changed in the 4- and 6-day-old untreated soybean compared to the 2-day-old soybean roots (Figure 12). Under flooding-stress conditions, 733 proteins were significantly changed in 4- and 6-day-old soybean flooded for 2 and 4 days, respectively, compared to the 2-day-old untreated soybean roots (Figure 12). In response to flooding with Ag NPs treatment, 919 proteins were significantly changed in the 4- and 6-day-old soybean roots treated for 2 and 4 days, respectively, compared to the 2-day-old untreated soybean roots (Figure 12).

2.3.3. Cluster analysis of identified proteins during the time-dependent exposure of soybean roots to Ag NPs

To further analyze the expression profiles of the 107 significantly changed proteins in the soybean roots under flooding with Ag NPs treatment (Table 3), a hierarchical clustering method was used. Using this approach, three clusters (I-III) of changed proteins were recognized (Figure 13). Cluster I consisted of only one protein, glyoxalase II 3, which is an important enzyme of the glyoxalase pathway. The abundance of glyoxalase II 3 time-dependently increased in roots under flooding stress, but decreased in response to Ag NPs treatment. Cluster II consisted of 11 proteins that were all increased after 2 and 4 days of flooding; however, the levels of these proteins

significantly decreased in roots exposed to Ag NPs under flooding conditions. Cluster III consisted of 95 proteins that displayed similar changes in abundance under flooding treatment without or with Ag NPs (Figure 13).

2.3.4. mRNA expression levels in soybean roots treated with Ag NPs

Based on the proteomic results, key enzymes involved in metabolic pathways, which showed changed abundances in response to flooding and Ag NPs treatment, were selected for mRNA expression analysis (Table 3). The flood responsive proteins with the opposite trend in abundance levels in the flooding and Ag NPs treatment were selected. The mRNA expression levels of *glyoxalase II 3* (Glyma15g39370.2), *alcohol dehydrogenase 1* (Glyma06g12780.1), *pyruvate decarboxylase 2* (Glyma13g30490.1), *sucrose synthase 4* (Glyma15g20180.2), *aluminum-induced protein with YGL and LRDR motifs* (Glyma12g35070.1), and *thiamine pyrophosphate-dependent pyruvate decarboxylase family protein* (Glyma01g29190.1) were analyzed (Figure 14). The mRNA expression level of *glyoxalase II 3* was slightly down-regulated and that of *alcohol dehydrogenase* was significantly down-regulated in roots after 2 days of flooding with Ag NPs treatment as compared to flooding alone (Figure 14). The mRNA expression levels of both *pyruvate decarboxylase 2* and *sucrose synthase 4* were up-regulated under flooding conditions (Figure 14), but following Ag NPs treatment, the expression levels of both genes in roots was down-regulated. Likewise, down-regulated mRNA expression levels were also evident in *aluminum-induced protein with YGL and LRDR motifs* and *thiamine pyrophosphate-dependent pyruvate decarboxylase family protein* (Figure 14).

2.3.5. Functional comparison of proteins affected by Ag NPs treatment in soybean roots and cotyledons

The effects of Ag NPs on protein profiles in the cotyledons of soybean under flooding stress were further examined by a gel-free proteomics. The differential analysis of cotyledon proteins revealed that a total of 676 proteins were significantly changed with 2-fold change in 4- and 6-day-old untreated soybean cotyledons compared to 2-day-old untreated soybean (Figure 15). Under flooding-stress conditions, 119 proteins

were significantly changed in the cotyledons of 4- and 6-day-old soybeans flooded for 2 and 4 days, respectively, compared to 2-day-old untreated soybean cotyledon (Figure 15). In response to flooding with Ag NPs treatment, 232 proteins were significantly changed in the cotyledons of 4- and 6-day-old soybeans treated for 2 and 4 days, respectively, with flooding and Ag NPs compared to 2-day-old untreated soybean (Figure 15). The proteomic results for soybean cotyledons indicated the abundance of beta-ketoacyl reductase was increased in response to Ag NPs treatment; whereas, that of Rmlc-like cupin superfamily protein was decreased. The abundances of 107 proteins were significantly changed in soybean roots exposed to flooding and Ag NPs compared to the untreated roots (Table 3). To investigate the effects of Ag NPs on the protein profiles of different organs, the proteomic analysis of proteins from cotyledons was also performed. In the differential analysis, 9 proteins were significantly changed in cotyledons under flooding and Ag NPs treatment compared to the untreated cotyledons (Table 4). The identified proteins in the cotyledons were functionally categorized using MapMan bin codes and compared to those identified in the roots (Usadel et al., 2005). The functional categorization and comparative analysis indicated that more proteins related to protein degradation/synthesis, fermentation, and photosynthesis were changed in roots, whereas proteins involved in carbohydrate metabolism, tetrapyrrole synthesis, and transport were predominantly affected in the cotyledon (Figure 16).

In the differential analysis of root and cotyledon proteins affected by Ag NPs treatment of soybean under flooding stress, only one protein, glyoxalase II 3, was found to be common between the two tissues (Figure 17). In root including hypocotyl, the abundance of glyoxalase II 3 was increased under flooding stress, but was decreased by Ag NPs treatment. In cotyledons, the abundance of glyoxalase II 3 was increased by 3- and 2-fold in response to flooding without or with Ag NPs treatments, respectively.

2.4. Discussions

2.4.1. Effects of Ag NPs on stress, signaling, and cell metabolism-related proteins in soybean roots under flooding stress

The results of the present quantitative proteomic analysis indicate that Ag NPs primarily affects the abundance of proteins related to stress, signaling, and cell

metabolism. The abundance of 36 signaling-related proteins, which were functionally categorized by MapMan bin codes as G-proteins, was changed in soybean roots in response to Ag NPs treatment under flooding stress. G-proteins are regulatory proteins that function as essential signal transducers in hypoxia signaling pathways (Steffens and Sauter, 2010). Under oxygen-deprived conditions, plants alter carbohydrate metabolic pathways to support ATP generation through glycolysis and subsequent fermentation (Banti et al., 2013). In *Arabidopsis*, the regulation of alcohol dehydrogenase activity under low-oxygen conditions is dependent on GTPase signaling (Steffens and Sauter, 2010). In maize, extensive aerenchyma formation through the lysis and death of root cells has been observed under flooding conditions (He et al., 2000). A decrease in the abundance of GTPase proteins would lead to the decreased hydrolysis of GTPγS and result in constitutively activated G proteins. In this study, numerous GTPase proteins were decreased in soybean roots exposed to flooding conditions, suggesting that the activation of G proteins induces the formation of aerenchyma under stress conditions.

The Ag NPs treatment of soybean under flooding stress increased the abundance of 32 stress-related proteins, which were comprised of Kunitz family trypsin and protease inhibitor proteins. The abundance of these proteins in the roots of flooding-stress soybean increased two-fold, whereas the magnitude of the increase was approximately four-fold in roots exposed to both flooding stress and 2 ppm Ag NPs. Stress conditions result in the aggregation of misfolded proteins (Liu et al., 2010). For maintaining the functional confirmation of proteins and preventing their aggregation, plant respond to stress by increasing the activity of protease inhibitors that degrade irreversibly damaged proteins. For example, the levels of trypsin inhibitors are increased in cereal crops under stress conditions (Domash et al., 2008). In the present study, Kunitz family trypsin and protease inhibitor proteins were increased in soybean roots treated with Ag NPs under flooding stress. However, these proteins are not typically found at high levels in soybean, suggesting that they might be involved in growth suppression in response to flooding stress.

The abundances of 30 cell metabolism-related proteins were affected by Ag NPs treatment under flooding stress. In addition, several cell organization-related proteins, including annexin 8, myosin heavy chain-related protein, and villin 2, were found to be

decreased. Lee et al. (2004) reported that annexins play important roles in osmotic stress and abscisic acid signaling in a calcium-dependent manner. In *Arabidopsis*, mutants lacking these annexins were reported to lack root hairs (Laohavisit et al., 2012). In soybeans, several cell organization-related proteins were recently found to be decreased under flooding, but were more significantly decreased in flooding-stress plants treated with abscisic acid (Komatsu et al., 2013b). In the present flooding experiments, Ag NPs treatment of soybean resulted in a decrease in cell organization-related proteins, which may be related to the quiescent status of cell division and elongation under these conditions.

2.4.2. Effects of Ag NPs on mRNA expression and protein abundance of alcohol dehydrogenase and pyruvate decarboxylase under flooding stress

Progressive decrease in soil oxygen concentration is one of the major physiological consequences of soil flooding (Hossain et al., 2009). Oxygen deprivation compromises ATP production and energy supply, as oxygen is the final acceptor of electrons in the mitochondrial respiration (Banti et al., 2013). Under low oxygen condition, plants shift their carbohydrate metabolism towards fermentative pathways. Previous studies on soybean reported that abundances of alcohol dehydrogenase and pyruvate decarboxylase, the two key enzymes that facilitate the inter-conversion between pyruvate and alcohol were increased on exposure to flooding to strengthen alcohol fermentation (Komatsu et al., 2014). This flood induced metabolic re-arrangement is important for soybean to adapt the initial phase of low oxygen condition (Yin et al., 2014; Komatsu et al., 2013b). In this study, the abundances of the fermentation-related proteins (pyruvate decarboxylase 2 and alcohol dehydrogenase 1) were significantly increased in roots under flooding stress, nevertheless decreased by Ag NPs treatment. Notably, the mRNA expression levels of *alcohol dehydrogenase 1* and *pyruvate decarboxylase 2 genes* were largely corroborate with the protein abundance. The expression of *alcohol dehydrogenase* gene was previously reported to be up-regulated in soybean under flooding stress to cope with the increased energy demand (Tougou et al., 2012). Similarly, in maize activity of pyruvate decarboxylase had been reported to be increased under flooding stress (Vantoai et al., 1987). The observed up-regulation of the

alcohol dehydrogenase 1 and *pyruvate decarboxylase 2* genes under flooding stress condition and its down-regulation in response to Ag NPs treatment might be related to a metabolic shift towards normal cellular processes.

2.4.3. Role of glyoxalase II 3 in soybean root and cotyledon under flooding stress with Ag NPs treatment

The glyoxalase II 3 is an important enzyme of the glyoxalase pathway that plays essential role in detoxification of methylglyoxal (Espartero et al., 1995). Methylglyoxal is a cytotoxic by-product of glycolysis generally accumulated in cell in response to various environmental stresses (Espartero et al., 1995). Enzymatic and non-enzymatic eliminations of phosphate from glycolytic intermediates including dihydroxy acetone phosphate and glyceraldehyde-3-phosphate lead to the formation of methylglyoxal (Thornalley, 1990). A recent finding suggests that glyoxalase II-1 is non-essential for the normal growth of *Arabidopsis;* however, it is required during unfavorable conditions such as anoxia, salinity, osmotic, chilling, and heat stresses (Devanathan et al., 2014). Comparative proteomic analysis of roots and cotyledons showed that abundance of glyoxalase II 3 was time-dependently increased under flooding stress; however, decreased in response to Ag NPs in both the organs. The mRNA expression level of the *glyoxalase II 3* gene also displayed similar trend with the changed protein abundance. The hierarchical clustering analysis reveals that cluster I is consisted of only protein i.e. glyoxalase II 3, that highlights the importance of glyoxalase II 3 protein in response of soybean to flooding stress. In the present study, comparatively low transcript level of glyoxalase II 3 under Ag NPs treatment might imply that less cytotoxic by-product of glycolysis are produced in Ag NPs exposed soybeans as compared to flooded soybean.

2.5. Conclusion

The present proteomic study highlights the effects of Ag NPs on soybean exposed to flooding stress. The major findings are as follows: (i) Ag NPs primarily affected the abundances of proteins predominantly associated with stress, signaling, and cell metabolism; (ii) comparative proteomic analysis revealed that abundances of the glyoxalase II 3 and fermentation related proteins (pyruvate decarboxylase 2 and alcohol

dehydrogenase 1) were significantly increased under flooding stress; however, decreased by Ag NPs treatment; and (iii) mRNA expression levels of these genes were largely corroborate with the protein abundance data (Figure 18). Taken together, these results suggest that Ag NPs treatment mediate the metabolic shift from fermentative pathways towards normal cellular processes as well as formation of comparatively low cytotoxic by-products that might be the key factors for better growth performance of Ag NPs treated soybeans under flooding stress.

Table 3. List of identified proteins in roots of flooded soybean in response to Ag NPs treatment.

No.	Protein ID	Description	M.P.	Control			Flooding			Flooding+Ag NPs			Functional Category
				Ratio 2(0)*	Ratio 4(0)	Ratio 6(0)	Ratio 2(0)	Ratio 4(2)	Ratio 6(4)	Ratio 2(0)	Ratio 4(2)	Ratio 6(4)	
1.	Glyma15g39370.2	Glyoxalase II 3	3	1	1.69	0.79	1	4.31	7.60	1	1.37	0.00	Biodegradation of xenobiotics
2.	Glyma01g29190.1	Thiamine pyrophosphate dependent pyruvate decarboxylase family protein	2	1	0.53	0.28	1	3.11	3.86	1	0.65	0.00	Fermentation
3.	Glyma13g33590.1	Glyoxalase II 3	7	1	1.36	0.64	1	2.99	5.17	1	0.77	0.00	Biodegradation of Xenobiotics
4.	Glyma12g35070.1	Aluminium induced protein with YGL and LRDR motifs	3	1	0.63	0.24	1	2.99	3.60	1	1.61	0.00	Hormone metabolism
5.	Glyma13g35480.1	Aluminium induced protein with YGL and LRDR motifs	3	1	0.63	0.24	1	2.99	3.60	1	1.61	0.00	Hormone metabolism
6.	Glyma07g18570.1	Thiamine pyrophosphate dependent pyruvate decarboxylase family protein	8	1	0.48	0.26	1	2.88	3.58	1	0.91	0.00	Fermentation
7.	Glyma13g30490.1	Pyruvate decarboxylase 2	10	1	0.61	0.28	1	2.28	2.48	1	0.62	0.00	Fermentation
8.	Glyma03g07300.2	Thiamine pyrophosphate dependent pyruvate decarboxylase family protein	2	1	0.53	0.28	1	2.04	3.06	1	0.68	0.00	Fermentation
9.	Glyma03g07380.1	Thiamine pyrophosphate dependent pyruvate decarboxylase family protein	2	1	0.53	0.28	1	2.04	3.06	1	0.58	0.00	Fermentation
10.	Glyma15g20180.2	Sucrose synthase 4	23	1	1.44	0.98	1	2.03	2.69	1	0.47	0.00	Major CHO metabolism
11.	Glyma06g12780.1	Alcohol dehydrogenase 1	15	1	0.65	0.25	1	2.03	2.49	1	1.08	0.00	Fermentation
12.	Glyma01g10900.1	Kunitz trypsin inhibitor 1	3	1	0.26	0.13	1	0.50	2.58	1	0.49	0.00	Stress.biotic
13.	Glyma17g18440.1	Granulin repeat cysteine protease family protein	3	1	0.49	0.18	1	0.48	0.36	1	0.52	0.00	Protein.degradation
14.	Glyma03g35530.1	Ribosomal protein l32e	4	1	0.39	0.06	1	0.48	0.51	1	0.32	0.00	Protein.synthesis
15.	Glyma11g34890.1	Ribosomal protein l32e	4	1	0.39	0.06	1	0.48	0.51	1	0.32	0.00	Protein.synthesis
16.	Glyma20g38480.1	Ribosomal L29 family protein	4	1	0.58	0.00	1	0.47	0.46	1	0.00	0.00	Protein.synthesis
17.	Glyma16g26630.1	Xyloglucan endotransglucosylase/hydrolase 5	6	1	2.01	0.89	1	0.47	0.49	1	0.14	0.00	Cell wall.modification
18.	Glyma05g20930.1	Granulin repeat cysteine protease family protein	4	1	0.49	0.05	1	0.47	0.37	1	0.48	0.00	Protein.degradation
19.	Glyma20g28631.1	O acetylserine (thiol) lyase (OAS TL) isoform A1	6	1	0.84	0.44	1	0.47	0.38	1	0.83	0.00	Amino acid metabolism
20.	Glyma09g36560.1	BCL 2 associated athanogene 7	6	1	0.39	0.05	1	0.44	0.74	1	0.12	0.00	Signalling.calcium
21.	Glyma19g28220.1	Xyloglucan endotransglucosylase/hydrolase 5	9	1	1.43	0.94	1	0.43	0.38	1	0.16	0.00	Cell wall.modification
22.	Glyma16g04950.1	Xyloglucan endotransglucosylase/hydrolase 5	13	1	1.43	0.97	1	0.43	0.37	1	0.17	0.00	Cell wall.modification
23.	Glyma12g03570.1	Subtilisin like serine protease 2	11	1	1.28	0.64	1	0.43	0.37	1	0.13	0.00	Protein.degradation

24.	Glyma02g45190.1	Photosystem II subunit P 1	3	1	1.79	2.82	1	0.41	0.40	1	0.41	0.01	PS
25.	Glyma14g03560.1	Photosystem II subunit P 1	3	1	1.79	2.82	1	0.41	0.40	1	0.41	0.01	PS
26.	Glyma20g33850.2	Oleosin 1	3	1	0.02	0.04	1	0.39	0.40	1	0.18	0.00	Lipid metabolism
27.	Glyma02g02140.1	Ribosomal L22e protein family	3	1	0.43	0.21	1	0.38	0.27	1	0.32	0.00	Protein.synthesis
28.	Glyma10g02270.1	Ribosomal L22e protein family	3	1	0.43	0.21	1	0.38	0.27	1	0.32	0.00	Protein.synthesis
29.	Glyma05g08880.1	Oleosin family protein	2	1	0.20	0.15	1	0.37	0.51	1	0.37	0.00	Lipid metabolism
30.	Glyma10g38450.1	Valyl trna synthetase / valine trna ligase (VALRS)	4	1	0.13	0.04	1	0.37	0.67	1	0.52	0.01	Protein.aa activation
31.	Glyma01g44700.1	Ribosomal protein S3Ae	12	1	0.67	0.11	1	0.37	0.23	1	0.08	0.00	Protein.synthesis
32.	Glyma11g00890.1	Ribosomal protein S3Ae	13	1	0.63	0.11	1	0.36	0.24	1	0.08	0.00	Protein.synthesis
33.	Glyma19g42090.2	Ribosomal L22e protein family	2	1	0.47	0.23	1	0.35	0.44	1	0.35	0.00	Protein.synthesis
34.	Glyma13g42830.1	Ribosomal L28e protein family	2	1	0.59	0.48	1	0.35	0.17	1	0.49	0.00	Protein.synthesis
35.	Glyma15g02610.1	Ribosomal L28e protein family	2	1	0.59	0.48	1	0.35	0.17	1	0.49	0.00	Protein.synthesis
36.	Glyma10g02290.1	NAD(P) binding Rossmann fold superfamily protein	6	1	1.04	0.39	1	0.34	0.30	1	0.50	0.01	Cell wall.precursor synthesis
37.	Glyma14g02700.3	OUT like cysteine protease family protein	3	1	0.29	0.13	1	0.33	0.21	1	0.11	0.00	Protein.degradation
38.	Glyma16g16290.1	Granulin repeat cysteine protease family protein	4	1	0.46	0.06	1	0.33	0.32	1	0.38	0.00	Protein.degradation
39.	Glyma05g29870.1	T complex protein 1 alpha subunit	10	1	0.64	0.49	1	0.32	0.68	1	0.81	0.00	Protein.folding
40.	Glyma06g20540.1	Ribosomal protein S4	6	1	0.67	0.34	1	0.32	0.46	1	0.50	0.00	Protein.synthesis
41.	Glyma10g39050.1	Ribosomal protein S3Ae	13	1	0.69	0.11	1	0.32	0.23	1	0.09	0.00	Protein.synthesis
42.	Glyma08g12970.1	T complex protein 1 alpha subunit	10	1	0.64	0.49	1	0.32	0.66	1	0.81	0.00	Protein.folding
43.	Glyma20g28780.1	Ribosomal protein S3Ae	14	1	0.67	0.10	1	0.32	0.24	1	0.09	0.00	Protein.synthesis
44.	Glyma04g33900.2	Ribosomal protein S4	5	1	0.68	0.33	1	0.31	0.45	1	0.50	0.00	Protein.synthesis
45.	Glyma20g28650.2	Cupin family protein	11	1	0.02	0.00	1	0.30	0.48	1	0.08	0.00	Development.storage proteins
46.	Glyma20g28660.1	Cupin family protein	13	1	0.02	0.00	1	0.30	0.01	1	0.07	0.00	Development.storage proteins
47.	Glyma08g16220.1	Leucine rich repeat (LRR) family protein	6	1	0.92	0.40	1	0.29	0.20	1	0.35	0.00	DNA.repair
48.	Glyma10g33760.1	Oleosin 1	2	1	0.04	0.04	1	0.28	0.33	1	0.15	0.01	Lipid metabolism
49.	Glyma09g08395.1	Ribosomal protein S3Ae	2	1	0.52	0.07	1	0.27	0.28	1	0.14	0.00	Protein.synthesis

50.	Glyma08g41220.3	S adenosyl L methionine dependent methyltransferases superfamily protein	3	1	0.65	0.39	1	0.26	0.27	1	0.45	0.00	Stress.abiotic
51.	Glyma18g15080.2	S adenosyl L methionine dependent methyltransferases superfamily protein	3	1	0.65	0.39	1	0.26	0.27	1	0.45	0.00	Stress.abiotic
52.	Glyma09g12430.1	Ribosomal protein S11 beta	2	1	0.30	0.15	1	0.25	0.06	1	0.17	0.00	Protein.synthesis
53.	Glyma17g16350.3	S adenosyl L methionine dependent methyltransferases superfamily protein	4	1	0.80	0.10	1	0.23	0.25	1	0.05	0.00	Stress.abiotic
54.	Glyma07g04470.1	Cytochrome P450 superfamily protein	11	1	1.84	1.55	1	0.22	0.04	1	0.05	0.03	Secondary metabolism
55.	Glyma01g31270.1	Ribosomal protein S4 (RPS4A) family protein	10	1	0.35	0.35	1	0.21	0.11	1	0.61	0.00	Protein.synthesis
56.	Glyma03g06440.1	Ribosomal protein S4 (RPS4A) family protein	10	1	0.35	0.35	1	0.21	0.11	1	0.61	0.00	Protein.synthesis
57.	Glyma01g38750.1	Photosystem II subunit O 2	10	1	2.41	1.63	1	0.21	0.16	1	0.37	0.01	PS
58.	Glyma02g06830.1	Photosystem II subunit O 2	7	1	1.88	1.31	1	0.21	0.16	1	0.37	0.01	PS
59.	Glyma11g06510.1	PS II oxygen evolving complex 1	10	1	2.48	1.65	1	0.21	0.16	1	0.37	0.01	PS
60.	Glyma16g25860.1	Photosystem II subunit O 2	10	1	2.04	1.38	1	0.21	0.16	1	0.37	0.01	PS
61.	Glyma13g19930.1	Ribosomal protein L4/L1 family	14	1	0.58	0.18	1	0.18	0.00	1	0.15	0.00	Protein.synthesis
62.	Glyma14g29145.1	Ribosomal protein L7Ae/l30e/s12e/Gadd45 family protein	3	1	0.72	0.13	1	0.17	0.17	1	0.15	0.00	Protein.synthesis
63.	Glyma13g23400.1	Ribosomal protein S11 beta	4	1	0.30	0.13	1	0.16	0.06	1	0.17	0.00	Protein.synthesis
64.	Glyma17g11430.1	Ribosomal protein S11 beta	4	1	0.30	0.13	1	0.16	0.06	1	0.17	0.00	Protein.synthesis
65.	Glyma10g37840.1	Ribosomal protein L36e family protein	2	1	0.44	0.14	1	0.15	0.15	1	0.20	0.00	Protein.synthesis
66.	Glyma20g29990.3	Ribosomal protein L36e family protein	2	1	0.44	0.14	1	0.15	0.15	1	0.20	0.00	Protein.synthesis
67.	Glyma13g36780.1	Late embryogenesis abundant domain containing protein	7	1	0.07	0.00	1	0.14	0.18	1	0.01	0.00	Not assigned
68.	Glyma10g05580.1	Ribosomal protein L4/L1 family	14	1	0.55	0.14	1	0.14	0.00	1	0.13	0.00	Protein.synthesis
69.	Glyma10g39150.1	Cupin family protein	15	1	0.03	0.00	1	0.14	0.32	1	0.05	0.00	Development.storage proteins
70.	Glyma05g03850.2	Ribosomal protein S13A	6	1	0.70	0.14	1	0.13	0.07	1	0.13	0.00	Protein.synthesis
71.	Glyma17g14370.1	Ribosomal protein S13A	6	1	0.70	0.14	1	0.13	0.07	1	0.13	0.00	Protein.synthesis
72.	Glyma12g33711.1	Late embryogenesis abundant domain containing protein	2	1	0.07	0.01	1	0.13	0.12	1	0.13	0.00	Not assigned
73.	Glyma13g31120.1	Late embryogenesis abundant protein (LEA) family protein	4	1	0.28	0.02	1	0.13	0.01	1	0.08	0.00	Not assigned
74.	Glyma05g26320.1	Ribosomal L27e protein family	5	1	0.50	0.21	1	0.13	0.08	1	0.20	0.00	Protein.synthesis
75.	Glyma09g05720.2	Ribosomal L27e protein family	5	1	0.51	0.23	1	0.12	0.07	1	0.15	0.00	Protein.synthesis

76.	Glyma14g39146.1	Ribosomal L27e protein family	4	1	0.53	0.28	1	0.12	0.07	1	0.15	0.00	Protein.synthesis
77.	Glyma15g17010.1	Ribosomal L27e protein family	5	1	0.49	0.21	1	0.12	0.07	1	0.19	0.00	Protein.synthesis
78.	Glyma11g07020.1	Rmlc like cupins superfamily protein	12	1	0.02	0.00	1	0.12	0.24	1	0.08	0.00	Not assigned
79.	Glyma10g07410.1	Embryonic cell protein 63	10	1	0.46	0.05	1	0.12	0.04	1	0.03	0.00	Development
80.	Glyma13g21291.1	Embryonic cell protein 63	6	1	0.52	0.04	1	0.11	0.06	1	0.13	0.00	Development
81.	Glyma07g02270.1	Ribosomal protein L30/L7 family protein	9	1	0.38	0.11	1	0.10	0.11	1	0.25	0.00	Protein.synthesis
82.	Glyma08g23750.3	Ribosomal protein L30/L7 family protein	9	1	0.37	0.11	1	0.10	0.10	1	0.25	0.00	Protein.synthesis
83.	Glyma06g01310.1	Ribosomal protein S25 family protein	3	1	0.63	0.11	1	0.10	0.01	1	0.03	0.00	Protein.synthesis
84.	Glyma11g12300.1	Ribosomal protein S25 family protein	3	1	0.63	0.10	1	0.10	0.01	1	0.03	0.00	Protein.synthesis
85.	Glyma12g04510.2	Ribosomal protein S25 family protein	3	1	0.63	0.10	1	0.10	0.01	1	0.03	0.00	Protein.synthesis
86.	Glyma11g37160.1	Ribosomal protein l22p/L17e family protein	5	1	0.43	0.15	1	0.09	0.09	1	0.47	0.00	Protein.synthesis
87.	Glyma16g03470.1	Late embryogenesis abundant protein	8	1	0.05	0.01	1	0.09	0.37	1	0.34	0.00	Development
88.	Glyma08g14995.1	Ribosomal protein L6 family protein	7	1	0.69	0.14	1	0.09	0.05	1	0.10	0.00	Protein.synthesis
89.	Glyma13g36400.1	ND	5	1	0.00	0.00	1	0.08	0.19	1	0.09	0.00	Not assigned
90.	Glyma08g09230.1	Ribosomal L27e protein family	5	1	0.50	0.15	1	0.07	0.07	1	0.17	0.00	Protein.synthesis
91.	Glyma01g38340.2	Rmlc like cupins superfamily protein	12	1	0.03	0.00	1	0.07	0.17	1	0.09	0.00	Not assigned
92.	Glyma05g27940.1	Ribosomal protein l22p/L17e family protein	5	1	0.44	0.16	1	0.07	0.07	1	0.45	0.00	Protein.synthesis
93.	Glyma08g10910.1	Ribosomal protein l22p/L17e family protein	5	1	0.44	0.16	1	0.07	0.07	1	0.45	0.00	Protein.synthesis
94.	Glyma16g28550.2	Ribosomal protein l22p/L17e family protein	5	1	0.44	0.16	1	0.07	0.07	1	0.45	0.00	Protein.synthesis
95.	Glyma18g01110.1	Ribosomal protein l22p/L17e family protein	5	1	0.44	0.16	1	0.07	0.07	1	0.45	0.00	Protein.synthesis
96.	Glyma08g16130.1	Ribosomal protein L6 family protein	8	1	0.59	0.10	1	0.07	0.05	1	0.05	0.00	Protein.synthesis
97.	Glyma05g31760.1	Ribosomal protein L6 family protein	6	1	0.61	0.13	1	0.06	0.04	1	0.11	0.00	Protein.synthesis
98.	Glyma08g15000.1	Ribosomal protein L6 family protein	5	1	0.58	0.12	1	0.06	0.04	1	0.10	0.00	Protein.synthesis
99.	Glyma15g42620.1	Ribosomal protein L6 family protein	6	1	0.62	0.14	1	0.05	0.04	1	0.15	0.00	Protein.synthesis
100.	Glyma02g05540.1	Ribosomal protein L2 family	7	1	0.56	0.08	1	0.05	0.14	1	0.15	0.00	Protein.synthesis
101.	Glyma01g37250.1	Ribosomal protein L2 family	6	1	0.59	0.08	1	0.04	0.15	1	0.21	0.00	Protein.synthesis

102. Glyma11g08050.1	Ribosomal protein L2 family	6	1	0.59	0.08	1	0.04	0.15	1	0.21	0.00	Protein.synthesis
103. Glyma11g15870.1	Rmlc like cupins superfamily protein	13	1	0.06	0.00	1	0.04	0.33	1	0.09	0.00	Development.storage proteins
104. Glyma12g03230.1	Ribosomal protein L7Ae/l30e/s12e/Gadd45 family protein	11	1	0.61	0.11	1	0.03	0.04	1	0.16	0.00	Protein.synthesis
105. Glyma02g00540.2	Ribosomal protein L7Ae/l30e/s12e/Gadd45 family protein	11	1	0.59	0.11	1	0.03	0.04	1	0.18	0.00	Protein.synthesis
106. Glyma10g00890.1	Ribosomal protein L7Ae/l30e/s12e/Gadd45 family protein	11	1	0.59	0.11	1	0.03	0.04	1	0.18	0.00	Protein.synthesis
107. Glyma11g11040.1	Ribosomal protein L7Ae/l30e/s12e/Gadd45 family protein	11	1	0.58	0.10	1	0.03	0.04	1	0.18	0.00	Protein.synthesis

Protein ID, according to the Phytozome database; M.P., matched peptide; Ratio, relative abundance of a protein compared to 2-day-old soybean root; *days after sowing (days after treatment); F, flooding; ND, no description.

Table 4. List of differentially abundant proteins in cotyledons of flooded soybean in response to Ag NPs treatment.

				Control			Flooding			Flooding+Ag NPs			
No.	Protein ID	Description	M.P.	Ratio 2(0)*	Ratio 4(0)	Ratio 6(0)	Ratio 2(0)	Ratio 4(2)	Ratio 6(4)	Ratio 2(0)	Ratio 4(2)	Ratio 6(4)	Functional Category
1.	Glyma02g16710.1	Eukaryotic aspartyl protease family protein	3	1	1.57	1.80	1	3.43	3.44	1	1.65	1.39	Protein.degradation
2.	Glyma13g33590.1	Glyoxalase II 3	3	1	2.25	3.79	1	3.16	3.39	1	2.21	2.29	Biodegradation of Xenobiotics
3.	Glyma06g38160.1	Protochlorophyllide oxidoreductase A	13	1	2.36	3.30	1	0.50	0.28	1	0.36	0.32	Tetrapyrrole synthesis.
4.	Glyma07g05580.3	UDP Glycosyltransferase superfamily protein	6	1	1.46	2.37	1	0.18	0.17	1	0.21	0.10	Major CHO metabolism
5.	Glyma16g02110.3	UDP Glycosyltransferase superfamily protein	6	1	1.46	2.37	1	0.18	0.17	1	0.21	0.10	Major CHO metabolism
6.	Glyma10g31540.3	UDP Glycosyltransferase superfamily protein	5	1	2.01	2.97	1	0.15	0.16	1	0.20	0.10	Major CHO metabolism
7.	Glyma20g36040.1	UDP Glycosyltransferase superfamily protein	4	1	1.91	2.95	1	0.15	0.16	1	0.20	0.10	Major CHO metabolism
8.	Glyma08g40800.1	Voltage dependent anion channel 1	6	1	1.26	1.64	1	0.10	0.58	1	0.24	0.12	Transport.porins
9.	Glyma03g32030.1	RmlC like cupins superfamily protein	26	1	0.93	0.00	1	0.02	0.00	1	1.13	0.00	Development

Protein ID, according to the Phytozome database; M.P., matched peptide; Ratio, relative abundance of a protein compared to 2-day-old soybean root; *days after sowing (days after treatment); F, flooding; ND, no description.

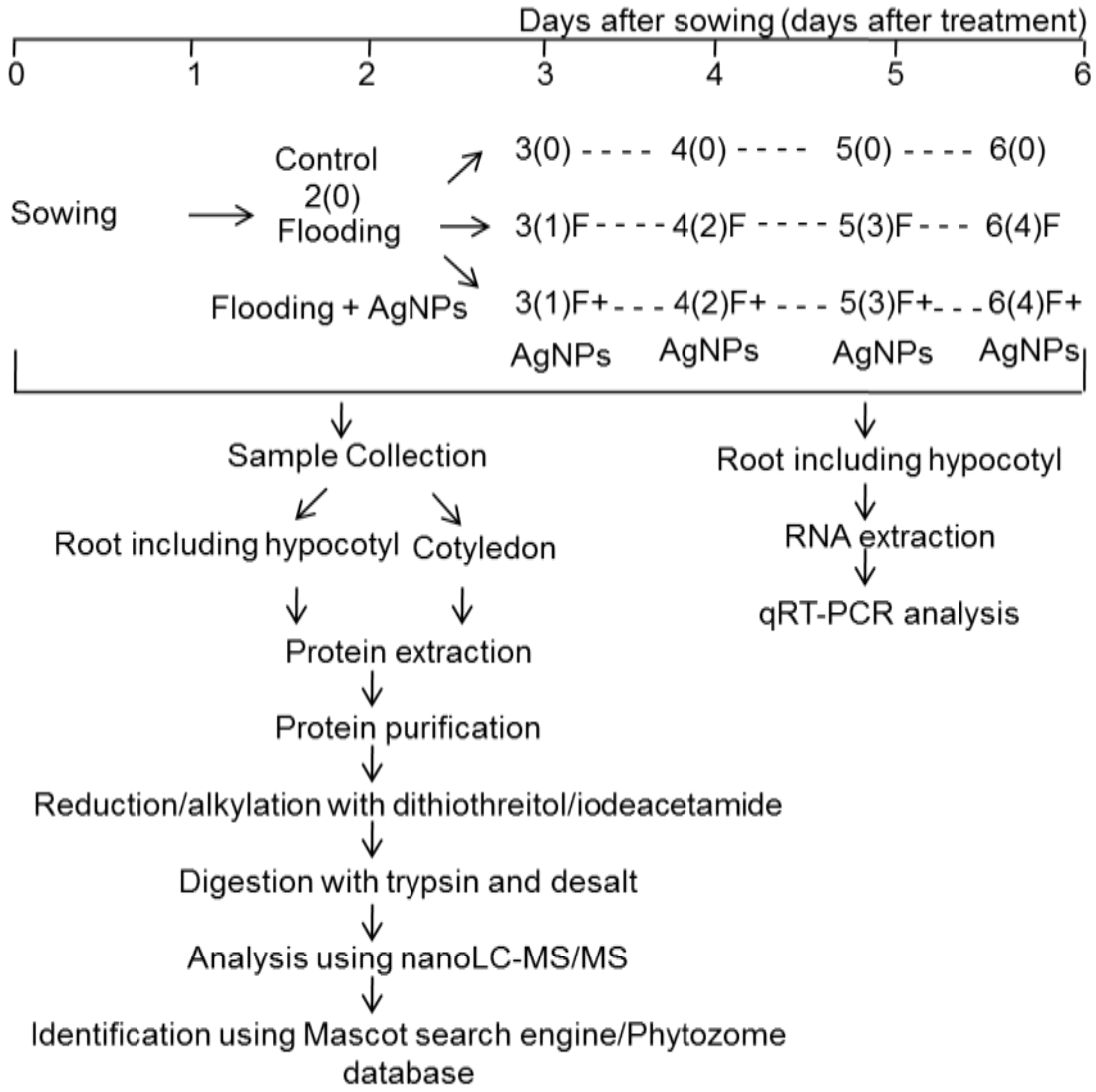

Figure 10. Experimental design to examine the effects of Ag NPs on soybean under flooding stress. Two-day-old soybeans were flooded without (F) or with (F+Ag NPs) Ag NPs for 1, 2, 3, and 4 days. Untreated plants served as controls. For proteomic analysis, proteins extracted from root including hypocotyl and cotyledons were analyzed using nanoLC-MS/MS. For transcriptional analysis, RNA was extracted from the root including hypocotyl and analyzed using qRT-PCR.

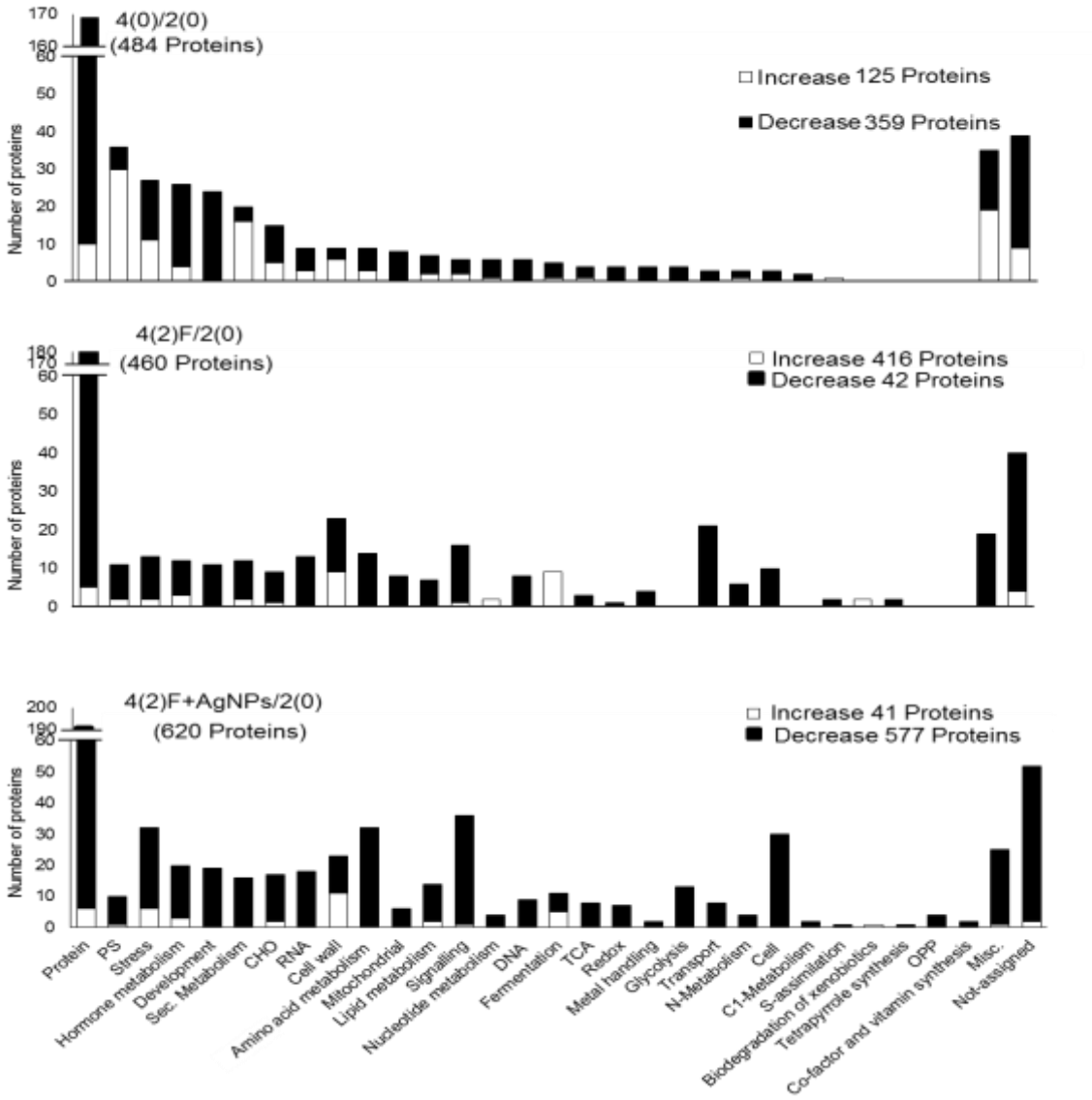

Figure 11. Functional categorization of the root proteins identified in soybean treated with Ag NPs. Two-day-old soybeans were flooded for 2 days without (F) or with (F+Ag NPs) Ag NPs treatment. Proteins were identified using a gel-free proteomic technique. MapMan bin codes were used to predict the functional categorization of the identified proteins. The *y*-axis indicates the number of identified proteins. Open and filled bars indicate increased and decreased proteins, respectively, in soybean roots under flooding stress with and without Ag NPs treatment. Abbreviations: Protein, protein synthesis/degradation/post-translational modification/targeting; PS, photosynthesis; Sec. metabolism, secondary metabolism; CHO, carbohydrate metabolism; RNA, RNA processing/transcription/binding; DNA, DNA synthesis; TCA, tricarboxylic acid cycle; N-Metabolism, nitrogen metabolism; C1-metabolism, carbon 1-metabolism; S-assimilation, sulfur assimilation; OPP, oxidative pentose pathway; and Misc., miscellaneous.

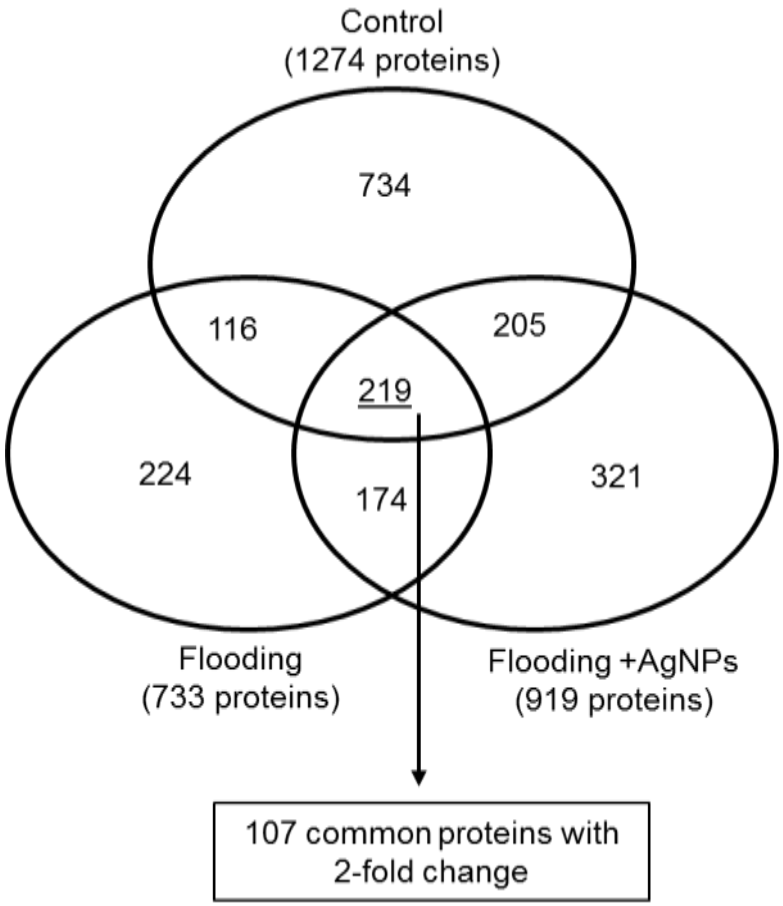

Figure 12. The Venn diagram represents the comparison of proteins identified among the control, flooding, and flooding with Ag NPs in soybean root including hypocotyl. The identified proteins for control, flooding, and flooding with Ag NPs were 1274, 733, and 919, respectively. Two-hundred and nineteen proteins were commonly identified among these three treatments.

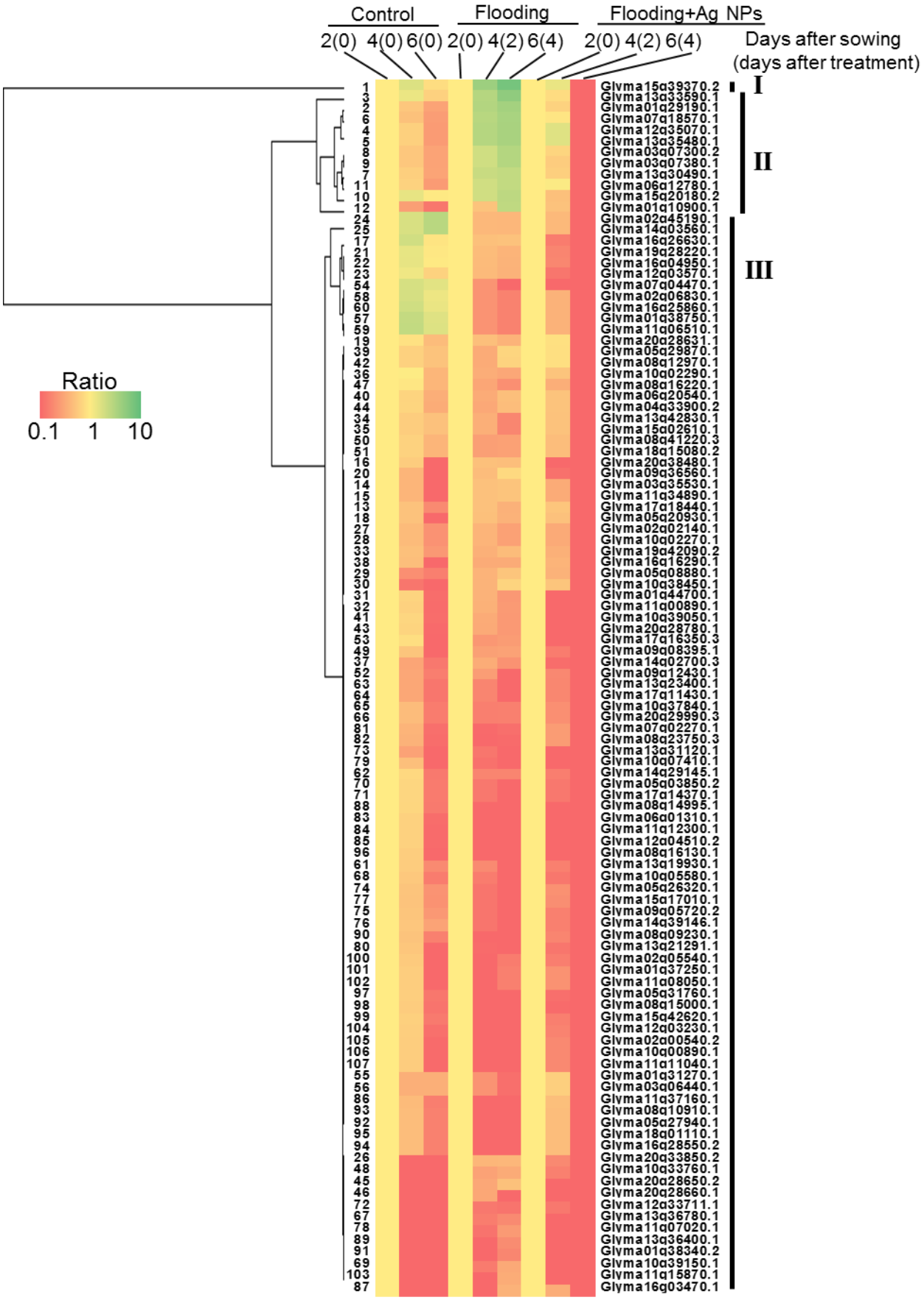
Control
Flooding
Flooding+Ag NPs
2(0) 4(0) 6(0) 2(0) 4(2) 6(4) 2(0) 4(2) 6(4)
Days after sowing
(days after treatment)
Ratio
0.1 1 10
I
II
III
1 Glyma15g39370.2
3 Glyma13g33590.1
2 Glyma01g29190.1
6 Glyma07g18570.1
4 Glyma12g35070.1
5 Glyma13g35480.1
8 Glyma03g07300.2
9 Glyma03g07380.1
7 Glyma13g30490.1
11 Glyma06g12780.1
10 Glyma15g20180.2
12 Glyma01g10900.1
24 Glyma02g45190.1
25 Glyma14g03560.1
17 Glyma16g26630.1
21 Glyma19g28220.1
22 Glyma16g04950.1
23 Glyma12g03570.1
54 Glyma07g04470.1
58 Glyma02g06830.1
60 Glyma16g25860.1
57 Glyma01g38750.1
59 Glyma11g06510.1
19 Glyma20g28631.1
39 Glyma05g29870.1
42 Glyma08g12970.1
36 Glyma10g02290.1
47 Glyma08g16220.1
40 Glyma06g20540.1
44 Glyma04g33900.2
34 Glyma13g42830.1
35 Glyma15g02610.1
50 Glyma08g41220.3
51 Glyma18g15080.2
16 Glyma20g38480.1
20 Glyma09g36560.1
14 Glyma03g35530.1
15 Glyma11g34890.1
13 Glyma17g18440.1
18 Glyma05g20930.1
27 Glyma02g02140.1
28 Glyma10g02270.1
33 Glyma19g42090.2
38 Glyma16g16290.1
29 Glyma05g08880.1
30 Glyma10g38450.1
31 Glyma01g44700.1
32 Glyma11g00890.1
41 Glyma10g39050.1
43 Glyma20g28780.1
53 Glyma17g16350.3
49 Glyma09g08395.1
37 Glyma14g02700.3
52 Glyma09g12430.1
63 Glyma13g23400.1
64 Glyma17g11430.1
65 Glyma10g37840.1
66 Glyma20g29990.3
81 Glyma07g02270.1
82 Glyma08g23750.3
73 Glyma13g31120.1
79 Glyma10g07410.1
62 Glyma14g29145.1
70 Glyma05g03850.2
71 Glyma17g14370.1
88 Glyma08g14995.1
83 Glyma06g01310.1
84 Glyma11g12300.1
85 Glyma12g04510.2
96 Glyma08g16130.1
61 Glyma13g19930.1
68 Glyma10g05580.1
74 Glyma05g26320.1
77 Glyma15g17010.1
75 Glyma09g05720.2
76 Glyma14g39146.1
90 Glyma08g09230.1
80 Glyma13g21291.1
100 Glyma02g05540.1
101 Glyma01g37250.1
102 Glyma11g08050.1
97 Glyma05g31760.1
98 Glyma08g15000.1
99 Glyma15g42620.1
104 Glyma12g03230.1
105 Glyma02g00540.2
106 Glyma10g00890.1
107 Glyma11g11040.1
55 Glyma01g31270.1
56 Glyma03g06440.1
86 Glyma11g37160.1
93 Glyma08g10910.1
92 Glyma05g27940.1
95 Glyma18g01110.1
94 Glyma16g28550.2
26 Glyma20g33850.2
48 Glyma10g33760.1
45 Glyma20g28650.2
46 Glyma20g28660.1
72 Glyma12g33711.1
67 Glyma13g36780.1
78 Glyma11g07020.1
89 Glyma13g36400.1
91 Glyma01g38340.2
69 Glyma10g39150.1
103 Glyma11g15870.1
87 Glyma16g03470.1

Figure 13. Cluster analysis of changed proteins in soybean treated with Ag NPs. Significant clusters are indicated by black bars to the right of the protein IDs. Abundance patterns of individual proteins are indicated based on the color legend for control and flooding-stress without and with Ag NPs samples at 0, 2, and 4 days (from left to right). Red indicates decreased protein abundances, green indicates increased protein abundances, and yellow means no change. The temporal abundance profiles of the 107 differentially changed proteins were used to group the proteins into 3 clusters. Protein IDs are indicated to the right of the abundance profile and the number to the left corresponds to the protein number in Table 3.

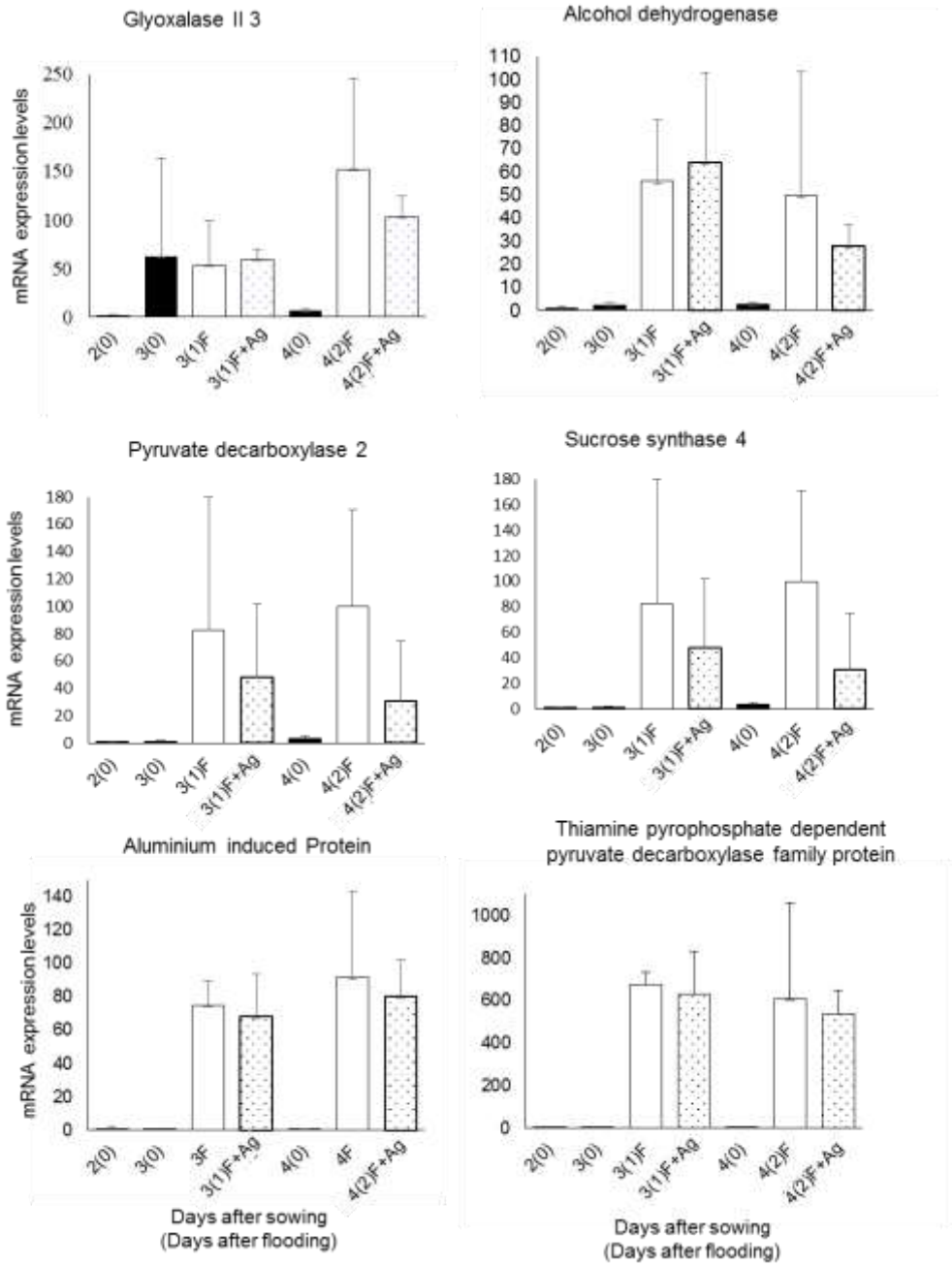

Figure 14. Effects of Ag NPs on the mRNA expression levels of selected proteins identified in the gel-free proteomic analysis. Two-day-old soybeans were flooded for 1 and 2 days without (white column) and with (dotted column) 2 ppm of 15 nm Ag NPs. Untreated plants served as controls (black columns). RNAs extracted from the root including hypocotyl of soybeans were analyzed by qRT-PCR. Relative mRNA abundances of *glyoxalase II 3* (Glyma15g39370.2), *alcohol dehydrogenase 1* (Glyma06g12780.1), *pyruvate decarboxylase 2* (Glyma13g30490.1), *sucrose synthase 4* (Glyma15g20180.2), *aluminum-induced protein with YGL and LRDR motifs* (Glyma12g35070.1), and *thiamine pyrophosphate-dependent pyruvate decarboxylase family protein* (Glyma01g29190.1) were normalized against 18S rRNA abundance. The data are presented as the mean ± S.D. from three independent biological replicates (n=3).

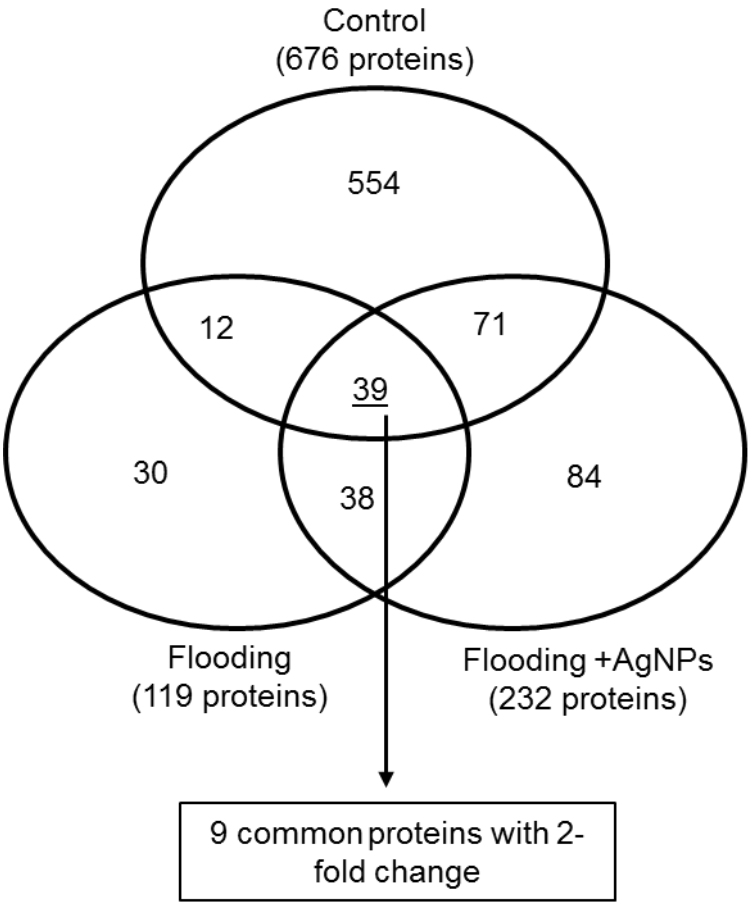

Figure 15. The Venn diagram represents the comparison of proteins identified among the control, flooding, and flooding with Ag NPs in soybean cotyledons. The identified proteins for control, flooding, and flooding with Ag NPs were 676, 119, and 232, respectively. Thirty-nine proteins were commonly identified among these three treatments.

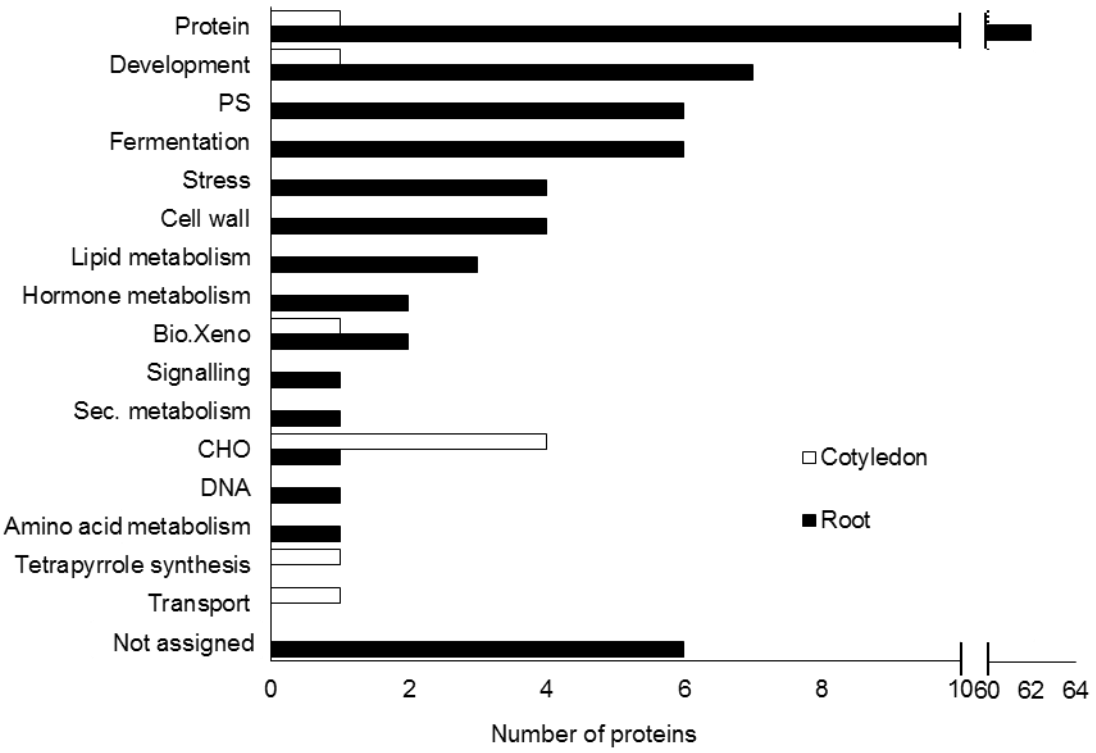

Figure 16. Functional categorization of the proteins identified in soybean root including hypocotyl and cotyledons treated with Ag NPs. Two-day-old soybeans were flooded without or with Ag NPs for 2 and 4 days, and changed proteins were identified using a gel-free proteomic technique. MapMan bin codes were used to predict the functional categorization of the identified proteins. The *x*-axis indicates the number of identified proteins. Open and filled bars indicate cotyledon and root proteins, respectively, in soybean under flooding stress with or without Ag NPs treatment. Abbreviations are the same as in Figure 11.

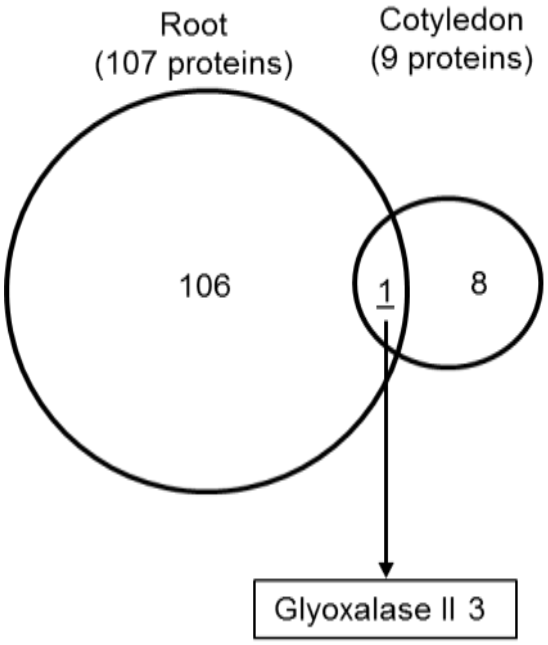

Figure 17. The Venn diagram represents the comparison of the commonly identified proteins from the root including hypocotyl and cotyledons under the Ag NPs treatement compared to the flooding and untreated soybean. One protein, glyoxalase II 3 was commonly identified among the two organs.

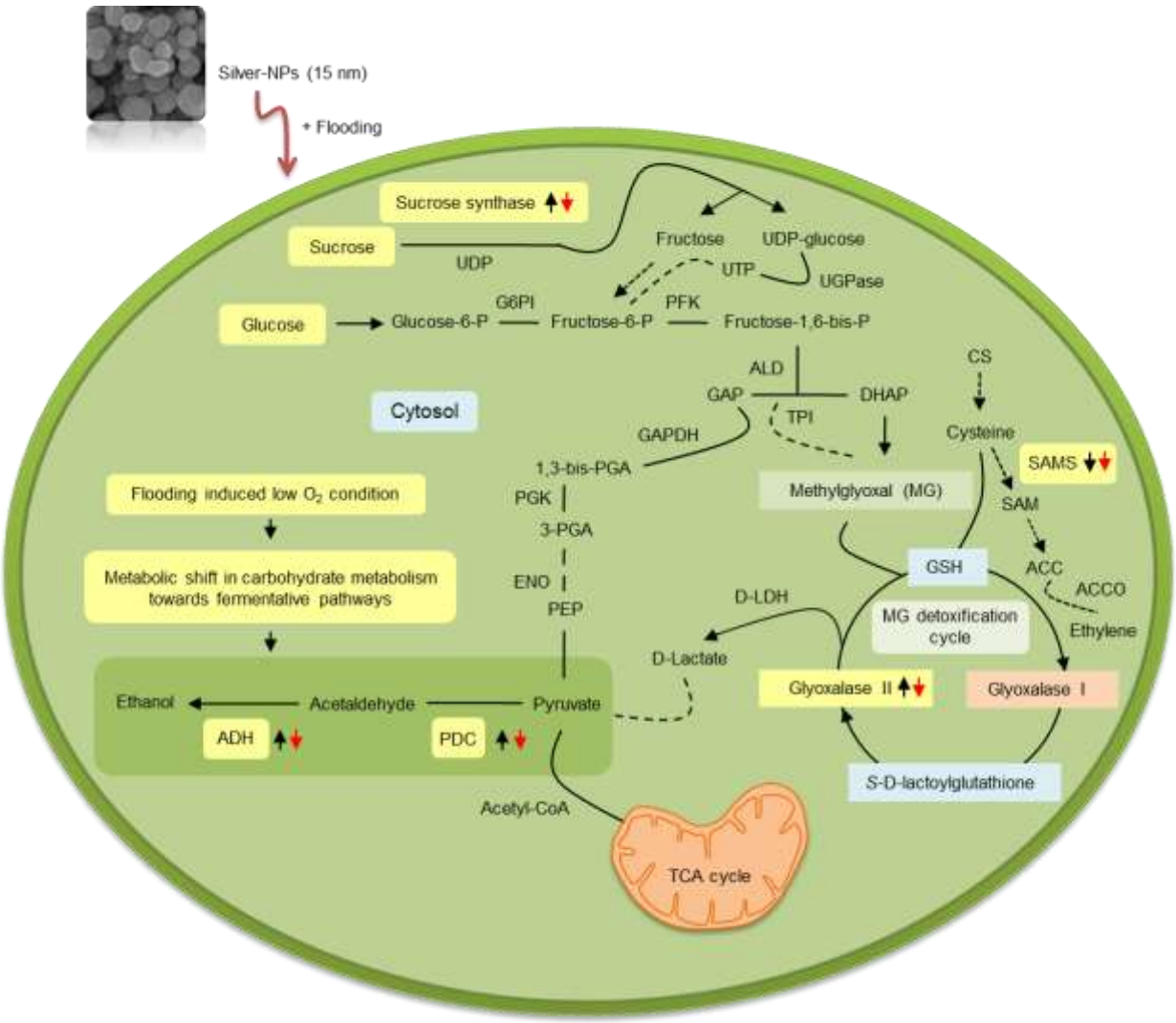

Figure 18. Ag NPs mediated changes in metabolic pathways under flooding stress. Black and red arrows indicate changes in protein abundance (upward arrows indicate increase and downward arrows indicate decrease) in response to flooding and Ag NPs, respectively. Proteomic analysis indicates that metabolic shift from fermentative pathways towards normal cellular processes as well as formation of comparatively low cytotoxic by-products (MG:methylglyoxal) might be the key factors for better growth performance of Ag NPs treated soybeans under flooding stress. Abbreviations: ACC, 1-aminocyclopropane-1-carboxylic acid; ACCO, ACC oxidase; ADH; alcohol dehydrogenase; CS, cysteine synthase; PDC, pyruvate decarboxylase; DHAP; dihydroxyacetone phosphate; SAM, *S*-adenosylmethionine; SAMS, SAM synthetase; ENO, enolase; UDP, uridine di-phosphate; UGPase , UDP-glucose pyrophosphorylase.

CHAPTER 3
CHARACTERIZATION OF SOYBEAN PROTEINS AFFECTED BY ALUMINUM OXIDE NANOPARTICLES UNDER FLOODING STRESS

3.1. Introduction

Aluminum is the most abundant metal in the earth surface. It is not essential for the crop growth and development. However, Al toxicity is one of the major limiting factor for crop growth in acidic soils with pH less than five (von Uexkull and Mutert, 1995). Aluminum toxicity is caused by the Al ions that is formed from the aluminosilicates. Aluminum ions are extremely toxic to plants at high concentration (Kochian et al., 2004). Physiological studies indicated that the plants follow two strategies while acquiring the Al tolerance. That is either by blocking the Al ions uptake or detoxifying the cellular Al by the formation of harmless complexes with organic ligands and then sequestering them to specific organelles (Ma, 2000; Ma and Furukawa, 2003). Toxic levels of Al inhibits the plant growth and caused yield reductions of Al-sensitive crops (Valle et al., 2009). Aluminum disrupt the cellular components and processes by binding with the phosphate, sulfate, and carbonyl functional groups (Poschenrieder et al., 2008).

Al_2O_3 NPs were reported to cause positive effects on the root elongation of radish, rape, ryegrass, and lettuce (Lin and Xing, 2007), but the root elongation of corn, cucumber, soybean, cabbage, and carrot was impaired by exposure to Al_2O_3 NPs (Yang and Watts, 2005). Al_2O_3 NPs altered the miRNA expression levels which play important role in mediating the stress response in the tobacco (Burklew et al., 2012). In wheat, the antioxidant enzymes activity that reduced the amount of free radiclas in root compensate the harmful effects of Al_2O_3 NPs (Riahi-Madvar et al., 2012). In the BY-2 plant cell suspension, Al_2O_3 NPs were responsible for the loss of mitochondrial activity, enhancement of caspase-like activity, and the fragmentation of DNA. These all factors point towards the execution of programmed cell death due to Al_2O_3 NPs (Poborilova et al., 2013). The molecular mechanisms affected by Al_2O_3 NPs on higher plants is still not clear.

Because of the possible interaction of the Al_2O_3 NPs with the plants and variable growth effects on the soybean under flooding stress, the molecular mechanisms affected by these NPs need to be investigated. Based on the results of Chapter 1, among the different sizes of Al_2O_3 NPs the 30-60 nm was more suitable in promoting the soybean growth under flooding stress. Furthermore, the 50 ppm of 30-60 nm Al_2O_3 NPs was

beneficial for the soybean growth compared to the other concentrations. This concentration and size of Al_2O_3 NPs was used for this proteomic experiment. In addition, bioinformatic and mRNA expression analyses were used to confirm the proteomic results.

3.2. Materials and Methods

3.2.1. Plant material and treatments

Soybean was used as the plant material in this study. Plant growth conditions are described in 1.2.1 in Chapter 1. To study the effects of Al_2O_3 NPs on the protein abundance and mRNA expression analyses, 2-day-old soybeans were flooded without or with 50 ppm Al_2O_3 NPs for 1, 2, and 3 days (Figure 19). After treatments, root including hypocotyl was collected.

3.2.2. Protein extraction, purification, and digestion

Protein extraction, purification, and digestion is described in 2.2.2 in Chapter 2. For protein digestion, lysyl endopeptidase was used along with the trypsin at 1:100 enzyme/protein concentration. The resulting tryptic peptides were acidified with 10 µL of 20% formic acid and analyzed by nanoLC MS/MS.

3.2.3. Mass spectrometry analysis

Mass spectrometry analysis is described in 2.2.3 in Chapter 2. The mass spectrometry proteomic data have been deposited with the ProteomeXchange Consortium (http://proteomecentral.proteomexchange.org) via the PRIDE partner repository (Vizcaíno et al., 2013) with the data set identifier: PXD002005.

3.2.4. Protein identification of acquired mass spectrometry data

Protein identifications of acquired mass spectrometry data is described in 2.2.4 in Chapter 2.

3.2.5. Differential analysis of the identified proteins

Differential analysis of the identified proteins is described in 2.2.5 in Chapter 2.

3.2.6. Bioinformatic analysis with MapMan software

To determine the functional role of the proteins identified in the MS analysis, functional categorization was performed using MapMan bin codes (Usadel et al., 2005). Visualization of protein abundance ratio was performed using MapMan software (Usadel et al., 2005, 2009). The software and mapping files (Gmax_109_peptide) were downloaded from the MapMan website (http://mapman.gabipd.org/web/guest). Log_2FC values with GmID were subjected to the MapMan software. The functional categories were based on MapMan bin codes.

3.2.7. Functional analysis of identified proteins

Functional analysis of identified proteins is described in 2.2.6 in Chapter 2.

3.2.8. Cluster analysis of protein abundance

Cluster analysis of protein abundance is described in 2.2.7 in Chapter 2.

3.2.9. *In-silico* protein-protein interaction

Interacting proteins were identified by comparisons of changes in abundance ratios over time. Clustered proteins were analyzed for *in silico* protein-protein interactions that were estimated by temporal expression profiling utilizing an *S*-system differential equation (Voit, 2000), as a mathematical model. Each interaction between proteins was tested based on a goodness-of-fit which indicates how well the *S*-system differential equation simulated the expression of the corresponding target protein. The interactions showing r^2 value (coefficient of determination) >0.98 were considered as candidate interactions. In the model protein interaction diagram, a red arrow indicates an inductive interaction and corresponds to $gij > 0$ in the *S*-system differential equation, and a T-bar indicates a suppressive interaction and corresponds to $gij < 0$ in the *S*-system differential equation (Tanaka et al., 2005).

3.2.10. RNA extraction and quantitative reverse transcription polymerase chain reaction analysis

RNA extraction and quantitative reverse transcription polymerase chain reaction analysis is described in 2.2.8 in Chapter 2. The primers used are listed in Supplemental Table 1.

3.2.11. Statistical analysis

Statistical analysis is described in 1.2.2 in Chapter 1.

3.3. Results

3.3.1. Functional analysis of soybean proteins identified during temporal exposure to Al_2O_3 NPs

To examine the effects of Al_2O_3 NPs on soybean under flooding stress, gel-free proteomic analysis was used. Proteins were extracted from the root including hypocotyl of 2-day-old soybeans flooded with or without 50 ppm Al_2O_3 NPs for 1, 2, and 3 days, and were then analyzed using a gel-free proteomic technique. In the differential analysis of proteins in the root including hypocotyl, the abundances of 586 proteins were significantly changed in 2-, 3-, 4-, and 5-day-old soybeans under control conditions (Figure 20). In response to flooding stress for 1, 2, and 3 days, the abundances of 782 proteins in soybean root were significantly changed (Figure 20). In flooding-stressed soybean exposed to Al_2O_3 NPs, the abundances of 453 proteins were significantly changed in the root including hypocotyl after 1, 2, and 3 days of stress exposure (Figure 20). To identify the commonly and specifically changed proteins in the control, flooding-stressed, and flooding-stressed soybean exposed to Al_2O_3 NPs, a Venn diagram was generated (Figure 20). In the Venn diagram, the abundances of 172 proteins were commonly changed among the soybean plants treated under the three different conditions. The analysis also revealed that the abundances of 235, 350, and 92 proteins were specifically changed in the control, flooding-stressed, and flooding-stressed plants exposed to Al_2O_3 NPs, respectively (Figure 20).

To determine the functional role of the identified proteins, functional categorization was performed using MapMan bin codes (Figure 21). The ‘protein’ category, which contained the highest proportion of identified proteins, included proteins related to protein synthesis, degradation, post-translational modification, folding, and targeting.

Under control conditions, proteins related to protein (13.14%), cell (9.04%), and stress (7.34%) were predominantly changed. In response to flooding stress, the highest proportions of differentially changed proteins were found in the protein (24.68%), cell (9.59%), and amino acid metabolism (6.39%) functional categories. In plants exposed to flooding with Al_2O_3 NPs, the changed proteins were predominantly associated with protein (22.52%), cell (10.60%), and glycolysis (6.40%) (Figure 21).

To examine the changing levels of the identified proteins in greater detail under control, flooding, and flooding condition with Al_2O_3 NPs, the identified proteins that significantly changed in soybean exposed to 1 day of stress were analyzed using MapMan software. The analysis identified the main functional categories of the significantly changed proteins: fermentation, glycolysis, and the tricarboxylic acid cycle (Figure 22). Under control condition, the proteins related to fermentation and glycolysis remained stable; however, under flooding condition, the proteins related to these two functional categories were clearly increased, but were similar to control levels in flooding-stressed plants exposed to Al_2O_3 NPs (Figure 22). Proteins related to amino acid and nucleotide metabolisms were also increased under flooding condition, but did not markedly differ between control and flooding-stressed soybean treated with Al_2O_3 NPs. However, the number of cell wall-related proteins was increased under flooding-stress conditions with and without Al_2O_3 NPs compared to control conditions (Figure 22).

3.3.2. Cluster and *in silico* protein-protein interaction analyses of commonly identified proteins during temporal exposure to Al_2O_3 NPs

To further analyze the abundance profiles of the changed proteins, which were commonly identified in soybean root including hypocotyl under flooding stress without and with Al_2O_3 NPs, hierarchical clustering and *in silico* protein-protein interaction analyses were performed. The abundance of 172 proteins were commonly changed among the control, flooding, and flooding with Al_2O_3 NPs (Figure 20). Out of these 172 commonly changed proteins, 128 significantly changed proteins were selected based on their unique description property (Table 5). These 128 significantly changed proteins were subjected to hierarchical clustering and *in silico* protein-protein interaction

analyses using their abundance ratios.

Using a hierarchical clustering approach, 4 clusters (I-IV) of significantly changed proteins were recognized (Figure 23). Cluster I consisted of a single protein, lipoxygenase 1. The abundance of lipoxygenase 1 was increased under control, flooding stress, and flooding stress conditions with Al_2O_3 NPs; however, the fold increase of lipoxygenase 1 was lower in response to flooding stress and treatment with Al_2O_3 NPs as compared to the control and flooding conditions. Cluster II also consisted of only one protein, HAD superfamily subfamily IIIB acid phosphatase, the abundance of which was increased under all three treatments. Similar to lipoxygenase 1, the increase in HAD superfamily subfamily IIIB acid phosphatase was least evident in flooding-stressed soybean exposed to Al_2O_3 NPs. Cluster III was comprised of 5 proteins that were decreased under control conditions, but were increased in response to flooding stress with and without Al_2O_3 NPs. Cluster IV consisted of 121 proteins that exhibited variable responses in control plants and flooding-stressed soybean treated with and without Al_2O_3 NPs (Figure 23). Within cluster IV, two sub-clusters, designated 'a' and 'b', were also identified. Cluster 'IV-a' contained 13 proteins that exhibited a decreased abundance in control soybeans; however, in response to flooding stress, the proteins increased in abundance after 1 day of stress, and then decreased with continued stress conditions. In contrast, the 13 proteins had decreased levels in flooding-stressed soybeans exposed to Al_2O_3 NPs throughout the treatment period. Cluster 'IV-b' consisted of 9 proteins that were decreased under control conditions, but were increased at each measurement point in response to flooding stress with and without Al_2O_3 NPs (Figure 23).

In silico protein-protein interactions in control and flooding-stressed soybeans with and without Al_2O_3 NPs were estimated based on temporal abundance patterns that were constructed utilizing the *S*-system differential equation as a mathematical model (Figure 24). Under control conditions, a well-coordinated network of protein interactions was formed. In contrast, under flooding conditions, 29 proteins were isolated from the protein-protein interaction network. In soybean exposed to flooding with Al_2O_3 NPs, a similar well-coordinated network of interacting proteins as observed in control soybeans was observed. Under control conditions, the most interactive protein was

glyceraldehyde-3-phosphate dehydrogenase C subunit 1 (protein no. 91), which displayed both inductive and repressive interactions. Under flooding conditions, the most interactive protein was tripeptidyl peptidase II (protein no. 78), which also exhibited both inductive and repressive interactions. In response to flooding stress with Al_2O_3 NPs, the most interactive protein in soybean root was poly (A)-binding protein 2 (protein no. 80), which also interacted both inductively and repressively interactions (Figure 24).

3.3.3. Functional analysis of Al_2O_3 NPs-responsive proteins

To better understand the temporal effects of Al_2O_3 NPs on proteins in soybean root including hypocotyl under flooding stress, Al_2O_3 NPs-responsive proteins were analyzed (Figure 20). In the differential analysis, the abundances of 92 proteins were specifically and significantly changed after 2, 3, 4, and 5 days in soybean root including hypocotyl treated with Al_2O_3 NPs (Table 6). To determine the functional role of these proteins in soybean stress responses, functional categorization was performed using MapMan bin codes. The functional categorization analysis predicted that the proteins predominantly affected by Al_2O_3 nanoparticle treatment were related to protein (35 proteins), glycolysis (6 proteins), and lipid metabolism (5 proteins) (Figure 25). Further sub-categorization within the 'protein' category revealed that the majority of proteins were related to protein synthesis (16 proteins), degradation (10 proteins), and post-translational modification (5 proteins) (Figure 25).

3.3.4. mRNA expression analysis of Al_2O_3 NPs-responsive proteins

From the above-described proteomic results, specifically responsive proteins that displayed a 5-fold change in the abundance ratio in response to Al_2O_3 NPs (Table 6) were selected for mRNA expression analysis. Two-day-old soybeans were flooded with or without Al_2O_3 NPs. mRNA was extracted from the root including hypocotyl and was analyzed using qRT-PCR. qRT-PCR products were analyzed by agarose gel electrophoresis and the sizes were equal to the expected product sizes. The mRNA expression levels of *NmrA-like negative transcriptional regulator family protein* (Glyma11g07490.1), *MLP-like protein 43* (Glyma08g24720.1), *flavodoxin-like quinone*

reductase 1 (Glyma08g06570.1), and *protein of unknown function DUF2359 transmembrane* (Glyma05g27090.1) were analyzed (Figure 26).

The mRNA expression level of *NmrA-like negative transcriptional regulator family protein* was slightly, but significantly, up-regulated under control conditions and remained relatively constant throughout the experimental period. However, the mRNA level of this gene was up-regulated more than 40-fold in soybean root including hypocotyl after one day of flooding-stress treatment in the presence of Al_2O_3 NPs. Under flooding stress, *NmrA-like negative transcriptional regulator family protein* was also significantly up-regulated after one day of stress treatment compared to control condition, but did not reach the level of that observed in Al_2O_3 NPs treated soybean. In both flooding stressed and Al_2O_3 NPs treated soybeans, this gene exhibited a similar pattern of decreasing expression over time (Figure 26). The mRNA expression level of *MLP-like protein 43* was up-regulated under control condition, but little or no change in the mRNA level of this gene was observed in flooding-stressed soybean treated additionally with and without Al_2O_3 NPs (Figure 26). *Flavodoxin-like quinone reductase 1* was significantly up-regulated in soybean root including hypocotyl compared to the control condition after 2 and 3 days of flooding stress with and without Al_2O_3 NPs. Under flooding stress condition with or without Al_2O_3 NPs, expression of the *flavodoxin-like quinone reductase 1* gene was initially up-regulated after one day of stress, but was down-regulated during the later stages of stress exposure (Figure 26). *Protein of unknown function DUF2359 transmembrane* was significantly up-regulated under control conditions at 5 days, but was down-regulated under flooding conditions with or without added Al_2O_3 NPs (Figure 26).

3.4. Discussion

3.4.1. Effects of Al_2O_3 NPs on energy metabolism- and glycolysis-related proteins in soybean root including hypocotyl

In soybean, ZnO and cerium oxide NPs impart differential effects on plant growth, but do not affect seed germination (Lopez-Moreno et al., 2010). In contrast, Al_2O_3 NPs at higher concentrations inhibit root growth in corn, cucumber, soybean, cabbage, and carrot (Yang and Watts, 2005). However, Lin and Xing (2007) reported that Al_2O_3 NPs

did not have toxic effects on the root elongation of radish, rape, ryegrass, lettuce, and cucumber, but did inhibit root elongation in corn. In the present study, moderate exposure to Al_2O_3 NPs had enhancing effects on soybean growth under flooding stress. However, lower (5 ppm) and higher (500 ppm) concentrations of Al_2O_3 did not positively affect soybean growth under flooding stress. Because the treatment with 50 ppm Al_2O_3 NPs enhanced soybean growth under flooding stress conditions, this concentration was used for the proteomic analysis.

Flooding stress is a major constraint for soybean growth that leads to reduced gaseous exchange (Fukao and Bailey-Serres, 2004). In addition, plants experience a reduced supply of oxygen, which leads to the rapid reduction of cellular ATP (Gibbs and Greenway, 2003). To overcome this decreased energy production, plants tend to shift from aerobic to anaerobic metabolism in response to flooding stress (Pedrazzini and Mckee, 1984). Sairam et al. (2009) reported that glycolysis may be an important mechanism in waterlogging tolerance in mung bean. In addition, low-oxygen conditions induce the synthesis of anaerobic proteins that are involved in sugar metabolism, glycolysis, and fermentation in rice (Huang et al., 2005).

Previous proteomic analyses of soybean under flooding stress revealed that proteins related to glycolysis are increased in abundance (Komatsu et al., 2013a; Komatsu et al., 2011a). In the present study, 3 glyceraldehyde-3-phosphate dehydrogenases were identified in the cluster and *in silico* protein-protein interaction analyses. In the predicted protein-protein interaction networks, glyceraldehyde-3-phosphate dehydrogenase, which is a ubiquitous enzyme involved in glycolysis, was the most interactive protein under control conditions, but was isolated in roots exposed to flooding stress. In flooding-stress soybean treated with Al_2O_3 NPs, glyceraldehyde-3-phosphate dehydrogenase was also detected in the protein interaction network. The increased accumulation of glyceraldehyde-3-phosphate dehydrogenase has also been reported in soybean root under flooding stress (Nanjo et al., 2010). In this study, the abundance of this protein was increased under flooding stress compared to the control condition, but was reduced by the exposure of flooding-stressed plants to Al_2O_3 NPs. This reduction in glyceraldehyde-3-phosphate dehydrogenase levels induced by Al_2O_3 NPs may lead to a metabolic shift towards aerobic pathways.

Several previous studies in soybean have revealed that proteins related to fermentation, scavenging, and glycolysis are affected by flooding stress (Nanjo et al., 2012; Hashiguchi et al., 2009), which limits the available oxygen supply (Colmer, 2003). Low oxygen conditions limit ATP generation and shift plant metabolism from oxidative pathways, such as carbohydrate metabolism, towards anaerobic pathways (Bailey-Serres and Voesenek, 2008). Komatsu et al. (2013a) reported the activation of a fermentative pathway in the early stage of flooding stress as a stress tolerance mechanism in soybean. As an acclimation response to reduced oxygen conditions, plants induce the activation of anaerobic pathways that generate ATP through glycolysis and regenerate NAD^+ through ethanol fermentation (Bailey-Serres and Voesenek, 2008). In the present study, several fermentation- and glycolysis-related proteins were decreased in flooding-stressed soybean treated with Al_2O_3 NPs compared to the levels found in plants exposed to flooding stress alone. Taken together, these results suggest that Al_2O_3 NPs may play a role in shifting plant metabolism towards pathways that operate under normal growth conditions.

3.4.2. Role of Al_2O_3 NPs towards the soybean response under flooding stress

NPs were reported to have both positive and negative effects on plant growth and development (Lin and Xing, 2007). To better understand how Al_2O_3 NPs influence soybean growth, the mRNA expression levels of several Al_2O_3 NPs-responsive proteins were analyzed. NmrA-like negative transcriptional regulator family protein is involved in the post-translational modification of the GATA-type transcription factor AreA (Stammers et al., 2001). In *Aspergillus nidulans*, NmrA interacts with AreA and control the regulation of the genes involved in nitrogen metabolism repression (Andrianopoulos et al., 1998). NmrA contains an NAD^+-binding domain that is essential for protein function (Stammers et al., 2001). Lamb et al. (2003) reported that NmrA is involved in redox-sensitive signal transduction pathways because it binds to the dinucleotides NAD^+ and $NADP^+$, but not to their reduced forms. As an acclimation response to flooding stress, plants activate anaerobic pathways that generate ATP through glycolysis and regenerate NAD^+ via ethanol fermentation by selectively synthesizing flooding marker proteins involved in sucrose breakdown, glycolysis, and fermentation (Bailey-

Serres and Voesenek, 2008). In the present study, *NmrA* was up-regulated in flooding-stressed soybean exposed to Al_2O_3 NPs. Consistent with this finding, the protein abundance ratio of NmrA was increased in response to flooding and treatment with Al_2O_3 NPs. These results suggest that Al_2O_3 NPs may be involved in ameliorating the effects of stress by regulating the levels of NmrA, which is involved in signal transduction pathways.

Major latex proteins (MLPs) were first identified in the latex of *Papaver somniferum* (Nessler et al., 1985) and were later found in many plant species, including soybean (Strömvik et al., 1999). MLPs are grouped in the pathogenesis-related Bet v1 family, along with other subfamilies (Radauer et al., 2008). Bet v1 family proteins and MLPs are involved in responses to biotic and abiotic stresses (Hashimoto et al., 2004; Ruperti et al., 2002). In *Gossypium hirsutum*, the *MLP* gene was cloned and its expression was induced in cotton root under salt stress by acting as a receptor that binds or transports ligand (Chen and Dai, 2010). MLPs have an important role in plant defense against biotic and abiotic stress by inhibiting protease activity (Tsukuda et al., 2006). Stress conditions often lead to the accumulation of trypsin inhibitors, suggesting that protease inhibitors such as MLPs play an important role in plant stress responses (Domash et al., 2008). In soybean, an increase in the abundance of MLP during post-flooding recovery has been reported (Khan et al., 2014). In the present study, the transcriptional level of *MLP-like protein 43* was down-regulated in flooding-stressed soybean exposed to Al_2O_3 NPs. These results suggest that Al_2O_3 NPs might affect the activity of protease inhibitors by regulating MLP-like protein 43 in soybean under flooding stress.

Quinone reductases are ubiquitous enzymes that protect organisms from oxidative stress by acting as detoxifying enzymes (Joseph et al., 1994). Flavodoxin-like quinone reductases (Fqr) form a four-member family. *Flavodoxin-like quinone reductase 1* was identified in *Arabidopsis* as an auxin-responsive gene (Laskowski et al., 2002). In soybean, Fqr1 was identified in a soluble protein fraction (Schopfer et al., 2008). The overexpression of Fqr1 in *Arabidopsis* leads to increased quinone reductase activity, which is speculated to reduce the effects of oxidative stress (Laskowski et al., 2002) and may protect cells against quinone-dependent oxidative cell damage. The levels of

quinone reductases were found to increase in plants in response to salt stress (Jiang et al., 2007) and pathogens (Greenshields et al., 2005). In necrotrophic fungal infections, quinone reductases are involved in redox reactions and thus mediate host resistance (Heyno et al., 2013). In soybean, ROS scavengers are increased under flooding stress (Hashiguchi et al., 2009). The ROS act as regulatory molecules in stress perception and signal transduction (Navrot et al., 2006). Quinone reductases protect cells against quinone-dependent oxidative cell damage. Fqr catalyzes the strict two-electron reduction of quinone, thereby avoiding the formation of semiquinone, which can induce oxidative stress (Deller et al., 2008). In the present study, the protein abundance of Fqr1 in the roots of Al_2O_3 NPs-treated soybean was decreased followed by its down-regulation at the transcript level. These results suggest that Al_2O_3 NPs might enhance the flavodoxin-like quinone reductase-mediated protection of cells against oxidative damage under flooding conditions.

3.5. Conclusion

Al_2O_3 NPs are extensively used in agricultural products (Vernikov et al., 2009) and cause various growth effects on different plant species (Yang and Watts, 2005). The present proteomic experiment investigated the effects of Al_2O_3 NPs on soybean under flooding stress. The major findings of this experiment are as follows: (i) Al_2O_3 NPs mainly affected proteins related to energy metabolism and cell wall synthesis; (ii) the abundance of glycolysis-related proteins was increased under flooding stress, but decreased by treatment with Al_2O_3 NPs; (iii) Al_2O_3 NPs-responsive proteins in the roots of soybean were related to protein synthesis/degradation, glycolysis, and lipid metabolism; and (iv) the mRNA expression levels of *NmrA-like negative transcriptional regulator family protein, flavodoxin-like quinone reductase 1,* and *protein of unknown function DUF2359 transmembrane* were consistent with the protein abundance data (Figure 27). Taken together, these results suggest that Al_2O_3 NPs mediate the shift from anaerobic to aerobic energy metabolism, under flooding conditions by regulating the energy metabolism related proteins. These responses are considered to be key factors for improving the growth performance of soybeans under flooding stress.

Table 5. List of identified proteins in root including hypocotyl of flooded soybean in response to Al_2O_3 NPs.

				Ratio[c]											
				Control				Flooding				Flooding+Al_2O_3 NPs			
No.	Protein ID[a]	Description	M.P.[b]	2(0)	3(0)	4(0)	5(0)	2(0)	3(1)	4(2)	5(3)	2(0)	3(1)	4(2)	Ratio 5(3)
1.	Glyma08g21410.2	HAD superfamily subfamily IIIB acid phosphatase	8	1	12.41	12.63	24.75	1	16.65	1.87	2.28	1	2.76	2.02	2.64
2.	Glyma07g00920.1	lipoxygenase 1	2	1	10.80	9.46	9.37	1	45.05	6.42	9.72	1	3.27	3.71	4.29
3.	Glyma08g20250.1	lipoxygenase 1	5	1	3.22	6.47	4.50	1	23.12	2.06	5.81	1	1.31	2.67	2.64
4.	Glyma13g42330.1	lipoxygenase 1	35	1	2.40	3.03	2.96	1	6.16	1.61	1.82	1	1.36	1.34	1.15
5.	Glyma16g08460.1	NADP malic enzyme 4	18	1	2.13	2.76	2.50	1	1.15	1.17	1.21	1	1.32	1.21	1.21
6.	Glyma14g35410.1	general regulatory factor 2	7	1	2.11	3.59	4.39	1	2.74	1.40	3.49	1	1.39	1.52	0.91
7.	Glyma08g38420.1	PLAT/LH2 domain containing lipoxygenase family protein	9	1	2.03	4.49	3.10	1	16.15	1.51	2.70	1	1.29	1.52	1.26
8.	Glyma15g03050.1	lipoxygenase 1	31	1	2.01	2.53	2.23	1	6.41	1.64	1.91	1	1.42	1.40	1.19
9.	Glyma19g29180.3	Cobalamin independent synthase family protein	24	1	1.78	1.49	1.38	1	4.48	1.49	8.35	1	1.47	1.26	1.68
10.	Glyma20g01180.2	peroxisomal 3 ketoacyl CoA thiolase 3	9	1	1.76	1.73	1.35	1	2.05	2.43	6.05	1	1.42	2.69	2.55
11.	Glyma02g02170.1	NAD(P) binding Rossmann fold superfamily protein	5	1	1.72	1.62	1.44	1	0.62	0.40	0.26	1	0.71	0.38	0.23
12.	Glyma01g01180.1	NADP malic enzyme 4	18	1	1.69	2.07	2.15	1	2.61	1.27	1.28	1	1.19	1.14	1.23
13.	Glyma07g00900.1	lipoxygenase 1	25	1	1.67	2.24	1.57	1	5.87	0.96	0.96	1	1.24	1.36	0.77
14.	Glyma03g28850.1	beta 1 3 glucanase 1	10	1	1.65	1.81	1.81	1	1.50	0.73	0.85	1	0.83	0.55	0.32
15.	Glyma05g22180.1	root hair specific 19	11	1	1.62	2.36	2.27	1	1.63	1.48	1.48	1	1.36	1.40	1.94
16.	Glyma07g13710.1	Nucleoside diphosphate kinase family protein	6	1	1.53	1.00	1.19	1	8.92	1.16	1.40	1	1.34	0.93	1.37
17.	Glyma04g09110.3	NADP malic enzyme 3	5	1	1.53	1.71	1.66	1	1.41	1.46	1.26	1	1.04	1.10	1.16
18.	Glyma08g03580.1	Insulinase (Peptidase family M16) protein	7	1	1.52	1.63	1.13	1	1.48	1.13	1.44	1	1.42	1.41	0.32
19.	Glyma17g04340.1	S adenosylmethionine synthetase family protein	10	1	1.48	1.34	1.29	1	0.97	0.55	0.42	1	0.94	0.71	0.65
20.	Glyma15g20180.2	sucrose synthase 4	19	1	1.47	1.68	1.79	1	2.35	2.33	2.59	1	1.94	1.63	2.46
21.	Glyma17g17730.1	root hair specific 19	11	1	1.47	2.49	2.33	1	1.68	1.53	1.55	1	1.36	1.35	1.56
22.	Glyma09g32430.1	Enoyl CoA hydratase/isomerase family	9	1	1.46	1.40	0.74	1	1.41	0.82	1.02	1	1.33	0.94	0.42
23.	Glyma15g43180.1	Protein of unknown function DUF642	7	1	1.46	1.34	3.89	1	3.48	0.58	0.52	1	1.35	0.76	0.44
24.	Glyma17g24366.1	Cobalamin independent synthase family protein	9	1	1.45	1.42	1.19	1	2.37	1.04	0.88	1	1.49	1.26	1.50
25.	Glyma1337s00200.1	S adenosylmethionine synthetase 2	8	1	1.44	1.34	1.29	1	0.96	0.55	0.42	1	0.94	0.72	0.65
26.	Glyma09g08550.1	sucrose synthase 4	17	1	1.44	2.00	2.13	1	2.44	2.39	2.65	1	1.95	1.67	2.23
27.	Glyma15g21890.1	S adenosylmethionine synthetase family protein	13	1	1.44	1.37	1.24	1	1.52	0.44	0.39	1	0.94	0.68	0.59
28.	Glyma13g17421.1	sucrose synthase 4	23	1	1.44	1.50	1.60	1	1.39	1.19	1.07	1	1.31	1.23	0.94
29.	Glyma18g52780.1	actin 11	14	1	1.43	1.34	1.13	1	1.92	1.21	1.17	1	1.62	1.43	1.29
30.	Glyma19g30770.1	beta 6 tubulin	18	1	1.40	1.39	1.12	1	1.65	1.20	0.93	1	1.33	0.71	0.44
31.	Glyma06g02650.1	tubulin beta 1 chain	19	1	1.36	1.31	1.14	1	1.32	0.99	0.86	1	1.18	0.76	0.44

32.	Glyma05g25610.1	tubulin beta 7 chain	16	1	1.36	1.36	1.04	1	1.68	1.11	0.82	1	1.23	0.63	0.42
33.	Glyma08g01740.1	beta 6 tubulin	13	1	1.35	1.37	1.99	1	1.56	1.20	0.91	1	1.26	2.08	0.51
34.	Glyma17g33050.1	aspartate aminotransferase 5	11	1	1.35	1.29	0.90	1	1.78	1.70	1.76	1	1.31	1.44	1.14
35.	Glyma15g13970.1	tubulin beta 8	19	1	1.35	1.32	1.01	1	1.64	1.11	0.89	1	1.20	0.68	0.54
36.	Glyma03g15020.1	tubulin beta chain 3	18	1	1.34	1.26	1.03	1	1.55	0.91	0.68	1	1.18	0.59	0.42
37.	Glyma19g00850.1	actin 11	12	1	1.34	1.21	1.00	1	1.90	1.19	1.16	1	1.39	1.35	1.20
38.	Glyma20g29840.1	tubulin beta 8	19	1	1.34	1.28	0.95	1	1.63	1.02	0.81	1	1.17	0.62	0.52
39.	Glyma08g05850.1	beta 6 tubulin	8	1	1.31	1.29	0.53	1	1.68	1.22	0.92	1	1.14	0.54	0.41
40.	Glyma08g08590.1	tubulin beta 7 chain	14	1	1.31	1.36	0.68	1	1.71	1.11	0.83	1	1.23	0.62	0.42
41.	Glyma11g14880.1	actin 11	11	1	1.30	1.15	0.98	1	1.85	1.14	1.19	1	4.06	1.63	1.16
42.	Glyma06g15520.3	actin 7	12	1	1.29	1.14	1.01	1	1.32	1.16	1.10	1	4.43	1.59	1.12
43.	Glyma15g04290.2	triosephosphate isomerase	7	1	1.25	1.11	0.95	1	1.60	1.29	1.15	1	1.43	1.33	1.22
44.	Glyma10g11620.1	Protein of unknown function DUF642	8	1	1.25	1.19	4.06	1	3.49	0.57	0.53	1	1.36	0.72	0.43
45.	Glyma11g35020.2	eukaryotic translation initiation factor 2	2	1	1.24	0.98	1.40	1	1.36	0.85	0.79	1	1.39	0.41	0.18
46.	Glyma13g41120.2	triosephosphate isomerase	10	1	1.24	1.15	1.04	1	1.55	1.27	1.09	1	1.44	1.34	1.22
47.	Glyma02g46200.1	Dihydrolipoamide succinyltransferase	7	1	1.24	1.14	0.69	1	1.11	1.25	1.21	1	1.30	1.31	0.69
48.	Glyma03g27290.2	RNA binding (RRM/RBD/RNP motifs) family protein	3	1	1.23	1.16	1.12	1	1.13	0.84	0.87	1	1.17	0.86	0.93
49.	Glyma14g13480.2	aspartate aminotransferase 5	6	1	1.23	1.36	1.21	1	1.95	1.70	1.84	1	1.38	1.51	1.21
50.	Glyma08g19420.3	actin 11	12	1	1.21	1.07	0.98	1	1.94	1.17	1.20	1	6.28	1.75	1.38
51.	Glyma05g35800.1	NADP malic enzyme 4	18	1	1.19	0.96	1.13	1	1.23	1.10	1.12	1	1.05	1.01	0.94
52.	Glyma08g12140.1	tubulin alpha 5	11	1	1.19	1.36	1.10	1	2.06	1.51	1.29	1	0.87	1.14	1.12
53.	Glyma07g03910.1	lipoxygenase 1	7	1	1.16	2.15	1.01	1	9.69	0.98	0.91	1	0.89	1.31	0.83
54.	Glyma0169s00210.1	monodehydroascorbate reductase 1	10	1	1.15	1.59	1.13	1	1.31	1.11	0.97	1	1.22	1.33	1.45
55.	Glyma01g03930.1	Threonyl tRNA synthetase	2	1	1.12	1.45	1.12	1	3.77	5.16	2.36	1	1.50	1.60	1.08
56.	Glyma04g30350.1	Cobalamin independent synthase family protein	15	1	1.10	0.85	1.05	1	2.16	1.12	2.11	1	1.27	1.19	1.25
57.	Glyma15g04360.2	actin 11	11	1	1.05	1.08	1.00	1	1.86	1.14	1.20	1	4.17	1.56	1.35
58.	Glyma13g15140.1	Cobalamin independent synthase family protein	16	1	1.03	0.75	0.57	1	3.08	1.38	0.96	1	1.13	1.02	1.06
59.	Glyma03g32850.2	heat shock cognate protein 70 1	21	1	1.01	1.04	0.79	1	1.24	1.00	0.90	1	1.09	0.91	0.34
60.	Glyma19g32990.2	actin 7	13	1	1.01	1.07	1.00	1	1.77	1.14	1.19	1	3.12	1.54	1.27
61.	Glyma02g29160.3	actin 1	10	1	0.99	1.09	1.22	1	2.19	1.15	1.45	1	3.24	1.60	1.40
62.	Glyma12g31620.1	DNAJ homologue 2	7	1	0.97	0.93	0.89	1	0.92	0.69	0.71	1	0.69	0.74	0.67
63.	Glyma11g33160.1	UDP glucose pyrophosphorylase 2	16	1	0.93	0.93	0.57	1	1.36	1.23	1.39	1	1.16	1.22	1.20
64.	Glyma20g38740.1	10 formyltetrahydrofolate synthetase	13	1	0.91	0.92	0.61	1	1.61	1.21	0.97	1	1.25	1.24	0.79
65.	Glyma13g20680.1	ATPase AAA type CDC48 protein	22	1	0.91	1.05	0.72	1	1.14	0.81	0.78	1	0.80	0.87	0.98
66.	Glyma13g19331.1	heat shock cognate protein 70 1	19	1	0.87	0.95	0.77	1	1.32	0.92	0.78	1	0.98	0.88	0.25

67.	Glyma03g30231.1	Aha1 domain containing protein	2	1	0.86	0.80	0.70	1	1.88	2.27	3.48	1	1.12	1.62	2.06
68.	Glyma05g33330.1	calnexin 1	11	1	0.86	1.09	0.93	1	30.51	1.37	1.26	1	1.18	1.41	2.07
69.	Glyma19g01210.1	formate dehydrogenase	11	1	0.86	0.82	0.55	1	1.64	2.15	2.96	1	1.02	1.66	1.67
70.	Glyma19g21200.1	ATPase AAA type CDC48 protein	4	1	0.85	0.78	0.51	1	1.05	0.99	0.80	1	0.90	1.03	4.14
71.	Glyma18g53600.1	Zinc binding dehydrogenase family protein	3	1	0.85	0.68	0.51	1	1.69	1.27	1.73	1	0.92	0.94	0.31
72.	Glyma08g00920.1	calnexin 1	9	1	0.84	1.02	0.88	1	33.37	1.28	1.30	1	1.21	1.65	2.36
73.	Glyma12g30060.1	ATPase AAA type CDC48 protein	19	1	0.84	1.11	0.71	1	1.13	0.81	0.78	1	0.80	0.90	1.17
74.	Glyma18g52610.1	heat shock cognate protein 70 1	17	1	0.84	0.92	0.72	1	1.33	1.13	1.06	1	0.94	1.11	0.32
75.	Glyma12g08410.2	ATPase AAA type CDC48 protein	7	1	0.84	0.79	0.33	1	1.06	0.81	0.73	1	0.74	0.83	2.35
76.	Glyma08g45531.1	kunitz trypsin inhibitor 1	5	1	0.83	0.56	0.09	1	2.89	1.04	1.28	1	0.89	0.78	0.57
77.	Glyma04g36860.3	glyceraldehyde 3 phosphate dehydrogenase C2	6	1	0.82	0.86	0.44	1	8.06	1.16	1.39	1	0.98	1.04	1.23
78.	Glyma09g25250.1	tripeptidyl peptidase ii	15	1	0.82	2.01	1.16	1	1.10	0.67	0.59	1	0.75	0.70	0.60
79.	Glyma04g36870.3	glyceraldehyde 3 phosphate dehydrogenase C subunit 1	13	1	0.82	0.68	0.42	1	4.08	1.09	1.23	1	0.91	1.04	1.25
80.	Glyma14g09300.1	poly(A) binding protein 2	7	1	0.81	0.76	0.43	1	1.52	0.80	0.63	1	0.90	0.85	0.13
81.	Glyma16g09225.1	Sec23/Sec24 protein transport family protein	2	1	0.80	0.64	0.66	1	1.03	1.11	0.90	1	1.21	1.68	0.49
82.	Glyma16g30190.1	tripeptidyl peptidase ii	17	1	0.79	1.91	1.21	1	1.13	0.74	0.61	1	0.74	0.68	0.46
83.	Glyma06g18110.4	glyceraldehyde 3 phosphate dehydrogenase C2	11	1	0.79	0.80	0.52	1	4.52	1.29	1.26	1	0.96	1.06	1.21
84.	Glyma18g02340.1	fibrillarin 2	7	1	0.78	0.80	0.39	1	0.72	0.61	0.23	1	0.62	0.45	0.17
85.	Glyma11g14950.1	heat shock protein 70	22	1	0.78	0.74	0.64	1	1.42	1.08	1.00	1	0.91	1.04	0.50
86.	Glyma19g00870.2	Pyruvate kinase family protein	10	1	0.77	0.77	1.53	1	1.38	1.16	1.46	1	1.51	1.39	1.30
87.	Glyma18g08070.2	ubiquitin family protein	3	1	0.77	0.67	0.53	1	1.37	0.97	0.87	1	0.88	0.35	0.16
88.	Glyma12g06910.1	heat shock protein 70	23	1	0.77	0.74	0.62	1	1.46	1.20	1.06	1	1.01	1.06	0.53
89.	Glyma18g52650.2	heat shock cognate protein 70 1	16	1	0.76	0.76	0.68	1	1.37	0.94	0.82	1	0.94	0.86	0.23
90.	Glyma10g07850.2	60S acidic ribosomal protein family	3	1	0.75	0.59	0.41	1	1.17	0.79	0.80	1	0.83	0.64	0.70
91.	Glyma11g37360.1	glyceraldehyde 3 phosphate dehydrogenase C subunit 1	10	1	0.74	0.68	0.40	1	4.76	1.25	1.37	1	1.08	1.15	0.90
92.	Glyma03g37441.2	sucrose synthase 3	8	1	0.73	0.76	0.66	1	2.61	2.33	2.13	1	1.79	1.76	2.09
93.	Glyma13g42320.1	lipoxygenase 1	33	1	0.72	0.52	0.38	1	4.91	1.03	1.20	1	0.79	0.81	0.70
94.	Glyma19g36630.2	adenosine kinase 1	5	1	0.71	0.79	0.57	1	1.29	1.15	0.87	1	1.02	0.94	0.81
95.	Glyma13g23790.1	formate dehydrogenase	9	1	0.71	0.65	0.40	1	1.40	0.93	0.91	1	0.92	0.91	0.81
96.	Glyma18g01330.4	glyceraldehyde 3 phosphate dehydrogenase C2	4	1	0.66	0.76	0.48	1	18.72	1.73	2.86	1	1.03	1.17	0.99
97.	Glyma15g03030.1	lipoxygenase 1	32	1	0.66	0.55	0.39	1	10.61	1.52	1.40	1	0.84	1.07	1.82
98.	Glyma04g35950.1	ATPase AAA type CDC48 protein	17	1	0.66	0.77	0.24	1	1.13	0.86	0.74	1	0.74	0.80	1.24
99.	Glyma17g08020.1	heat shock protein 70B	16	1	0.65	0.62	0.51	1	1.26	0.88	0.78	1	0.91	0.80	0.58
100.	Glyma06g12780.2	alcohol dehydrogenase 1	9	1	0.65	0.60	0.46	1	5.92	2.39	3.10	1	1.90	2.96	3.61
101.	Glyma18g43390.1	metallopeptidase M24 family protein	2	1	0.64	1.03	0.35	1	1.09	1.04	0.77	1	0.76	0.53	0.21

102.	Glyma04g41990.1	alcohol dehydrogenase 1	9	1	0.63	0.58	0.43	1	4.19	2.24	2.66	1	1.87	3.02	3.77
103.	Glyma13g42310.1	lipoxygenase 1	31	1	0.63	0.48	1.07	1	2.94	1.23	1.31	1	0.78	0.96	0.88
104.	Glyma14g27940.1	alcohol dehydrogenase 1	3	1	0.62	0.54	0.42	1	3.78	2.79	3.12	1	1.95	2.87	2.83
105.	Glyma18g43460.1	pyruvate decarboxylase 2	5	1	0.62	0.52	0.26	1	4.13	2.46	3.01	1	1.83	2.31	2.65
106.	Glyma07g18500.1	metallopeptidase M24 family protein	4	1	0.61	0.91	0.32	1	1.09	1.04	0.77	1	0.76	0.53	0.21
107.	Glyma06g35680.1	ARM repeat superfamily protein	3	1	0.60	0.62	0.43	1	2.74	1.46	1.78	1	0.98	0.97	1.12
108.	Glyma12g09390.1	NAD ADP ribosyltransferases	10	1	0.60	0.83	1.66	1	1.69	0.91	0.66	1	0.67	1.11	0.76
109.	Glyma15g10210.1	Ribosomal protein S11 family protein	3	1	0.57	0.64	0.41	1	0.85	0.70	0.19	1	0.68	0.55	0.16
110.	Glyma02g36700.1	heat shock protein 70B	13	1	0.56	0.57	0.34	1	1.26	0.96	0.77	1	0.93	0.81	0.66
111.	Glyma05g27840.1	Urease	15	1	0.56	0.43	0.19	1	1.24	1.56	1.45	1	0.93	0.94	2.85
112.	Glyma03g06780.1	PEBP (phosphatidylethanolamine) family protein	3	1	0.53	0.43	0.13	1	4.98	0.87	0.71	1	0.57	0.73	0.43
113.	Glyma07g18570.1	Thiamine pyrophosphate dependent pyruvate decarboxylase	5	1	0.52	0.41	0.25	1	4.81	2.51	3.25	1	1.91	3.02	2.68
114.	Glyma20g37670.1	NAD(P) binding Rossmann fold superfamily protein	12	1	0.50	0.30	0.14	1	1.55	0.81	0.78	1	0.89	0.87	0.96
115.	Glyma15g07760.1	proline rich spliceosome associated (PSP) family protein	2	1	0.49	0.20	0.35	1	0.62	0.48	0.50	1	0.68	0.41	0.43
116.	Glyma14g06160.1	ferritin 4	5	1	0.47	0.44	0.10	1	0.51	0.69	0.24	1	0.37	0.40	0.27
117.	Glyma12g30600.1	histone deacetylase 2C	2	1	0.46	0.49	0.28	1	0.50	0.02	0.04	1	0.15	0.05	0.00
118.	Glyma11g33700.3	dehydroascorbate reductase 1	3	1	0.45	0.27	0.37	1	0.87	0.53	0.70	1	0.33	0.53	0.51
119.	Glyma10g39150.1	cupin family protein	12	1	0.41	0.37	0.27	1	1.14	0.72	0.51	1	0.51	0.32	1.05
120.	Glyma09g25830.2	CAP160 protein	10	1	0.41	0.17	0.31	1	0.80	1.37	0.86	1	0.67	0.80	0.57
121.	Glyma11g19070.2	NAD ADP ribosyltransferases	18	1	0.33	0.18	0.48	1	2.92	0.90	0.37	1	0.83	1.17	1.34
122.	Glyma20g28650.2	cupin family protein	8	1	0.32	0.27	0.29	1	0.54	0.33	0.37	1	0.55	0.26	0.20
123.	Glyma19g13060.1	Oleosin family protein	4	1	0.22	0.10	0.06	1	3.12	2.38	1.89	1	0.63	0.75	0.46
124.	Glyma03g07470.1	Stress induced protein	4	1	0.22	0.15	0.06	1	3.36	1.10	0.72	1	0.36	0.62	0.41
125.	Glyma01g38340.2	RmlC like cupins superfamily protein	4	1	0.17	0.16	0.03	1	0.32	0.24	0.03	1	0.13	0.07	0.11
126.	Glyma11g15870.1	RmlC like cupins superfamily protein	7	1	0.11	0.06	0.07	1	3.35	1.71	0.27	1	0.07	0.06	0.05
127.	Glyma09g31740.2	ND	6	1	0.10	0.09	0.06	1	10.39	0.90	0.68	1	0.34	0.34	0.26
128.	Glyma07g10030.1	ND	5	1	0.05	0.03	0.03	1	1.68	1.29	0.74	1	0.35	0.63	0.49

[a] Protein ID, according to the Phytozome database; [b] M.P., matched peptide; [c] Ratio, relative abundance of protein; ND, no description; p-value<0.05.

Table 6. List of proteins identified from soybean root including hypocotyl flooded for 1-, 2-, and 3 days with Al_2O_3 NPs compared to 2-day-old soybean.

No.	Protein ID[a]	Description	M.P.[b]	Ratio[c]				Functional Category[d]
				2(0)	3(1)F+Al_2O_3	4(2)F+ Al_2O_3	5(3)F+ Al_2O_3	
1.	Glyma11g07490.1	NmrA like negative transcriptional regulator family protein	3	1	8.17	14.68	15.75	Secondary metabolism
2.	Glyma08g24720.1	MLP like protein 43	5	1	8.92	6.67	10.95	Stress.abiotic
3.	Glyma05g27090.1	Protein of unknown function DUF2359 transmembrane	2	1	3.34	6.44	2.92	Not assigned
4.	Glyma05g02670.2	RAB GTPase homolog E1B	7	1	2.05	4.31	4.04	Protein.synthesis
5.	Glyma17g03350.1	ND	5	1	3.15	3.73	2.42	Not assigned
6.	Glyma15g10910.1	GTP binding Elongation factor Tu family protein	2	1	4.29	3.69	2.61	Protein.synthesis
7.	Glyma06g23081.1	enolase 1	2	1	1.48	3.29	1.84	Glycolysis
8.	Glyma01g02300.1	Mitochondrial substrate carrier family protein	2	1	1.86	2.56	1.76	Transport
9.	Glyma09g33690.2	Mitochondrial substrate carrier family protein	2	1	1.86	2.56	1.76	Transport
10.	Glyma13g44170.3	phospholipase D alpha 1	7	1	1.82	2.49	1.63	Lipid metabolism
11.	Glyma08g10070.1	Protein of unknown function DUF2359 transmembrane	2	1	2.04	2.18	1.59	Not assigned
12.	Glyma08g19290.1	UDP Glycosyltransferase superfamily protein	5	1	2.09	2.15	3.75	Secondary metabolism
13.	Glyma03g30720.1	GTP binding Elongation factor Tu family protein	7	1	2.55	2.05	1.53	Protein.synthesis
14.	Glyma19g33570.1	GTP binding Elongation factor Tu family protein	7	1	2.55	2.05	1.53	Protein.synthesis
15.	Glyma07g15480.2	ACC oxidase 1	2	1	1.19	2.03	2.17	Hormone metabolism
16.	Glyma05g37190.1	vacuolar H ATPase subunit E isoform 3	3	1	1.33	1.81	2.59	Transport
17.	Glyma10g39540.1	long chain acyl CoA synthetase 6	2	1	1.79	1.77	0.45	Lipid metabolism
18.	Glyma20g28200.1	long chain acyl CoA synthetase 7	2	1	1.79	1.77	0.45	Lipid metabolism.
19.	Glyma13g01870.1	annexin 1	6	1	1.52	1.76	1.78	Cell.organisation
20.	Glyma07g10000.1	protein phosphatase 2A subunit A2	2	1	1.02	1.54	0.09	Protein.postranslational modification
21.	Glyma09g31760.1	protein phosphatase 2A subunit A2	2	1	1.02	1.54	0.09	Protein.postranslational modification
22.	Glyma03g40050.1	glutathione synthetase 2	3	1	1.42	1.52	1.73	Redox
23.	Glyma10g42250.1	protein phosphatase 2A subunit A2	3	1	1.05	1.52	0.62	Protein.postranslational modification
24.	Glyma20g24790.1	protein phosphatase 2A subunit A2	3	1	1.05	1.52	0.62	Protein.postranslational modification
25.	Glyma11g28731.1	AAA type ATPase family protein	2	1	0.77	1.40	1.72	Protein.degradation
26.	Glyma06g43050.1	phosphoenolpyruvate carboxylase 1	9	1	1.36	1.39	1.34	Glycolysis
27.	Glyma20g02980.1	Pyruvate kinase family protein	8	1	1.37	1.38	0.41	Glycolysis
28.	Glyma07g35110.3	Pyruvate kinase family protein	9	1	1.37	1.38	0.36	Glycolysis
29.	Glyma12g33820.1	phosphoenolpyruvate carboxylase 2	7	1	1.36	1.38	1.26	Glycolysis

30.	Glyma13g36670.1	phosphoenolpyruvate carboxylase 1	7	1	1.36	1.38	1.26	Glycolysis
31.	Glyma20g31980.1	chorismate synthase putative	2	1	2.02	1.27	1.40	Amino acid metabolism
32.	Glyma03g37191.1	HSP20 like chaperones superfamily protein	2	1	0.49	1.26	0.76	Not assigned
33.	Glyma19g39800.1	HSP20 like chaperones superfamily protein	2	1	0.49	1.26	0.76	Not assigned
34.	Glyma06g39800.1	Adenine nucleotide alpha hydrolases like superfamily protein	6	1	0.90	1.13	1.05	Stress.abiotic
35.	Glyma05g04940.1	acyl CoA oxidase 1	8	1	1.25	1.10	0.92	Lipid metabolism
36.	Glyma19g34900.2	ribophorin II (RPN2) family protein	4	1	0.75	1.07	0.80	Development
37.	Glyma01g07930.1	reversibly glycosylated polypeptide 3	10	1	1.13	1.06	0.90	Cell wall
38.	Glyma02g13330.1	reversibly glycosylated polypeptide 3	11	1	1.06	1.04	0.89	Cell wall
39.	Glyma10g15910.1	S formylglutathione hydrolase	4	1	1.46	1.01	1.08	C1-metabolism
40.	Glyma05g29870.1	T complex protein 1 alpha subunit	2	1	0.56	1.00	1.41	Protein.folding
41.	Glyma08g12970.1	T complex protein 1 alpha subunit	2	1	0.56	1.00	1.41	Protein.folding
42.	Glyma18g04940.1	glutamate decarboxylase 4	6	1	1.63	0.98	0.81	Amino acid metabolism
43.	Glyma05g24110.1	GTP binding Elongation factor Tu family protein	10	1	0.82	0.93	0.54	Protein.synthesis
44.	Glyma19g07240.3	GTP binding Elongation factor Tu family protein	11	1	0.82	0.93	0.53	Protein.synthesis
45.	Glyma08g39241.1	ATPase AAA type CDC48 protein	2	1	0.75	0.93	5.86	Cell.division
46.	Glyma10g35700.2	GTP binding Elongation factor Tu family protein	11	1	0.79	0.92	0.55	Protein.synthesis
47.	Glyma16g07350.1	GTP binding Elongation factor Tu family protein	11	1	0.79	0.92	0.55	Protein.synthesis
48.	Glyma05g11630.2	GTP binding Elongation factor Tu family protein	11	1	0.79	0.91	0.53	Protein.synthesis
49.	Glyma17g23900.1	GTP binding Elongation factor Tu family protein	12	1	0.81	0.91	0.52	Protein.synthesis
50.	Glyma19g03490.1	Glycosyl transferase family 35	14	1	1.13	0.89	0.72	Major CHO metabolism
51.	Glyma01g39700.2	ADP ribosylation factor A1E	2	1	1.00	0.86	1.75	Protein.targeting
52.	Glyma11g05581.1	ADP ribosylation factor A1F	2	1	1.00	0.86	1.75	Protein.postranslational modification
53.	Glyma10g01760.1	20S proteasome alpha subunit E2	5	1	0.92	0.86	0.77	Protein.degradation
54.	Glyma02g01700.1	20S proteasome alpha subunit E2	6	1	0.93	0.86	0.83	Protein.degradation
55.	Glyma18g43710.1	20S proteasome alpha subunit C1	4	1	0.83	0.83	0.80	Protein.degradation
56.	Glyma20g24380.1	20S proteasome alpha subunit E2	6	1	0.89	0.79	0.77	Protein.degradation
57.	Glyma12g03070.1	nucleolin like 2	5	1	0.87	0.77	1.50	Protein.synthesis
58.	Glyma12g29340.1	Preprotein translocase Sec Sec61 beta subunit protein	3	1	0.83	0.77	0.80	Protein.targeting
59.	Glyma13g40276.1	Seven transmembrane MLO family protein	3	1	0.83	0.77	0.80	Stress.biotic
60.	Glyma19g23760.1	ubiquitin 5	2	1	0.65	0.77	0.68	Protein.degradation
61.	Glyma08g02390.1	vacuolar ATP synthase subunit E1	3	1	0.62	0.71	0.58	Transport
62.	Glyma09g07120.1	Transducin family protein	4	1	0.65	0.71	0.57	Development

63.	Glyma15g18450.1	Transducin family protein	4	1	0.65	0.71	0.57	Development
64.	Glyma13g42660.3	Transducin family protein	2	1	0.64	0.69	0.56	Development
65.	Glyma02g07340.1	Ubiquinol cytochrome C reductase iron sulfur subunit	4	1	0.83	0.68	0.61	Mitochondrial electron transport
66.	Glyma10g43770.2	Ribosomal L29 family protein	2	1	1.03	0.68	0.04	Protein.synthesis
67.	Glyma20g38480.1	Ribosomal L29 family protein	2	1	1.03	0.68	0.04	Protein.synthesis
68.	Glyma17g34040.1	early nodulin like protein 15	2	1	0.76	0.67	0.54	Misc
69.	Glyma10g28370.1	Saposin like aspartyl protease family protein	3	1	0.74	0.66	0.35	Protein.degradation
70.	Glyma08g09310.1	1 cysteine peroxiredoxin 1	5	1	0.69	0.62	0.36	Redox
71.	Glyma11g35610.1	ferritin 4	3	1	0.48	0.60	0.15	Metal handling
72.	Glyma18g02800.1	ferritin 4	3	1	0.48	0.60	0.15	Metal handling.binding
73.	Glyma01g03530.1	ATP citrate lyase A 1	3	1	0.86	0.54	0.45	Tricarboxylic acid cycle
74.	Glyma06g08650.1	La protein 1	2	1	0.63	0.50	0.44	RNA
75.	Glyma08g25150.1	metacaspase 5	2	1	0.38	0.49	0.95	Protein.degradation
76.	Glyma08g25170.1	metacaspase 4	2	1	0.38	0.49	0.95	Protein.degradation
77.	Glyma15g31750.1	metacaspase 4	2	1	0.38	0.49	0.95	Protein.degradation
78.	Glyma14g39170.1	glutamate decarboxylase	3	1	1.60	0.45	0.40	Amino acid metabolism
79.	Glyma08g00910.1	TUDOR SN protein 1	3	1	0.56	0.44	0.16	RNA
80.	Glyma18g12210.1	spermidine hydroxycinnamoyl transferase	3	1	1.35	0.43	0.15	Secondary metabolism
81.	Glyma08g17010.3	ATP citrate lyase A 1	2	1	0.55	0.39	0.31	Tricarboxylic acid cycle
82.	Glyma15g42140.2	ATP citrate lyase A 1	2	1	0.55	0.39	0.31	Tricarboxylic acid cycle
83.	Glyma15g11200.2	Aluminium induced protein with YGL and LRDR motifs	2	1	0.50	0.34	0.25	Metal handling
84.	Glyma13g27800.1	Aluminium induced protein with YGL and LRDR motifs	3	1	0.42	0.32	0.24	Metal handling
85.	Glyma11g37610.1	Pectate lyase family protein	2	1	0.38	0.31	0.18	Cell wall
86.	Glyma18g01560.1	Pectate lyase family protein	2	1	0.38	0.31	0.18	Cell wall
87.	Glyma06g01310.1	Ribosomal protein S25 family protein	2	1	0.40	0.29	0.08	Protein.synthesis
88.	Glyma19g36080.1	Glutathione S transferase family protein	3	1	0.27	0.27	0.22	Misc
89.	Glyma11g29350.1	Thioredoxin superfamily protein	2	1	0.12	0.24	0.16	Not assigned
90.	Glyma11g12300.1	Ribosomal protein S25 family protein	2	1	0.39	0.23	0.08	Protein.synthesis
91.	Glyma12g04510.2	Ribosomal protein S25 family protein	2	1	0.39	0.23	0.08	Protein.synthesis
92.	Glyma08g06570.1	flavodoxin like quinone reductase 1	2	1	0.41	0.20	0.02	Lipid metabolism

[a] Protein ID, according to the Phytozome database; [b] M.P., matched peptide; [c] Ratio, relative abundance of protein; ND, no description; p-value<0.05; [d] Functional classification using MapMan bin codes.

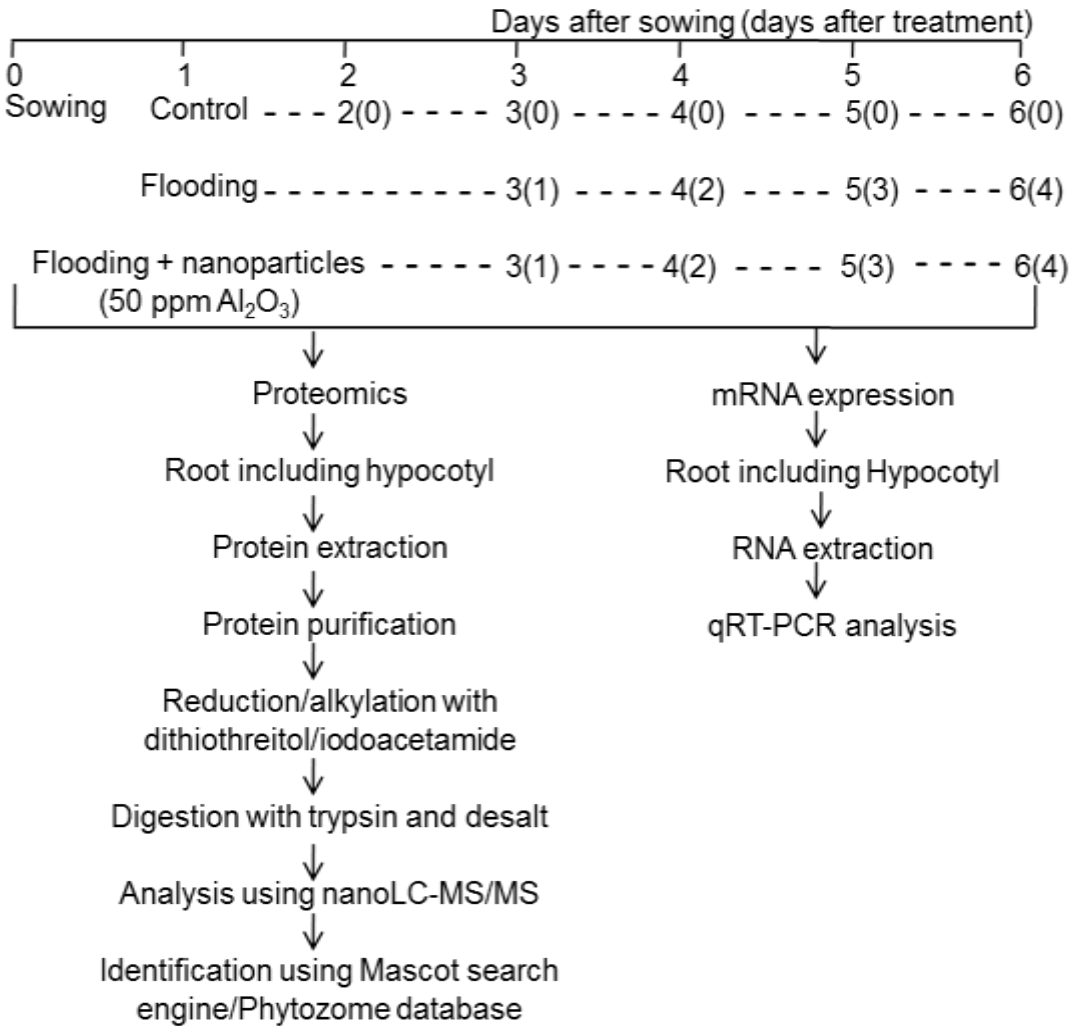

Figure 19. Experimental design to study the effects of Al_2O_3 NPs on soybean under flooding stress. Two-day-old soybeans were flooded without or with 50 ppm Al_2O_3 NPs for 0, 1, 2, and 3 days. For proteomic analysis, proteins extracted from root including hypocotyl were analyzed using nanoLC-MS/MS. For mRNA expression analysis, RNAs extracted from root including hypocotyl were analyzed by qRT-PCR.

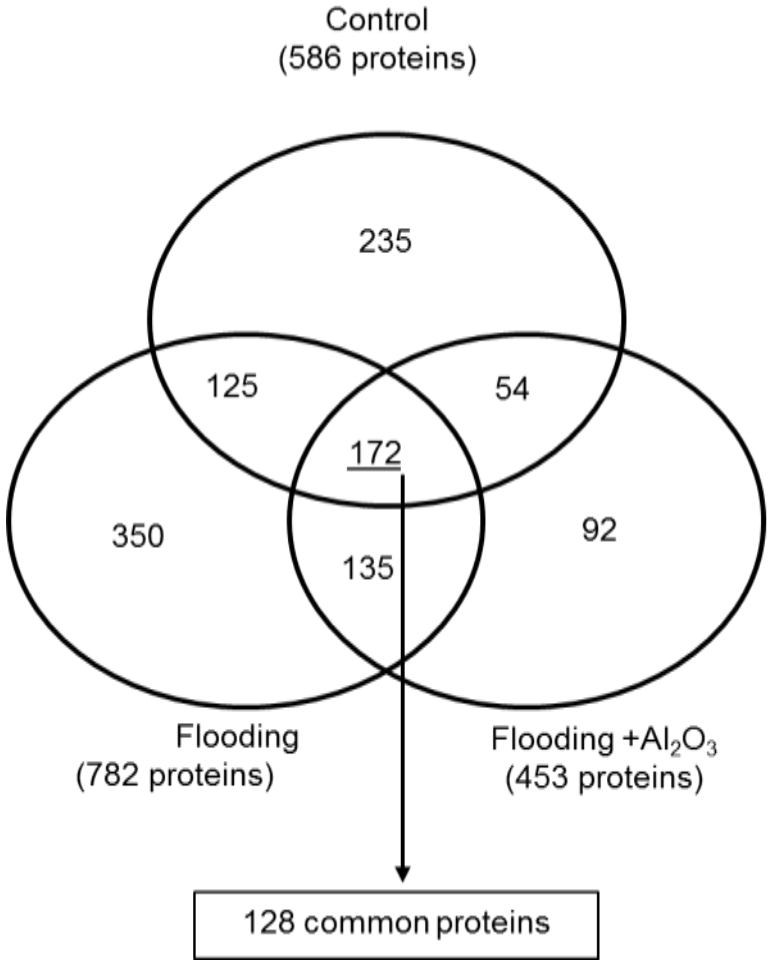

Figure 20. The Venn diagram represents the comparison of proteins identified among the control, flooding, and flooding with Al_2O_3 NPs in soybean root including hypocotyl. The identified proteins for control, flooding, and flooding with Al_2O_3 NPs were 586, 782, and 453, respectively. One-hundred and seventy-two proteins were commonly identified among these three treatments.

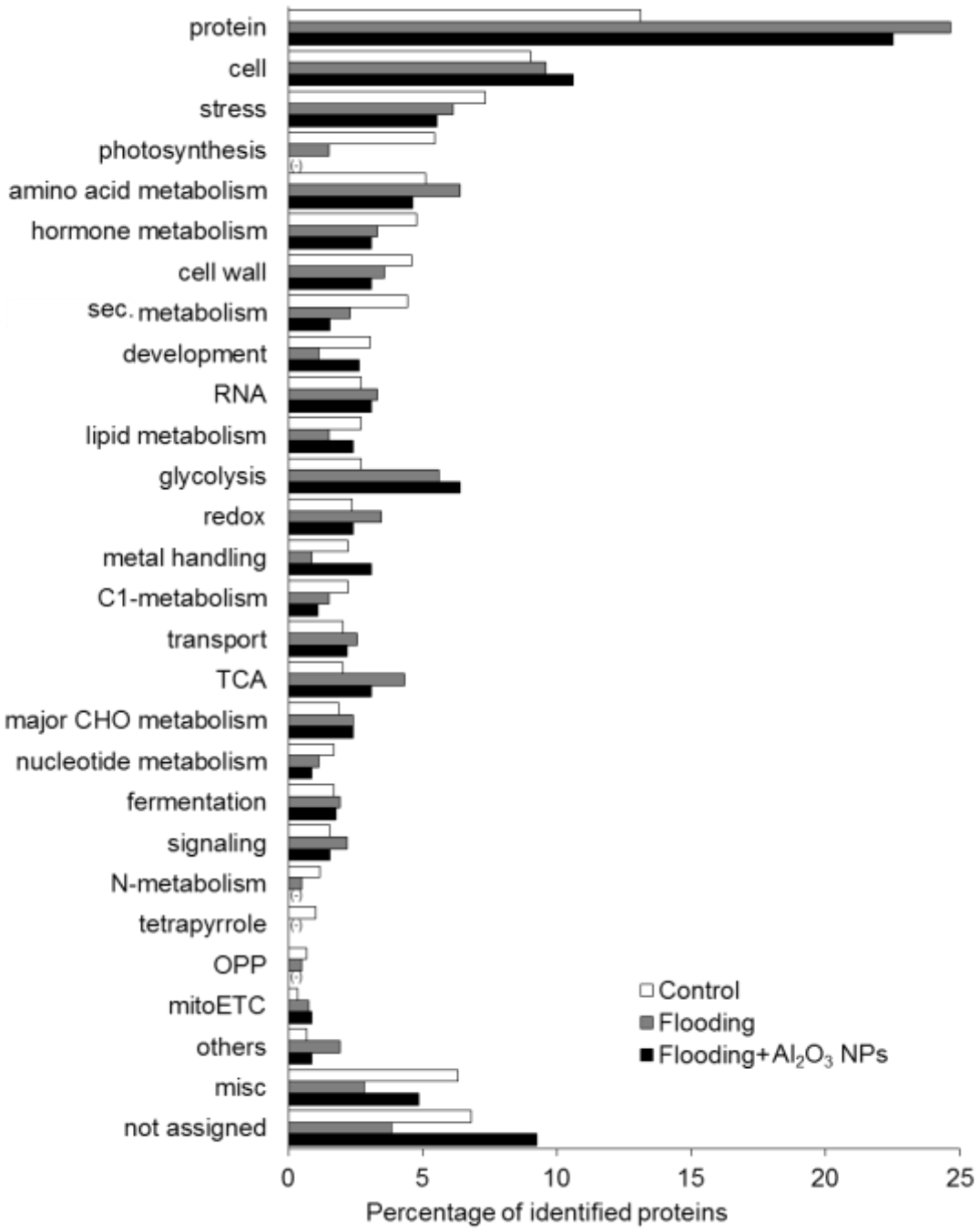

Figure 21. Functional categorization of the proteins identified in flooding-stressed soybean treated with Al_2O_3 NPs. Two-day-old soybeans were flooded for 1, 2, and 3 days without (Flooding, grey columns) or with Al_2O_3 NPs (Flooding + Al_2O_3 NPs, black columns). Untreated plants served as the control (white columns). Proteins were extracted from root including hypocotyl, and identified using a gel-free proteomic technique. Significantly changed proteins ($p < 0.05$) were analyzed. MapMan bin codes were used to predict the functional categorization of the identified proteins. The *x*-axis indicates the percentage of identified proteins. The identified functional categories with zero proteins are marked with (-). Abbreviations are the same as in Figure 11.

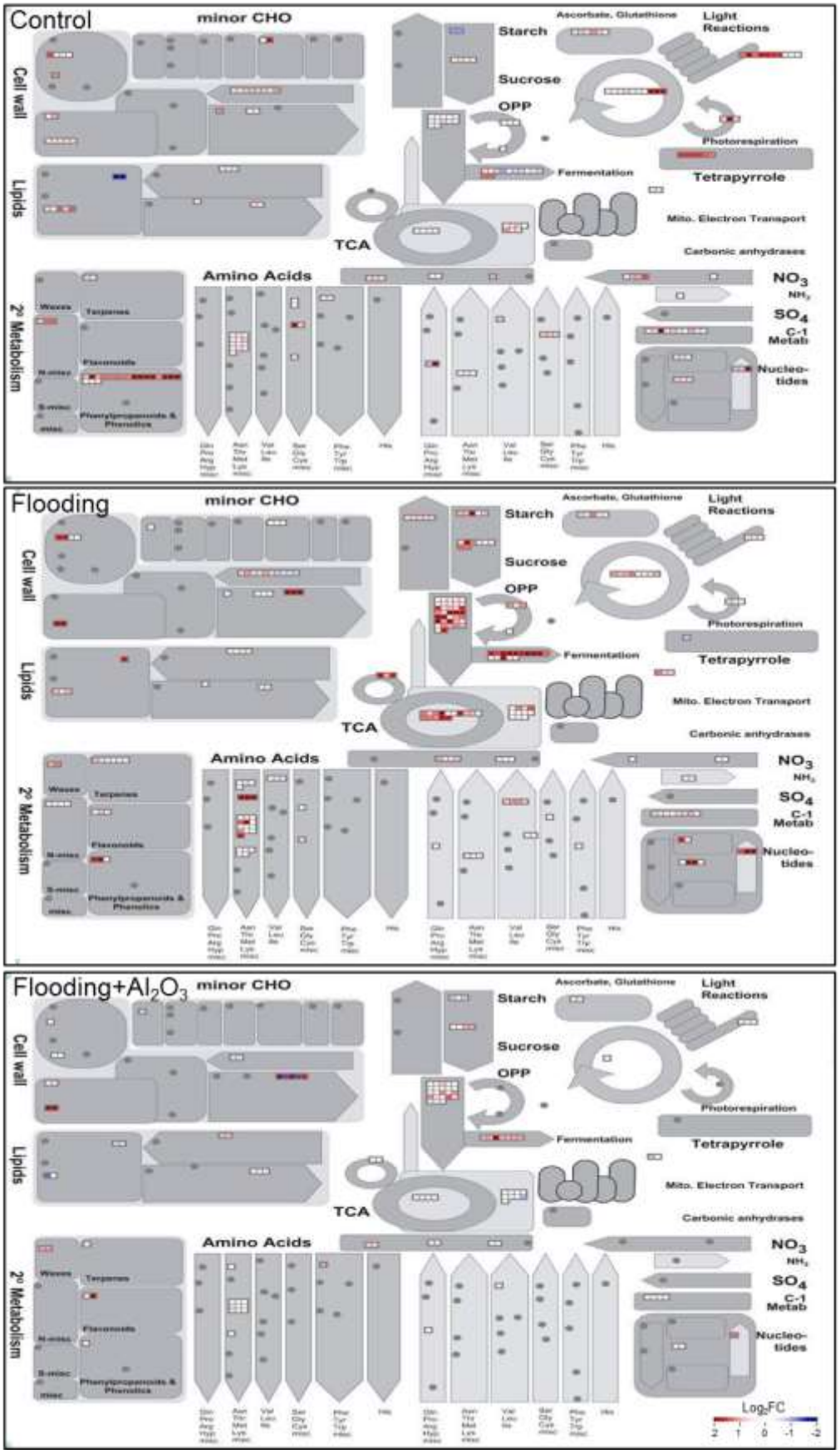
Control
minor CHO
Cell wall
Lipids
2º Metabolism
Starch
Sucrose
OPP
Fermentation
TCA
Amino Acids
Ascorbate, Glutathione
Light Reactions
Photorespiration
Tetrapyrrole
Mito. Electron Transport
Carbonic anhydrases
NO3
NH3
SO4
C-1 Metab
Nucleo-tides
Waxes
Terpenes
Flavonoids
Phenylpropanoids & Phenolics
Flooding
minor CHO
Flooding+Al2O3
minor CHO
Log2FC
2
1
0
-1
-2

Figure 22. Abundances of proteins identified in flooding-stressed soybean treated with Al_2O_3 NPs. The 586, 782, and 453 significantly changed proteins in the control, flooding-stressed, and flooding-stressed plants treated with Al_2O_3 NPs, respectively, after 1 day of stress were used. The abundance changes of proteins grouped into the functional categories related to primary metabolism were visualized using MapMan software. Each square and color indicates the Log_2FC value of a differentially changed protein. Red, blue, and white colors indicate an increase, decrease, and no change in the Log_2FC value in each treatment compared to those of 2-day-old untreated soybean.

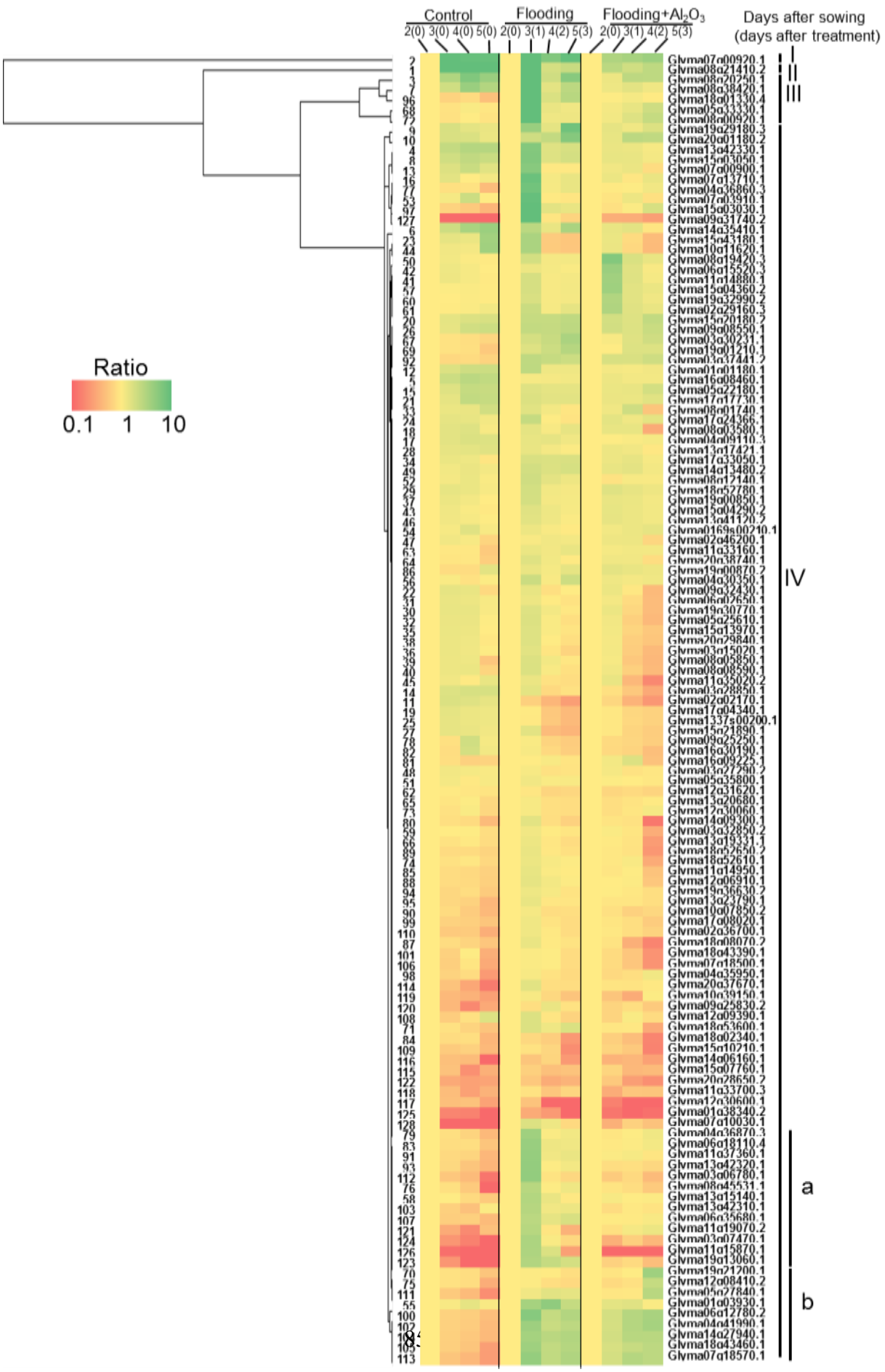
Control
Flooding
Flooding+Al2O3
Days after sowing
(days after treatment)
2(0) 3(0) 4(0) 5(0) 2(0) 3(1) 4(2) 5(3) 2(0) 3(1) 4(2) 5(3)
Ratio
0.1 1 10
I
II
III
IV
a
b

Figure 23. Cluster analysis of significantly changed proteins in soybean during temporal exposure to Al_2O_3 NPs. Abundance patterns of individual proteins are indicated based on the color legend for the control and flooding stress treatments without and with Al_2O_3 NPs at 0, 1, 2, and 3 days (from left to right). Red, green, and yellow colors indicate a decrease, increase, and no change of protein abundance, respectively, compared to those of 2-day-old soybeans. The temporal abundance profiles of the 128 changed proteins that were commonly identified among the control, flooding-stressed, and flooding-stressed plants treated with Al_2O_3 NPs were used to group the proteins into four clusters, which are indicated by black bars to the right of the protein IDs. Sub-clusters 'a' and 'b' indicate significant clusters within cluster IV. Protein IDs are indicated to the right of the abundance profile and the number to the left corresponds to the protein number in Table 5.

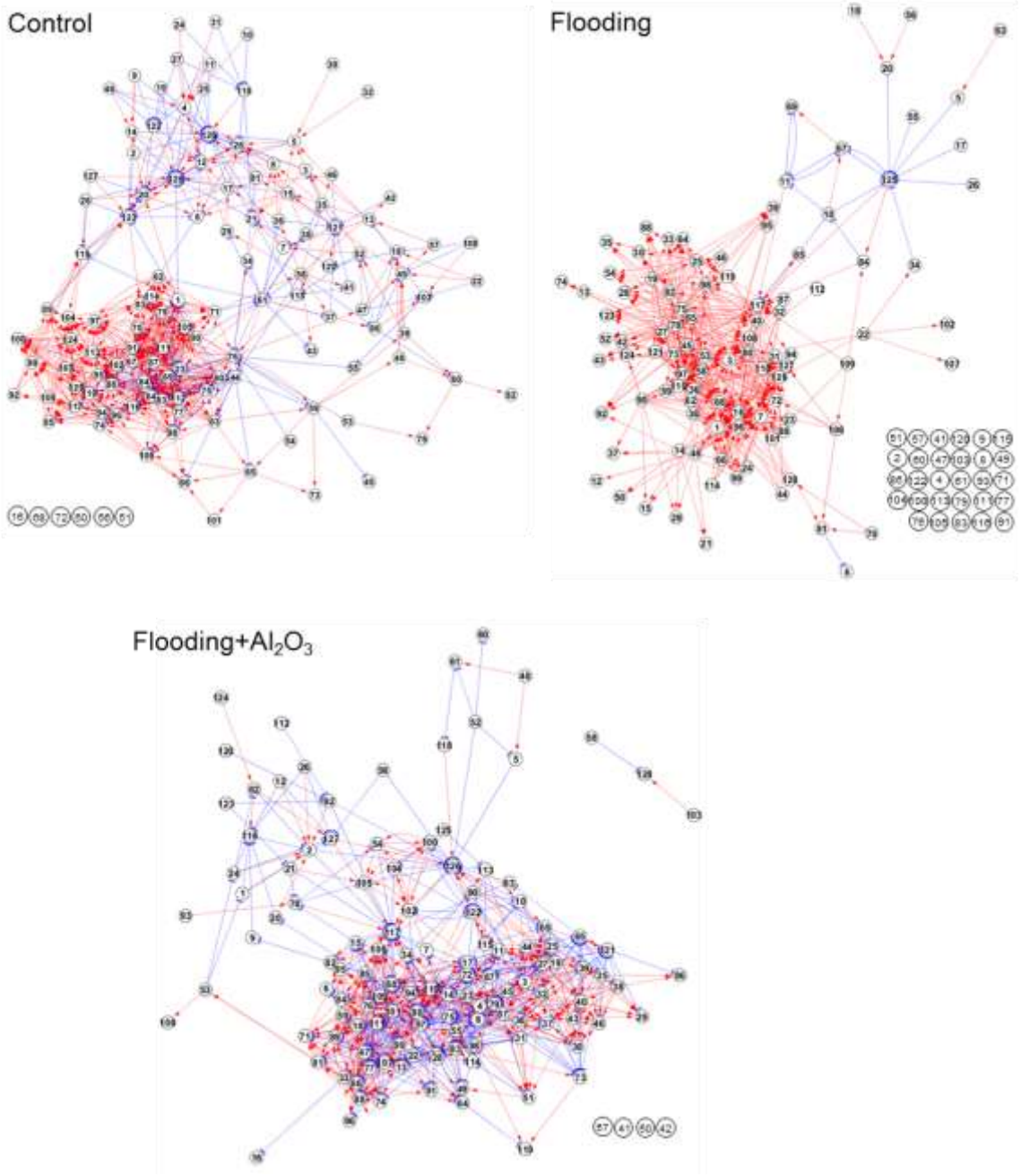

Figure 24. *In silico* protein-protein interaction analysis of significantly changed proteins in soybean during temporal exposure to Al_2O_3 NPs. Protein interactions of the control, flooding-stressed, and flooding-stressed plants treated with Al_2O_3 NPs were analyzed based on time course data compared to 2-day-old soybeans. Red arrows indicate inductive interactions, and blue T-bar show suppressive interactions. Protein numbers are the same as in Table 5.

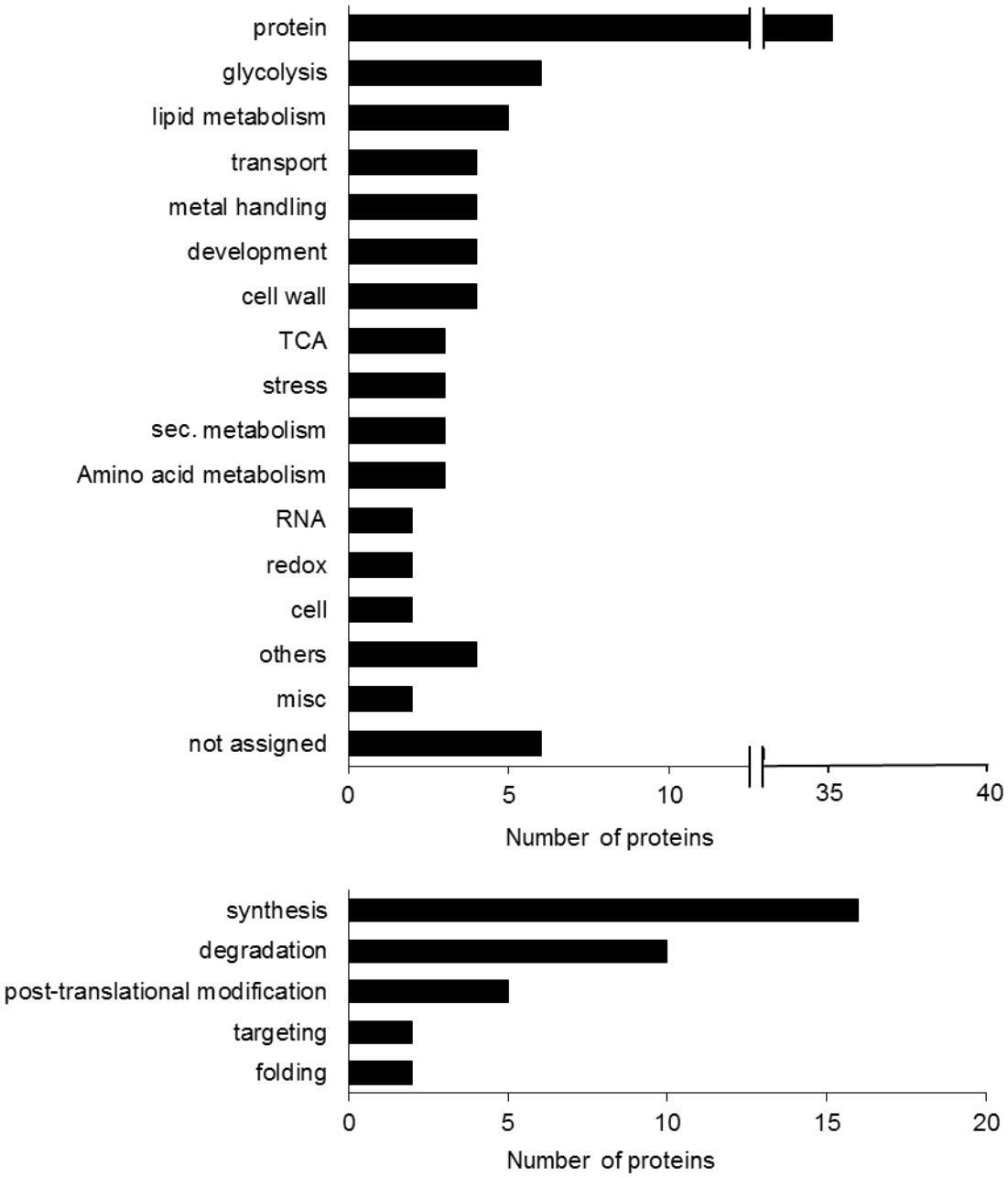

Figure 25. Functional categorization of Al_2O_3 NPs responsive proteins identified in flooding-stressed soybean. Two-day-old soybeans were flooded without or with Al_2O_3 NPs for 1, 2, and 3 days, and proteins were identified using a gel-free proteomic technique. The 92 identified Al_2O_3 NPs-responsive proteins were functionally categorized using MapMan bin codes. The *x*-axis indicates the number of identified proteins. The proteins in the 'protein' functional category were further divided into five sub-categories. Abbreviations are the same as in Figure 11.

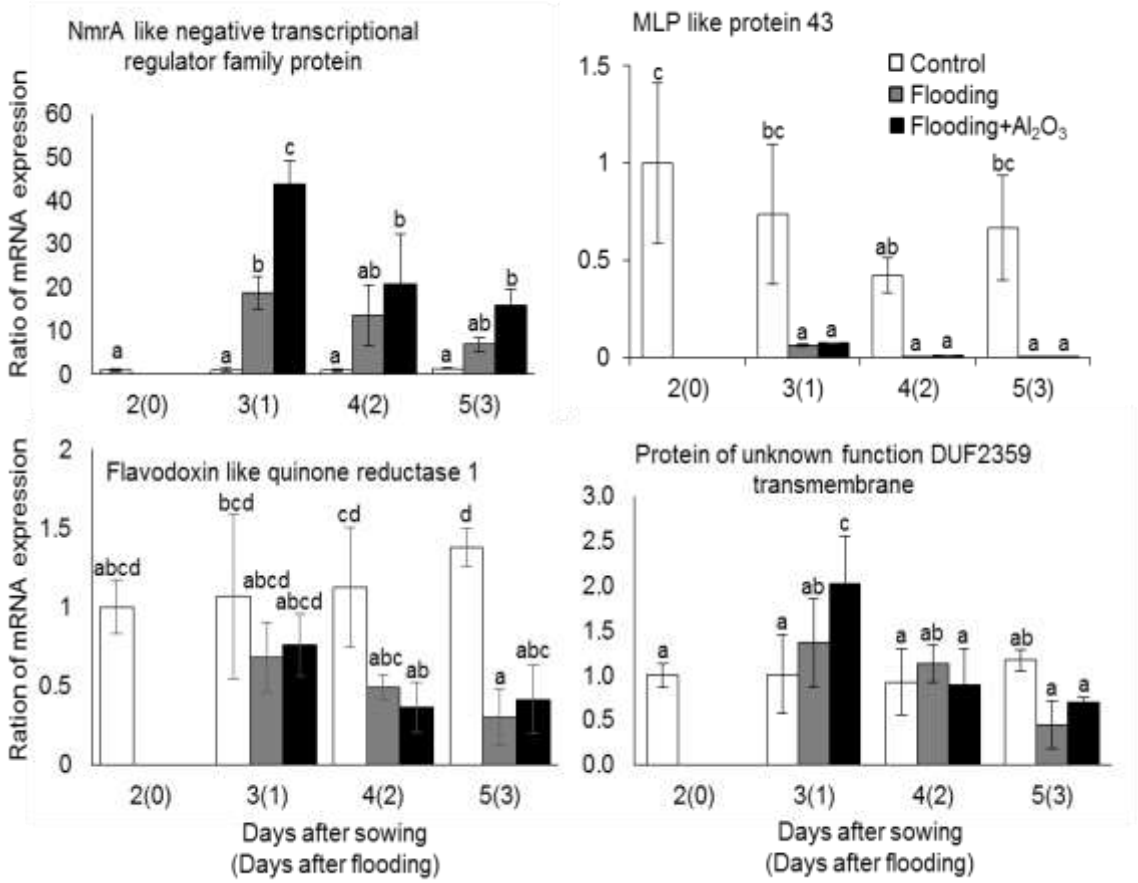

Figure 26. Effects of Al_2O_3 NPs on the mRNA expression levels of proteins with significantly changed abundance ratios. Two-day-old soybeans were flooded without (grey columns) and with (black columns) 50 ppm Al_2O_3 NPs for 1, 2, and 3 days. Untreated plants served as controls (white columns). RNAs extracted from the root including hypocotyl of soybeans were analyzed by qRT-PCR. Relative mRNA abundances of *NmrA-like negative transcriptional regulator family protein* (Glyma11g07490.1), *MLP like protein 43* (Glyma08g24720.1), *flavodoxin-like quinone reductase 1* (Glyma08g06570.1), and *protein of unknown function DUF2359 transmembrane* (Glyma05g27090.1) were normalized against 18S rRNA abundance. The data are presented as the mean ± S.D. from three independent biological replicates (n=3). Statistical analysis is same as described in Figure 5.

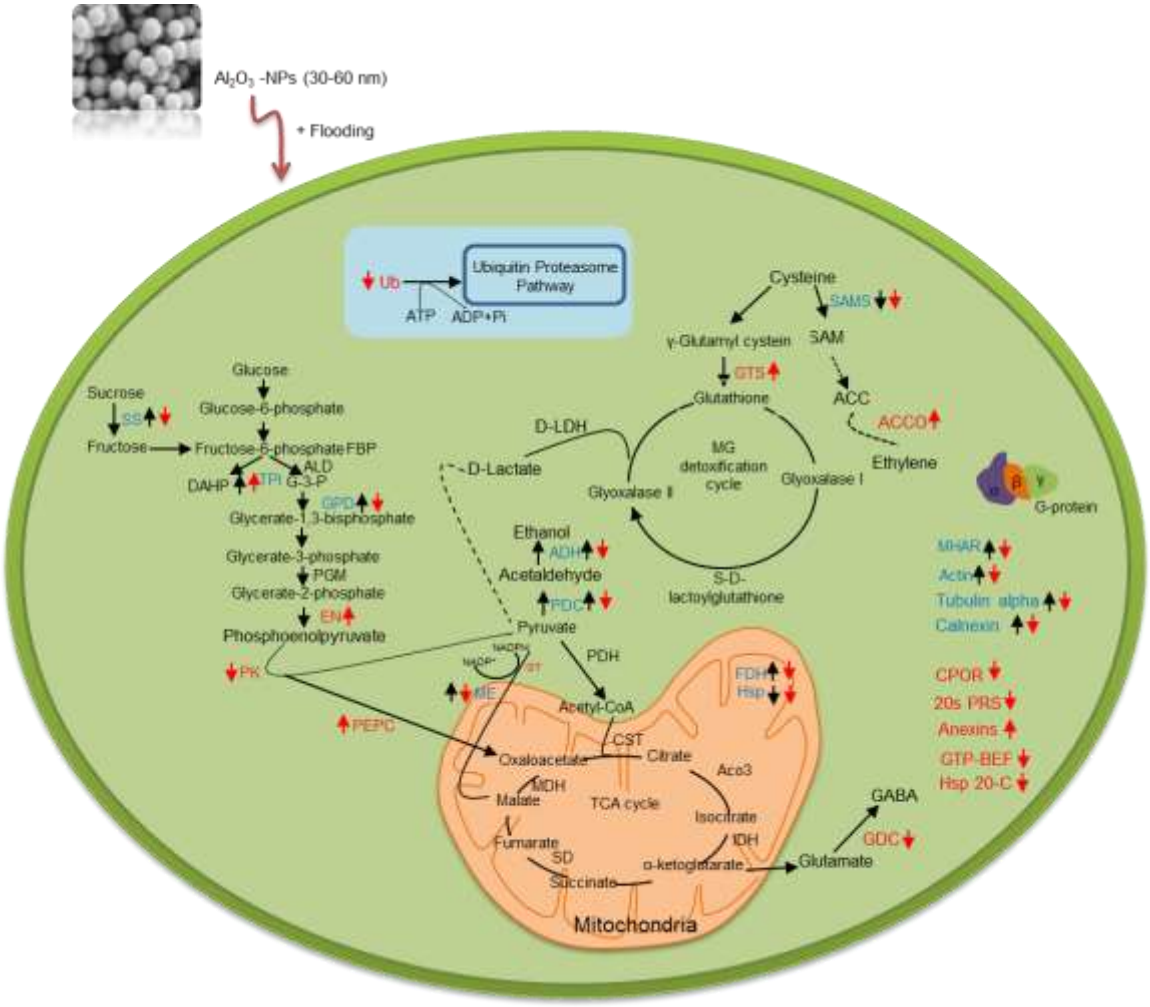

Figure 27. Al_2O_3 NPs mediated changes in metabolic pathways under flooding stress. Black and red arrows indicate changes in protein abundance (upward arrows indicate increase and downward arrows indicate decrease) in response to flooding and Al_2O_3 NPs, respectively. Protein names in blue color indicate their identifications from both flooding and Al_2O_3 NPs treatments; however, red color indicate proteins only identified in Al_2O_3 NPs treatment. Proteomic findings indicate that Al_2O_3 NPs mediate the metabolic shift from anaerobic to aerobic energy metabolism. Abbreviations: ACC, 1-aminocyclopropane-1-carboxylic acid; ACCO, ACC oxidase; ADH; alcohol dehydrogenase; CPOR, cysteine peroxiredoxin; CS, cysteine synthase; DHAP; dihydroxyacetone phosphate; ENO, enolase; PDC, pyruvate decarboxylase; SAM, *S*-adenosylmethionine; SAMS, SAM synthetase; SS, sucrose synthase; ME, NADP malic enzyme; MHAR, monohydroascorbate reductase; GS, glutathione synthetase; PK, pyruvate kinase; PEPC, phosphoenolpyruvate carboxylase; GDC, glutamate decarboxylase; GABA, gamma-aminobutyric acid; GT, glycosyl transferase; 20s PRS, 20s proteasome alpha subunit; GTP-BEf, GTP binding elongation factor.

CHAPTER 4
CHARACTERIZATION OF NANOPARTICLES-MEDIATED SOYBEAN PROTEINS UNDER FLOODING STRESS

4.1. Introduction

The NPs are responsible for changing biological activities including ROS generation (Manke et al., 2013). Various reports suggested the deposition and accumulation of metal NPs on cellular surface as well as inside organelles caused oxidative stress (Buzea et al., 2007). NP-mediated oxidative stress depends on NPs size, surface area, composition, and presence of metals; while, cellular factors include mitochondrial respiration, NP-cell interaction, and immune cell activation (Manke et al., 2013). Various studies indicated the entry of Ag NPs into cells causing mitochondrial dysfunction, generation of ROS, leading to damage to proteins, and finally inhibition of cell proliferation (He et al., 2012). Verano-Braga et al. (2014) reported that the NP induced cellular damage is size-dependent. They reported that the 20 nm Ag NPs could enter the cell and caused cellular stress including the generation of ROS and protein carbonylation. On the other hand, 100 nm Ag NPs indirectly generated the oxidative stress (Verano-Braga et al., 2014). Based on the differential growth effects caused by varying sizes of NPs, the molecular mechanisms affected by the varying sizes of NPs need intensive investigation.

In *Arabidopsis*, different sizes of Ag NPs caused ROS accumulation and root growth promotion (Syu et al., 2014). Forty five and 2 nm Ag NPs caused the lowest and highest accumulation of superoxide dismutase, respectively. Along with this, Ag NPs activated the gene expression involved in cellular events (Syu et al., 2014). In another study, 6 nm Ag NPs reduced plant growth compared to 20 nm Ag NPs (Yin et al., 2012). The NPs toxicity mechanism could be related to size-dependent effects on plants. In the case of Ag NPs, the toxicity was reported to be influenced by NPs surface area (Yin et al., 2012). Six nm NPs more strongly affected the growth compared to 25 nm Ag NPs at similar concentrations (Yin et al., 2012). Therefore, NPs could impart differential effects on plants depending on the size and surface area.

In the previous proteomic experiments of Chapters 2 and 3, Al_2O_3 and Ag NPs mediated the energy metabolism of soybean leading to better growth under flooding stress. This response was evaluated for the 15 and 30-60 nm of Ag and Al_2O_3 NPs, respectively. The Al_2O_3 and Ag NPs had positive effects on soybean under flooding stress. This proteomic experiment is carried out to study whether the variable sizes of

these two NPs also caused similar growth enhancing effects or not. For this purpose, soybean proteome with varying sizes of NPs under flooding stress was explored. In addition, bioinformatic analysis was used to confirm the proteomic results.

4.2. Materials and Methods

4.2.1. Plant material and treatments

Soybean was used as the plant material in this study. Plant growth conditions are described in 1.2.1 in Chapter 1. To study the effects of different NPs on the proteomics of soybean, Al_2O_3 (5, 30-60, and 135 nm), and Ag (2, 15, and 50-80 nm) NPs at 50 and 5 ppm concentration were used, respectively. Two-day-old soybeans were treated with NPs for 0, 1, 2, and 3 days. For proteomic analysis, root including hypocotyl was collected as sample (Figure 28).

4.2.2. Protein extraction, purification, and digestion

Protein extraction, purification, and digestion is described in 2.2.2 in Chapter 2. For protein digestion, lysyl endopeptidase was used along with the trypsin at 1:100 enzyme/protein concentration. The resulting tryptic peptides were acidified with 10 μL of 20% formic acid and analyzed by nanoLC MS/MS.

4.2.3. Mass spectrometry analysis and protein identification of acquired mass spectrometry data

Mass spectrometry analysis is described in 2.2.3 in Chapter 2. Protein identifications of acquired mass spectrometry data is described in 2.2.4 in Chapter 2.

4.2.4. Differential analysis of the identified proteins

Differential analysis of the identified proteins is described in 2.2.5 in Chapter 2.

4.2.5. Functional analysis of identified proteins

Functional analysis of identified proteins is described in 2.2.6 in Chapter 2.

4.2.6. Subcellular localization of identified proteins

The *Arabidopsis* subcellular localization database, SUBA3 was used to determine all the homologous proteins that are likely to be found in mitochondria (Tanz et al., 2013).

4.2.7. Cluster analysis using protein abundance

Protein abundance ratios at different time points of flooding stress with Ag and Al_2O_3 NPs treatments were used for the cluster analysis, which was performed with the Genesis software (version 17.6, http://genome.tugraz.at) (Sturn et al., 2002).

4.2.8. Statistical analysis

Statistical analysis is described in 1.2.2 in Chapter 1.

4.3. Results

4.3.1. Functional analysis of soybean proteins identified with varying sizes of Ag NPs under flooding stress

To examine the effects of various sizes of Ag NPs on soybean under flooding stress, gel-free proteomic analysis was performed. Proteins were extracted from the root including hypocotyl of 2-day-old soybeans treated with and without flooding in the presence of Ag NPs for 1, 2, an 3 days. In the differential analysis of the proteins identified in soybean root including hypocotyl, 1,541 proteins were significantly changed in 1, 2, and 3-day-old soybeans under flooding stress condition. In response to 2 nm Ag NPs, the abundances of 870 proteins were differentially changed in the soybean root including hypocotyl after 1, 2, and 3 days of exposure. In flooding stress soybean root including hypocotyl exposed to 15 nm Ag NPs, the abundances of 1,002 proteins were differentially changed. In response to 50-80 nm Ag NPs, the abundances of 1,190 proteins were differentially changed after 1, 2, and 3 days of exposure. To identify the commonly and specifically responsive proteins among the flooding, flooding with 2, 15, and 50-80 nm Ag NPs, a Venn diagram was generated. In the Venn diagram, the abundances of 504 proteins were commonly changed among the soybean plants under the four different treatments (Figure 29).

To determine the functional role of the identified proteins, functional categorization

was performed using MapMan bin codes (Figure 29). The functional categorization revealed that the proteins related to protein, cell, amino acid metabolism, and stress were differentially changed under the different treatments (Figure 29). The most affected categories under the varying sizes of Ag NPs were tricarboxylic acid cycle, redox, and mitochondrial electron transport chain (Figure 29).

4.3.2. Functional analysis of soybean proteins identified with varying sizes of Al_2O_3 NPs under flooding stress

To examine the effects of various sizes of Al_2O_3 NPs on soybean under flooding stress, gel-free proteomic analysis was performed. Proteins were extracted from the root including hypocotyl of 2-day-old soybeans treated with and without flooding in the presence of Al_2O_3 NPs for 1, 2, and 3 days. In the differential analysis of the proteins identified in soybean root including hypocotyl, the 1,541 proteins were significantly changed in 1, 2, and 3-day-old soybeans under flooding stress condition. In response to 5 nm Al_2O_3 NPs, the abundances of 1,360 proteins were differentially changed in the soybean root including hypocotyl after 1, 2, and 3 days of exposure. In flooding stress soybean root including hypocotyl exposed to 30-60 nm Al_2O_3 NPs, the abundances of 1,856 proteins were differentially changed. In response to 135 nm Al_2O_3 NPs, the abundances of 1,668 proteins were differentially changed after 1, 2, and 3 days of exposure. To identify commonly and specifically responsive proteins among the flooding, flooding with 5, 30-60, and 135 nm Al_2O_3 NPs, a Venn diagram was generated. In the Venn diagram, the abundances of 1,045 proteins were commonly changed among the soybean plants under the four different treatments (Figure 30).

To determine the functional role of the identified proteins, their functional categorization was performed using MapMan bin codes (Figure 30). Among the treatments, differentially changed proteins were related to the protein, cell metabolism, amino acid metabolism, and stress related proteins. The most affected categories under the varying sizes of Al_2O_3 NPs were tricarboxylic acid cycle, redox, and mitochondrial electron transport chain.

4.3.3. Subcellular localization of the identified proteins during temporal exposure to

Ag and Al_2O_3 NPs

In order to interpret the localization of the proteins which were identified under flooding stress without or with Ag NPs of 2, 15, and 50-80 nm, the subcellular localization was performed using SUBA3 (Tanz et al., 2013). The subcellular localization data revealed that the identified proteins were mainly localized in the cytosol, mitochondria, and plastids (Figure 31). Mitochondria was identified as the target organelle affected under the flooding stress without or with Ag NPs of 2, 15, and 50-80 nm. Out of total proteins, 1541, 870, 1002, and 1190, the proteins localized in the mitochondria were 91, 40, 65, and 65 proteins under flooding without or with Ag NPs of 2, 15, and 50-80 nm, respectively (Figure 31). In Al_2O_3 NPs treated soybean, the subcellular localization data revealed that the identified proteins were mainly localized in the cytosol, mitochondria, and plastids (Figure 32). Mitochondria was identified as the target organelle affected under the flooding stress without or with Al_2O_3 nanoparticles of 5, 30-60, and 135 nm. Out of total proteins, 1541, 1360, 1856, and 1668, the proteins localized in the mitochondria were 91, 65, 104, and 86 proteins under flooding without or with Al_2O_3 NPs of 5, 30-60, and 135 nm, respectively (Figure 32).

4.3.4. Cluster analysis of the identified mitochondrial proteins during temporal exposure to Ag and Al_2O_3 NPs

To further analyze the abundance profiles of the significantly changed mitochondrial proteins that were commonly identified in soybean root including hypocotyl under flooding stress without and with Ag NPs of 2, 15, and 50-80 nm, hierarchical clustering analysis was performed. The abundance of 25 mitochondrial proteins were commonly changed among the flooding and flooding with Ag NPs of 2, 15, and 50-80 nm (Figure 34). These 25 significantly changed proteins were subjected to hierarchical clustering analysis using their abundance ratios. Using a hierarchical clustering approach, 4 clusters (I-IV) of significantly changed mitochondrial proteins were recognized (Figure 33). Cluster I consisted of two mitochondrial proteins whose abundances were increased under the flooding and flooding with Ag NPs of 2, 15, and 50-80 nm compared to the control condition (Figure 33). Cluster II consisted of three mitochondrial proteins whose abundances were increased on exposure to flooding while this increase was less evident

on exposure to flooding with Ag NPs of 2, 15, and 50-80 nm (Figure 33). Cluster III consisted of 7 mitochondrial proteins whose abundances were almost same like the control under flooding and flooding with Ag NPs of 2, 15, and 50-80 nm (Figure 33). Cluster IV consisted of 13 mitochondrial proteins whose abundances were decreased under flooding and flooding with Ag NPs of 2, 15, and 50-80 nm (Figure 33).

To further analyze the abundance profiles of the significantly changed mitochondrial proteins that were commonly identified in soybean root including hypocotyl under flooding stress without and with Al_2O_3 NPs of 5, 30-60, and 135 nm, hierarchical clustering analysis was performed. The abundance of 58 mitochondrial proteins were commonly changed among the flooding and flooding with Al_2O_3 NPs of 5, 30-60, and 135 nm (Figure 34). These 58 significantly changed proteins were subjected to hierarchical clustering analysis using their abundance ratios. Using a hierarchical clustering approach, 4 clusters (I-IV) of significantly changed mitochondrial proteins were recognized (Figure 34). Cluster I consisted of two mitochondrial proteins whose abundances were increased under the flooding and flooding with Al_2O_3 NPs of 5, 30-60, and 135 nm compared to the control condition (Figure 34). Cluster II consisted of 20 mitochondrial proteins whose abundances were increased on exposure to flooding and flooding with Al_2O_3 NPs of 5 nm while decreased with Al_2O_3 NPs of 30-60 and 135 nm. On the other hand, the abundances of these proteins were increased almost equal to the level of control on exposure to Al_2O_3 NPs of 135 nm (Figure 34). Cluster III consisted of 16 mitochondrial proteins whose abundances were increased under flooding and flooding with Al_2O_3 NPs of 5 and 30-60 nm while decreased on exposure to Al_2O_3 nanoparticles of 5, 30-60, and 135 nm (Figure 34). Cluster IV consisted of 20 mitochondrial proteins whose abundances were decreased under flooding and flooding with Al_2O_3 NPs of 5, 30-60, and 135 nm (Figure 34).

4.4. Discussion

4.4.1. Effect of varying sizes of Ag and Al_2O_3 NPs on the mitochondrial proteins under flooding stress

The different morphologies of NPs were reported to cause the differential growth effects on the plants. Syu et al. (2014) reported that the different sizes of Ag NPs caused

differential growth effects on the *Arabidopsis* by regulating the different proteins. Verano-Braga et al. (2014) reported that the smaller NPs could enter the cell and cause direct effects; however, larger NPs cause indirect effects because of their inability to cross the plasma membrane. In the present study, the different sizes of NPs mainly affected the tricarboxylic acid cycel, redox, and mitochondrial electron transport chain related proteins. The smaller NPs affected the cell wall related proteins; however, larger NPs affected the signaling related proteins. These results suggest that the different sizes of NPs cause alterations in the soybean proteins under flooding stress.

Plant mitochondria are the principle organelle responsible for the aerobic respiration. In these organelles, the organic acids are oxidized to generate energy in the form of ATP. In the mitochondrial matrix, the TCA cycle oxidized the organic acids into CO_2 and H_2O, thereby providing electrons from reducing NADH to O_2 through the electron transport chain (Sweetlove et al., 2007). Along with this, mitochondria are also responsible for the synthesis of nucleotides, metabolism of amino acids and vitamins, cofactors, and participation in the photorespiratory pathways (Millar et al., 2005). Mitochondria has central role in plant metabolic processes. Previous studies reported that the flooding stress damaged the mitochondria and directly impairs the electron transport chain; however, the NADH production was increased through the TCA cycle (Komatsu et al., 2011b). In the present study, the mitochondrial proteins were predominantly affected under the varying sizes of Ag and Al_2O_3 NPs. The varying sizes of NPs might regulate the molecular mechanisms by regulating the mitochondrial proteins.

4.5. Conclusion

The NPs are extensively used in agricultural products (Vernikov et al., 2009) and cause various growth effects on different plant species (Yang and Watts, 2005). The present proteomic experiment investigated the effects of varying sizes of Ag and Al_2O_3 NPs on soybean under flooding stress. The major findings of this experiment are as follows: (i) the different sizes of Ag NPs mainly affected the proteins related to tricarboxylic acid cycle, redox, and mitochondrial electron transport chain; (ii) the different sizes of Al_2O_3 NPs changed the abundances of tricarboxylic acid cycle, redox,

and mitochondrial electron transport chain; (iii) mitochondria was the target organelle for the varying sizes of Ag and Al_2O_3 NPs under flooding stress; (iv) mitochondrial proteins were differentially regulated under the varying sizes of Ag and Al_2O_3 NPs. Taken together, these results suggest that Ag and Al_2O_3 NPs affected the mitochondria as the target organelle by causing the changes in the mitochondrial proteins suggesting the involvement of size dependency of NPs.

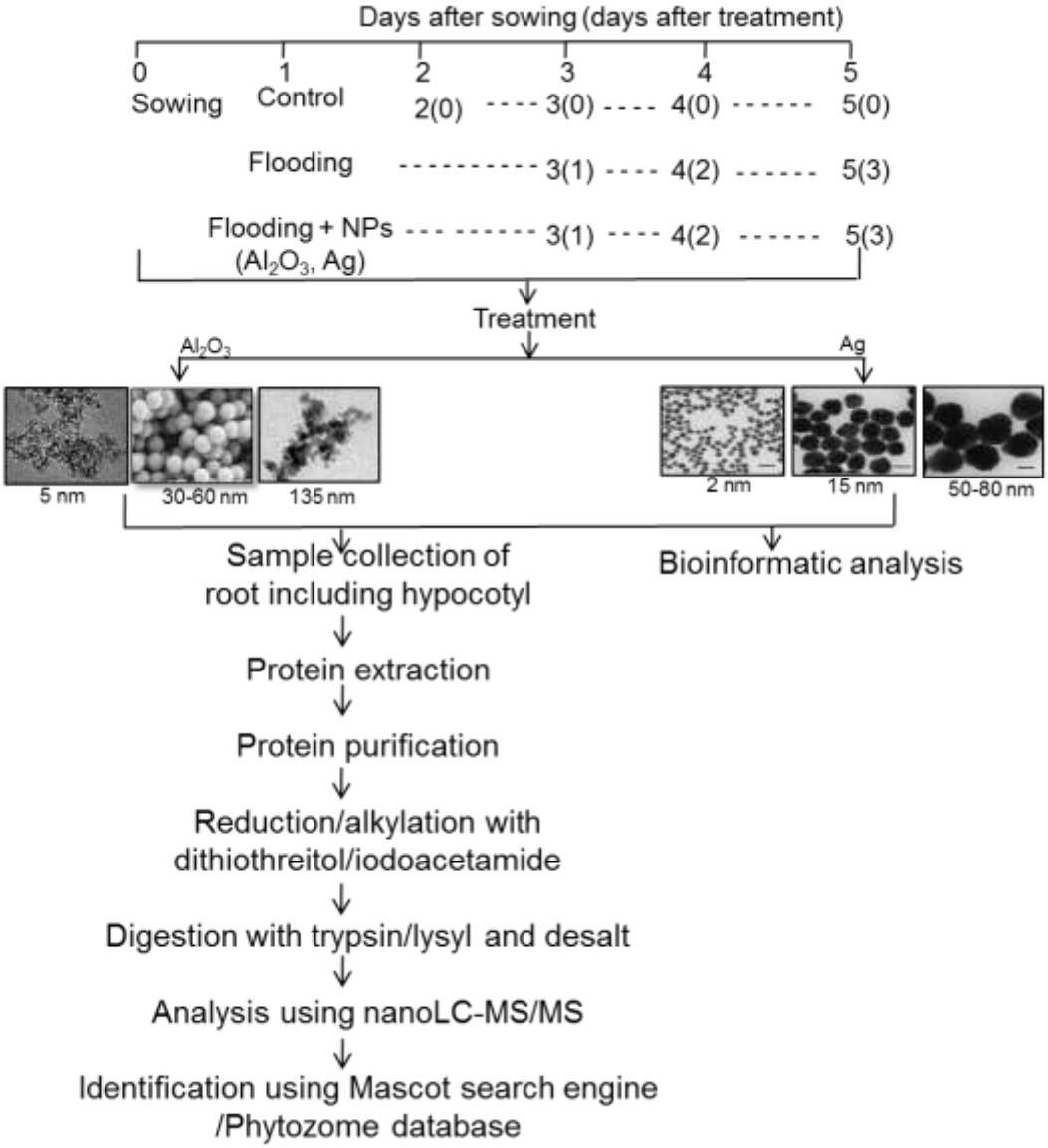

Figure 28. Experimental design to examine the effects of varying sizes of Ag and Al_2O_3 NPs on soybean under flooding stress. Two-day-old soybeans were treated without (F) or with (Flooding+Ag NPs 2, 15, and 50-80 nm) or (Flooding+ Al_2O_3 NPs 5, 30-60, 135 nm) flooding stress and Ag or Al_2O_3 NPs for 1, 2, and 3 days. Untreated plant served as control. For proteomic analysis, proteins extracted from root including hypocotyl were analyzed using nanoLC-MS/MS.

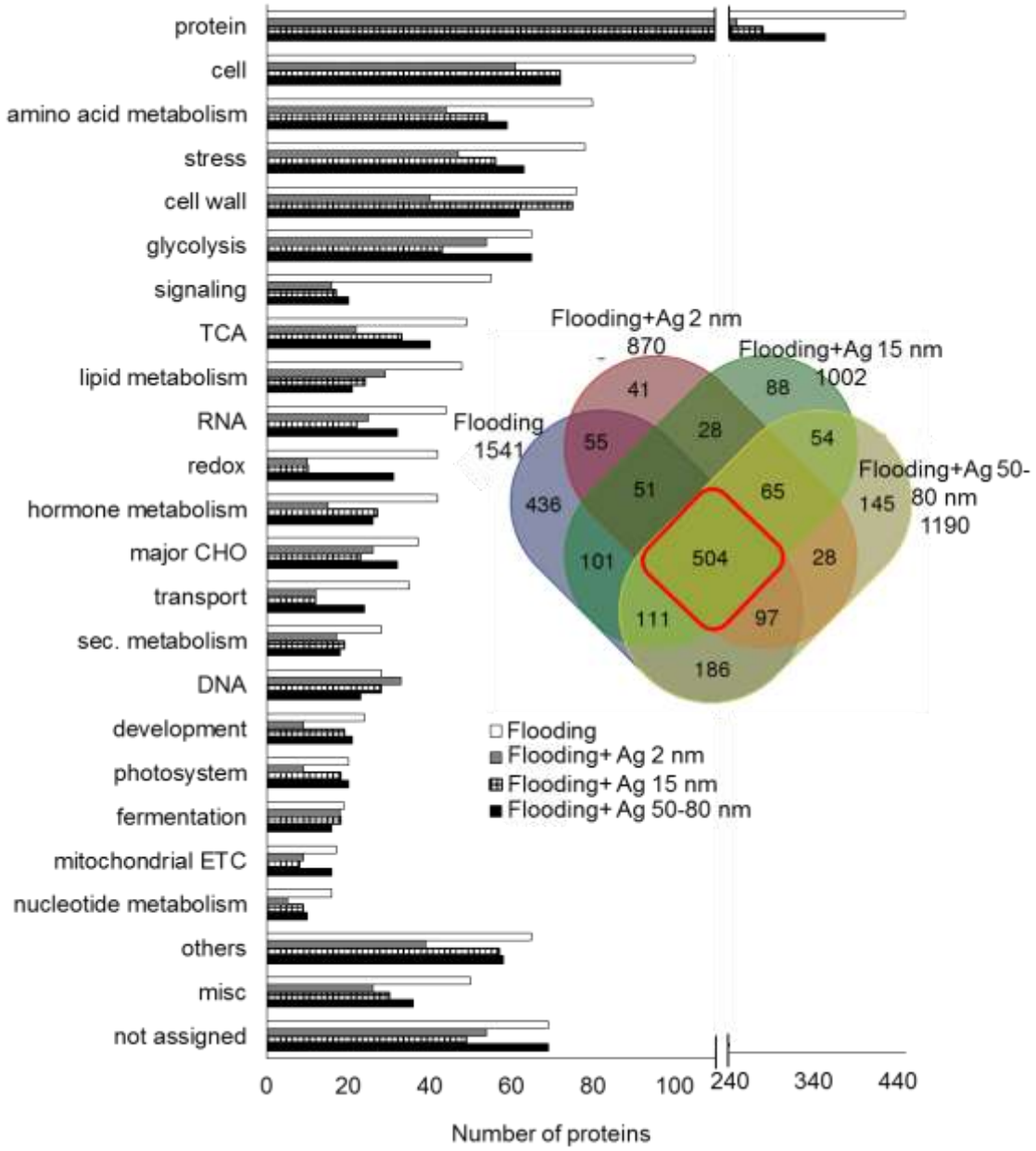

Figure 29. Functional categorization of Ag NPs responsive proteins identified in flooding-stressed soybean. Two-day-old soybeans were flooded for 1, 2, and 3 days without or with Ag NPs (Flooding + Ag 2, 15, 50-80). Untreated plants served as the control. Proteins were extracted from root including hypocotyl, and identified using a gel-free proteomic technique. Significantly changed proteins according to SIEVE software ($p < 0.05$) were analyzed. MapMan bin codes were used to predict the functional categorization of the identified proteins. The *x*-axis indicates the number of identified proteins. Abbreviations are the same as in Figure 11.

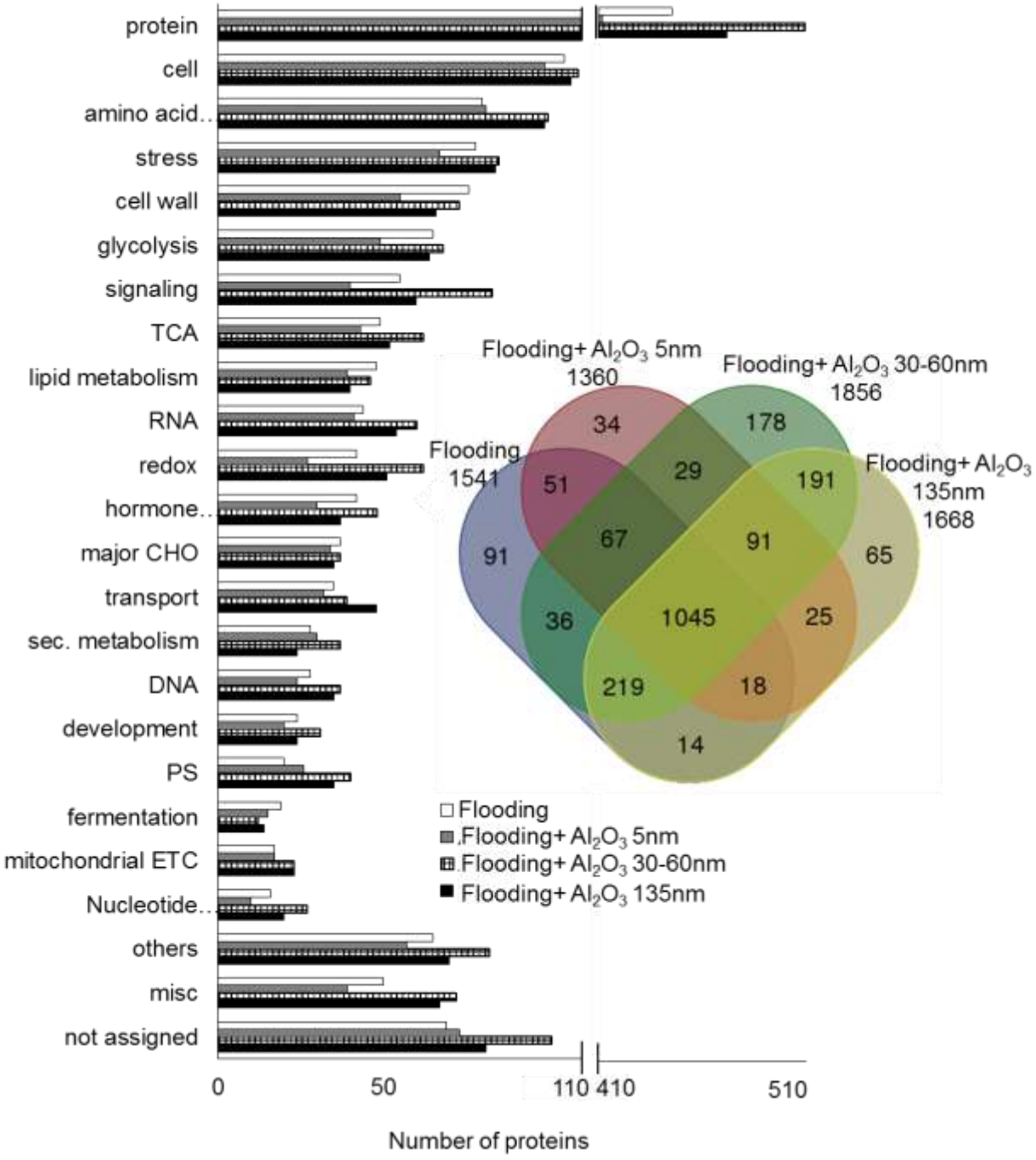

Figure 30. Functional categorization of Al_2O_3 NPs responsive proteins identified in flooding-stressed soybean. Two-day-old soybeans were flooded for 1, 2, and 3 days without or with Al_2O_3 NPs (Flooding + Al_2O_3 5, 30-60, 135). Untreated plants served as the control. Proteins were extracted from root including hypocotyl, and identified using a gel-free proteomic technique. Significantly changed proteins according to SIEVE software ($p < 0.05$) were analyzed. MapMan bin codes were used to predict the functional categorization of the identified proteins. The *x*-axis indicates the number of identified proteins. Abbreviations are the same as in Figure 11.

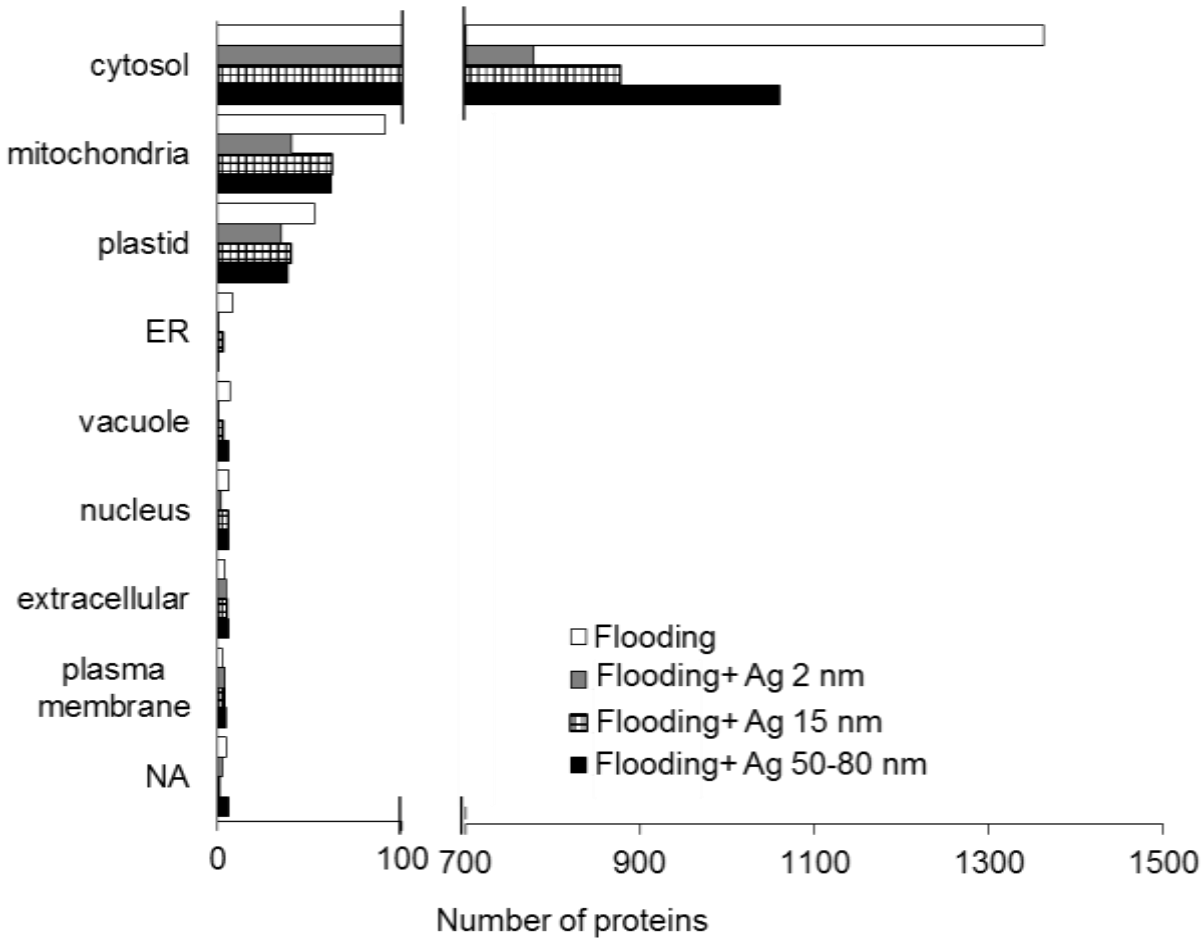

Figure 31. Subcellular localization of significantly changed proteins in soybean during temporal exposure to varying sizes of Ag NPs. SUBA3 was used to predict the subcellular localization of the identified proteins. The *x*-axis indicates the number of identified proteins. The subcellular localization of identified proteins are indicated without (Flooding, white columns) or with Ag 2 nm (grey columns), 15 nm (white square columns), and 50-80 nm (black columns) NPs.

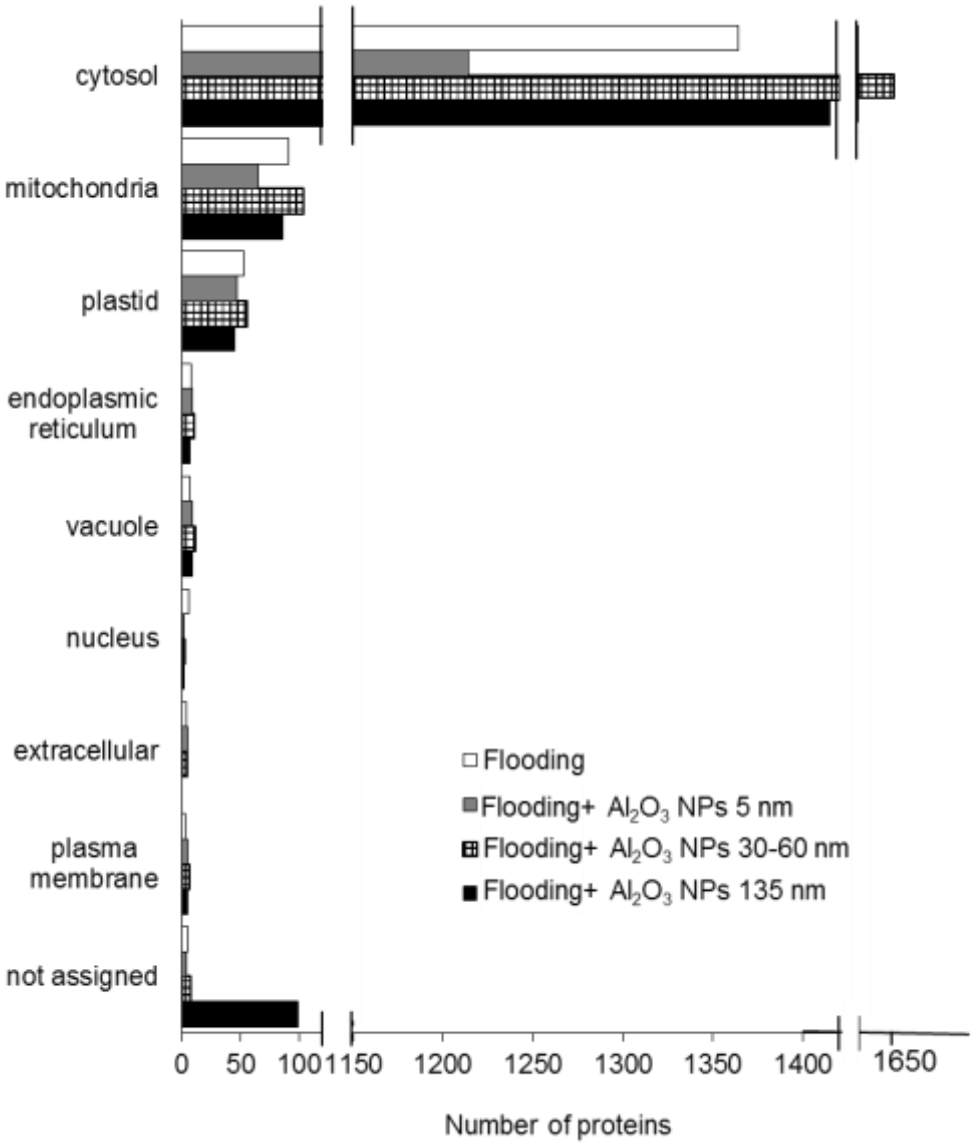

Figure 32. Subcellular localization of significantly changed proteins in soybean during temporal exposure to varying sizes of Al_2O_3 NPs. SUBA3 was used to predict the subcellular localization of the identified proteins. The *x*-axis indicates the number of identified proteins. The subcellular localization of identified proteins are indicated without (Flooding, white columns) or with Al_2O_3 5 nm (grey columns), 30-60 nm (white square columns), and 135 nm (black columns) nanoparticles.

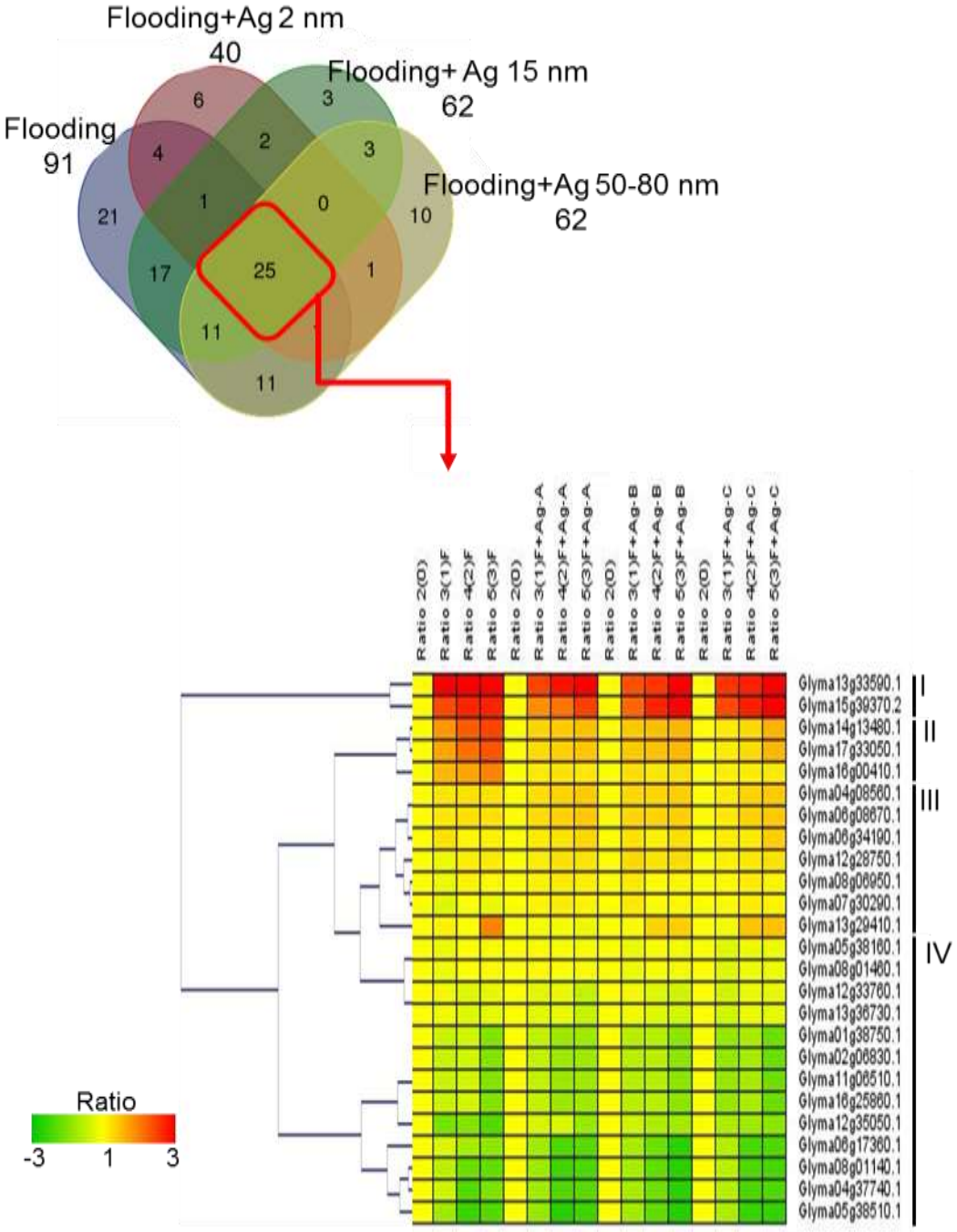

Figure 33. Cluster analysis of significantly changed mitochondrial proteins in soybean during exposure to varying sizes of Ag NPs. Abundance patterns of individual proteins are indicated based on the color legend for the flooding stress treatments without and with Ag NPs of 2, 15, and 50-80 nm at 0, 1, 2, and 3 days (from left to right). Red, green, and yellow colors indicate an increase, decrease, and no change of protein abundance, respectively, compared to those of 2-day-old soybeans. The temporal abundance profiles of the 25 changed mitochondrial proteins that were commonly identified among the flooding, flooding with Ag NPs of 2, 15, and 50-80 nm treated plants were used to group the proteins into four clusters, which are indicated by black bars to the right of the protein IDs. Protein IDs are indicated to the right of the abundance profile.

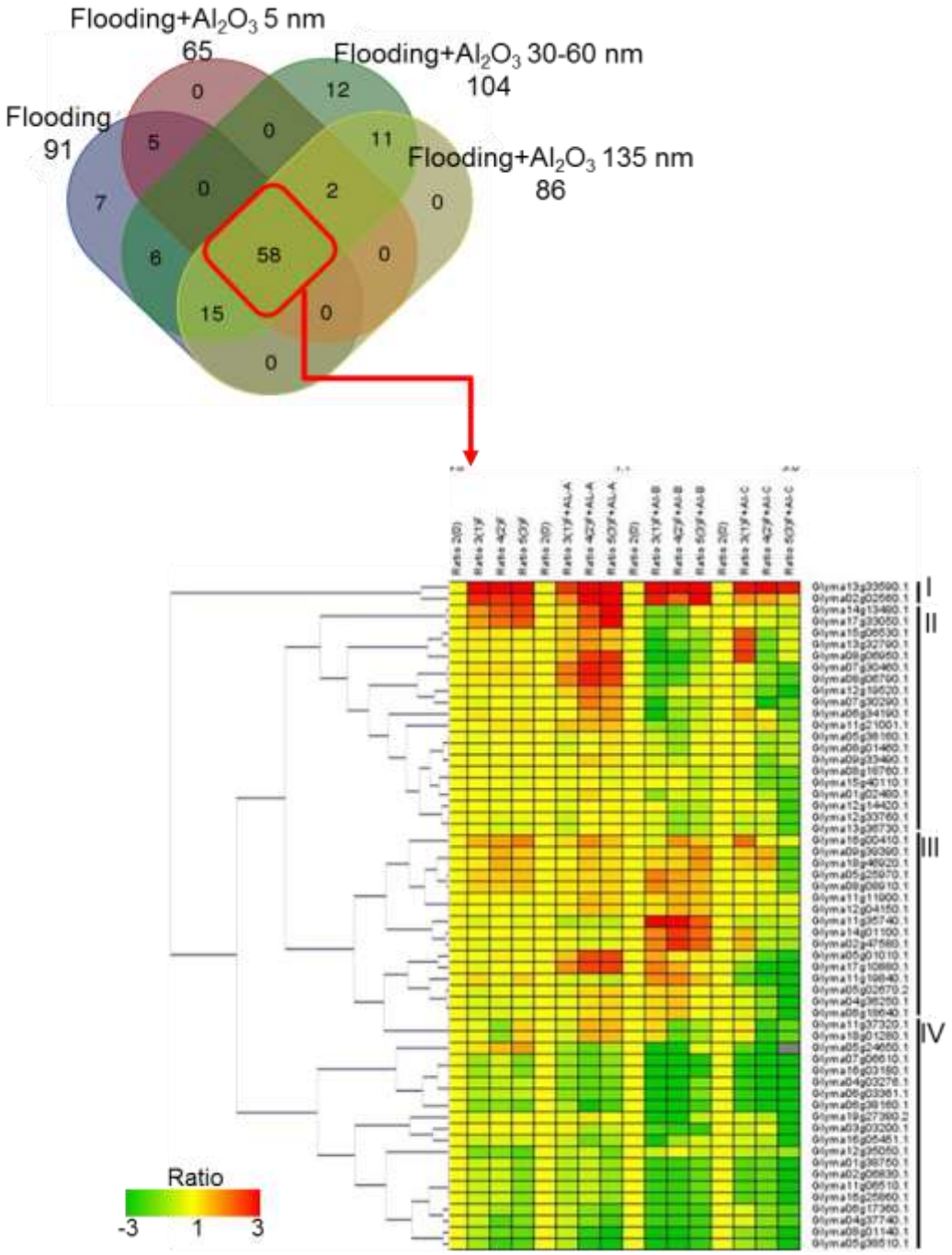

Figure 34. Cluster analysis of significantly changed mitochondrial proteins in soybean during exposure to varying sizes of Al_2O_3 NPs. Abundance patterns of individual proteins are indicated based on the color legend for the flooding stress treatments without and with Al_2O_3 NPs of 5, 30-60, and 135 nm at , 1, 2, and 3 days (from left to right). Red, green, and yellow colors indicate an increase, decrease, and no change of protein abundance, respectively, compared to those of 2-day-old soybeans. The temporal abundance profiles of the 58 changed mitochondrial proteins that were commonly identified among the flooding, flooding with Al_2O_3 NPs of 5, 30-60, and 135 nm treated plants were used to group the proteins into four clusters, which are indicated by black bars to the right of the protein IDs. Protein IDs are indicated to the right of the abundance profile.

CONCLUSION AND FUTURE PROSPECTS

Climate change around the globe is responsible for the imbalance in the earth's ecosystem. These changing climatic conditions are a major threat to crop production (Eigenbrod et al., 2015). Under these variations, plants are at the foreface of many abiotic stresses. The global climate variation significantly increased annual rainfall and this trend is likely to continue in the future (Kreuzwieser and Gessle, 2010). It has been estimated that almost 17 million square kilometer of land is affected by soil flooding every year with an annual damage exceeding 60 billion euro (Voesenek and Sasidharan, 2013). Flooding has deleterious effects on crop growth and cause a severe reduction in the yield (Normile, 2008). In different parts of the world, flooding caused severe crop destruction that leads to decreased, maize yield in Australia (Olesen et al., 2011), wheat and cotton yield in Pakistan (Arshad and Shafi, 2010), and maize and soybean yield in Europe (Bailey-Serres et al., 2012). Soybean is an important crop due to its high protein and oil content (Medic et al., 2014). The consumption of soybean-based products is increasing in the world (Medic et al., 2014). Mainly the soybean plant is intolerant to flooding stress (Hou et al., 1991). In the past, researches have been focused on exploring soybean response towards flooding stress. However, the molecular mechanisms being affected by flooding stress is yet to be unveiled.

Towards the development of modern agricultural techniques, nanotechnology occupies a prominent technological innovation that transforms the agriculture and food production. The production of nanodevices and nanomaterials could open up novel applications in the plant biotechnology and agriculture (Scrinis and Lyons, 2007). The rapid advancement and potential release of NPs into the ecosystem have raised concerns about their behavior of interaction due to their characteristic properties (Ma et al., 2010). Plants have naturally evolved in the presence of these NPs because of their production in the ecosystem (Pan and Xing, 2010). However, the probability of NPs interaction with the plants is increasing due to their ongoing increasing production and usage in the agricultural sector (Pan and Xing, 2010). The NPs interaction with plants cause both enhancive and inhibitive effects depending on their physical and chemical properties. Due to their ongoing production and interaction with plant species the

molecular mechanisms being affected are essential to explore. In this study, to understand the alterations in the molecular mechanisms caused by the NPs under flooding stress, the effect of different NPs was investigated using gel-free proteomic technique.

Different kinds of NPs are reported to cause different growth effects on plants depending on the plant species (Yang and Watts, 2005). Lee et al. (2010) investigated the phytotoxicity effects of four NPs on *A. thaliana*, and reported that the ZnO and Al_2O_3 NPs were the most and least toxic to the plant, respectively. Yin et al. (2012) reported that the smaller Ag NPs caused growth reduction compared to those of lager sizes. Tobacco growth was reduced on exposure to higher concentration of Al_2O_3 NPs compared to the low concentrations (Burklew et al., 2012). The Ag NPs are often detrimental to plant growth; however, a few studies demonstrated the growth-enhancing effects of Ag NPs on plants. In *E. sativa* and *B. juncea*, the Ag NPs stimulated the growth (Vannini et al., 2013; Sharma et al., 2012). The differential effects of NPs on the plant species are dependent on the size and concentration of the NPs.

In peanut, soybean, wheat, and onion, relatively low concentrations of ZnO NPs caused beneficial growth effects on seed germination (Prasad et al., 2012; Sedghi et al., 2013; Ramesh et al., 2014; Raskar and Laware, 2014). Along with this, the *Cyamopsis tetragonoloba* plant biomass, shoot/root length, chlorophyll content, and protein synthesis were improved with the application of ZnO NPs. ZnO NPs in the media promoted the somatic embryogenesis, shooting, regeneration, and activity of various antioxidant enzymes thus facilitating the tolerance against biotic stress (Helaly et al., 2014). In the present study, the medium sizes of Al_2O_3 and Ag NPs at very low concentrations facilitated the soybean growth under flooding stress. Under flooding stress, the Ag NPs promoted the growth of *C. sativus* by blocking the ethylene signaling (Rezvani et al., 2012). Plants are at the expense of various abiotic stresses. These multiple abiotic stresses might have positive or negative interactions with each other. As the cold and osmotic stress have negative effect on each other (Xiong et al., 1999). In the present study, the Al_2O_3/Ag NPs suppresses the effects of flooding stress; however, ZnO NPs did not show positive effects (Figure 35).

Proteins related to fermentation and glycolysis were increased under flooding

stress; however, decreased with the application of Al_2O_3 NPs. Several previous studies in soybean have revealed that proteins related to fermentation, scavenging, and glycolysis are affected by flooding stress (Nanjo et al., 2012; Hashiguchi et al., 2009), which limits the available oxygen supply (Colmer, 2003). Low oxygen conditions limit ATP generation and shift plant metabolism from oxidative pathways, such as carbohydrate metabolism, towards anaerobic pathways (Bailey-Serres and Voesenek, 2008). Komatsu et al. (2013) reported the activation of a fermentative pathway in the early stage of flooding stress as a stress tolerance mechanism in soybean. As an acclimation response to reduced oxygen conditions, plants induce the activation of anaerobic pathways that generate ATP through glycolysis and regenerate NAD^+ through ethanol fermentation (Bailey-Serres and Voesenek, 2008). In the present study, several fermentation- and glycolysis-related proteins were decreased in flooding-stressed soybean treated with Al_2O_3 NPs compared to the levels found in plants exposed to flooding stress alone (Figure 35). These results suggest that Al_2O_3 NPs might play a role in shifting plant energy metabolism towards cellular processes that operate under normal growth conditions.

The proteomic analysis of soybean treated with Ag NPs under flooding stress revealed that the proteins were mainly related to stress, signaling, and cell metabolism. Along with this, the fermentation related proteins showed similar behavior to those of Al_2O_3 NPs under flooding stress, suggesting that these proteins might be important for soybean growth under flooding stress. In this study, the alcohol dehydrogenase and pyruvate decarboxylase were increased under flooding stress; however, decreased with the Ag NPs treatment. The activity of pyruvate decarboxylase was 9-fold increased in rice during anoxia stress period (Rivoal et al., 1997). The overexpression of *pyruvate decarboxylase* gene resulted in improved plant survival in *Arabidopsis* under anaerobic conditions, suggesting that pyruvate decarboxylase controls ethanol fermentation (Ismond et al., 2003). The metabolic adjustment to low oxygen stress involved the down-regulation of storage metabolism (Geigenberger et al., 2000; van Dongen et al., 2004) and energy-conserving shift from invertase to sucrose synthase route of sucrose degradation (Bologa et al., 2003; Huang et al., 2008). The alcohol dehydrogenase, pyruvate decarboxylase, and sucrose synthase were increased under flooding stress and

decreased with the application of Ag NPs, indicating the metabolic shift from fermentative pathways towards normal cellular processes (Figure 35). These findings indicate that energy metabolism might be one of the regulatory processes involved in the flooding stress response in soybean.

Another important finding was the identification of glyoxalase II 3, whose abundance was time-dependently increased under flooding stress; however, decreased in response to Ag NPs. The glyoxalase pathway has an important role in chemical detoxification by converting acyclic alpha oxoaldehydes to their corresponding alpha hydroxyl acids (Rhee et al., 1986; Marmstål et al., 1979; Irsch and Krauth-Siegel, 2004). The glyoxalase pathway mainly consist of two enzymes, glyoxalase I and II. The removal of phosphate group from the glycolytic intermediates lead to the formation of methylglyoxal (Thornalley, 1990). In response to environmental stresses, the methyglyoxal becomes accumulated as a by-product of glycolysis. In *Arabidopsis*, the findings suggested that glyoxalase II is non-essential for the normal growth; however, it is required under the unfavorable stress conditions (Devanathan et al., 2014). The role of glyoxalase was reported to be linked to stress tolerance (Espartero et al., 1995). The overexpression of glyoxalase pathway enzymes caused the salt tolerance in the transgenic tobacco (Yadav et al., 2005). In the present study, the abundance of glyoxalase II 3 was time-dependently increased under flooding stress; however, decreased with the application of Ag NPs (Figure 35). The elevated level of glyoxalase activity under flooding stress might be related to the efficient removal of methylglyoxal in order to maintain the cellular processes under stress conditions; however, its low production under Ag NPs treatment showed that less cytotoxic by-products are being produced compared to flooding stress. Furthermore, glyoxalase II 3 was identified as a marker protein and this could be used to develop the transgenic soybean. Under flooding stress, the plant can not survive due to the overproduction of the toxic substances. This glyoxalase II 3 could help to detoxify the toxic substances and confer tolerance in soybean under flooding stress.

In this study, the two NPs mainly influenced the energy metabolism of soybean under flooding stress. The fermentation-related proteins were increased under flooding stress at the initial stage; however, it was decreased with the progression of the stress

condition. On the other hand, the Ag and Al_2O_3 NPs treatment reduced the abundance of these proteins with little or no change with the advancement in the stress condition. In this study, the Ag and Al_2O_3 NPs mainly affected the energy metabolism of the soybean under flooding stress. The change in the energy metabolism was similar on exposure to these NPs. However, the Ag NPs characteristically controlled the detoxicfication process under flooding stress thereby facilitating the soybean growth. These findings suggest that along with the toxicological effects of NPs on plants, NPs could be used to enhance the plant growth under stress conditions.

Conventionally, the agrochemicals are applied to the crops either by spraying or broadcasting. However, very low concentration of these chemicals could reach the target site due to leaching, photolysis, hydrolysis, and microbial degradation. In order to get the effective concentration, these agrochemicals had been applied in much larger quantities to achieve the real benefits (Green and Beestman, 2007). These repeated applications would cause deleterious effects like soil and water pollution. Towards the developments in nanotechnology, nano-encapsulated agrochemicals are the future goal to be achieved (Boehm et al., 2003). The control of parasitic weeds with nano-encapsulated herbicides thereby reducing the phytotoxicity of herbicides on crops and facilitating the efficient delievery is one example (Perez-de-Luque and Diego, 2009). Nanotechnology is progressing towards the application of these NPs in agriculture for the genetic improvement of plants (Eapen and D'Souza, 2005), delievery of genes to the target sites (Maysinger, 2007), delievery system for agrochemicals, and buildup of nutrients in the soil (Bhalla and Mukhopadhyay, 2010). The overwhelming use of NPs for the improvement of agriculture needs the critical evaluation of the impact of these NPs with the plants. This study will be helpful to understand the molecular basis of the possible interaction mechanisms of NPs with the cellular components of plants. By examining the mode of molecular interaction between plants and NPs, the efficient usage of these NPs in the agricultural sector could be estimated. These findings suggest that the NPs could be used in the agricultural products as a delivery system at a low concentrations. In this way, the agricultural products can be improved.

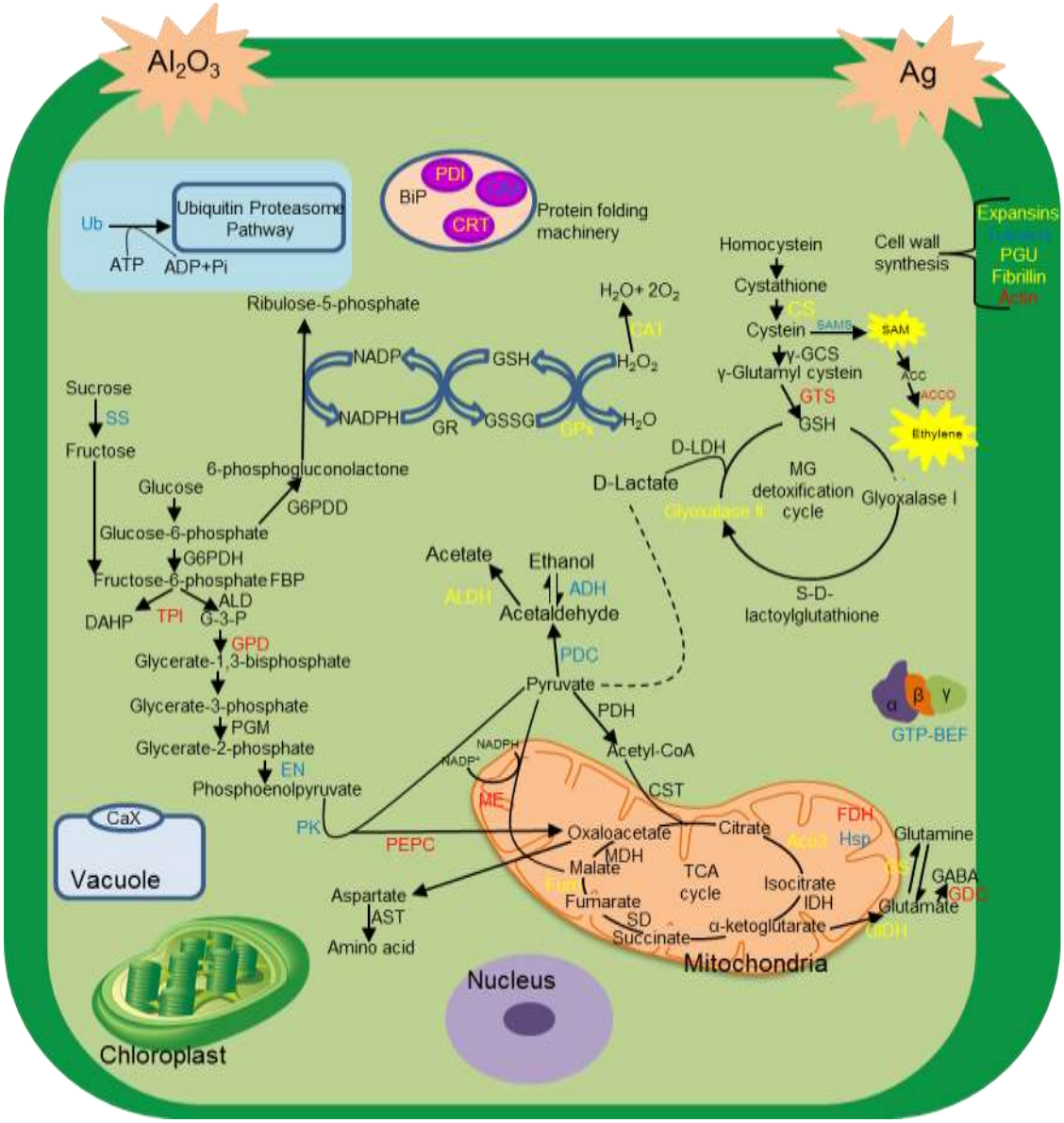

Figure 35. NPs mediated changes in metabolic pathways under flooding stress. Protein names in yellow and red colors indicate their identifications from Ag and Al_2O_3 NPs, respectively; however, protein names in blue color indicate their identification from both the NPs treatments. Proteomic findings indicate that Ag and Al_2O_3 NPs mediate the metabolic shift from anaerobic to aerobic energy metabolism. Abbreviations: ACC, 1-aminocyclopropane-1-carboxylic acid; ACCO, ACC oxidase; ADH; alcohol dehydrogenase; ALDH, aldehyde dehydrogenase; CS, cysteine synthase; CNX, calnexin; CRT, calreticulin; CAT, catalase; DHAP; dihydroxyacetone phosphate; ENO, enolase; Fum, fumarase; GIDH, glutamate dehydrogenase; GPx, glutathione peroxidase; GS, glutamine synthase; GABA, gamma-aminobutyric acid; GT, glycosyl transferase; GTP-BEf, GTP binding elongation factor, GDC, glutamate decarboxylase; GTS, glutathione synthetase; PDC, pyruvate decarboxylase; SAM, *S*-adenosylmethionine; SAMS, SAM synthetase; SS, sucrose synthase; ME, NADP malic enzyme; PK, pyruvate kinase; PEPC, phosphoenolpyruvate carboxylase; 20s PRS, 20s proteasome alpha subunit; PGU, polygalacturonase inhibiting protein.

Supplemental Table 1. Primer sequences of genes selected for qRT-PCR.

Protein ID[a)]	Description	Sequence of primers
Glyma15g39370.2	Glyoxalase II 3	F: 5'-CTCCTCCTCCTCCAAGCTCT-3'
		R: 5'-GATAAGGCCAGTCCCAGTGA-3'
Glyma01g29190.1	Thiamine pyrophosphate dependent pyruvate decarboxylase family protein	F: 5'-GCGTACAGCGAGAATCTTCC-3'
		R: 5'-TTGCTTTCTTTCAGGCAGGT-3'
Glyma12g35070.1	Aluminium induced protein with YGL and LRDR motifs	F: 5'-GGGTATTGCAGCTGATGGAT-3'
		R: 5'-CACTCGAGGAATGCTGTTGA-3'
Glyma13g30490.1	Pyruvate decarboxylase 2	F: 5'-GGGCCAAAACTAAGGGTAGC-3'
		R: 5'-ATGGGGCCAACAAAAACATA-3'
Glyma15g20180.2	Sucrose synthase 4	F: 5'-TACCCTGACACTGGTGGACA-3'
		R: 5'-TTGCGAACAATTCCCTTTTC-3'
Glyma06g12780.1	Alcohol dehydrogenase 1	F: 5'-GGTTGGGGTGTTGCTGTACT-3'
		R: 5'-TTCCAATTCCCCATTCATGT-3'
Glyma11g07490.1	NmrA like negative transcriptional regulator family protein	F: 5'-CCCTGCAAATGTTTTGACCT-3'
		R: 5'-AGTGGCCTAATGCCAACATC-3'
Glyma08g24720.1	MLP like protein 43	F: 5'-AAATTGGTGTTCAGGCAACC-3'
		R: 5'-TGTCTCCATCGAAGAGCTTG-3'
Glyma05g27090.1	Protein of unknown function DUF2359 transmembrane	F: 5'-CGAAGAAGCCTAAGGTGACG-3'
		R: 5'-TTTCACCCAGGGAAACTGAG-3'
Glyma08g06570.1	Flavodoxin like quinone reductase 1	F: 5'-CACACAGGCACTAGCTGGAA-3'
		R: 5'-TCCCAGCACCAAATGTGTAA-3'
18S rRNA	X02623.1[b)]	F: 5'-TGATTAACAGGGACAGTCGG-3'
		R: 5'-ACGGTATCTGATCGTCTTCG-3'

a, Protein ID according to the Phytozome database; b, according to Genebank.

SUMMARY

Changing climatic conditions can alter physiological state of plant and stimulate different biological pathways in order to combat unfavorable stress conditions. This alteration results in various abiotic stresses including flooding, which acts as a major constraint for crop productivity. Towards the advancement of modern agricultural techniques, mankind opened a new gateway for the development of nanomaterials. NPs are used in agricultural products and cause various adverse growth effects on different plant species. Flooding mainly affects the growth and NPs have the ability to improve the plant growth. To study the effects of the NPs on soybean under flooding stress, a gel-free proteomic technique was used.

Phenotypic analysis revealed that Al_2O_3 NPs enhanced fresh weight of soybean and length of root including hypocotyl while Ag NPs promoted the soybean growth under flooding stress. However, ZnO NPs did not affect the soybean growth and lies in between Al_2O_3 and Ag NPs. Among various sizes of Ag NPs, 15 nm NPs enhanced soybean growth under flooding stress compared to 2 and 50-80 nm NPs. Concentration analysis revealed that 2 ppm of 15 nm NPs was suitable for promoting soybean growth under flooding stress. Among various sizes of Al_2O_3 NPs, 30-60 nm facilitated the soybean growth under flooding stress compared to 5 and 135 nm NPs. Concentration analysis revealed that 50 ppm of 30-60 nm NPs was the best suitable for ameliorating soybean growth under flooding stress. These results indicate that among various NPs, 30-60 nm Al_2O_3 NPs at 50 ppm and 15 nm Ag NPs at 2 ppm concentration were the best suitable for promoting the soybean growth under flooding stress. For the following proteomic study, 2 ppm of 15 nm Ag and 50 ppm of 30-60 nm Al_2O_3 NPs were used.

With Ag NPs, the commonly changed root proteins were predominantly associated with stress, signaling, and cell metabolism. Hierarchical clustering divided these proteins into 3 clusters. Based on cluster analysis, the abundances of glyoxalase II 3 and fermentation-related proteins were time-dependently increased under flooding stress, but decreased in response to Ag NPs. At the transcriptional level, the fermentation- and glycolysis-related genes were down-regulated in response to Ag NPs. *Glyoxalase II 3* was also down-regulated with Ag NPs compared to flooding stress. These results suggest that Ag NPs mediated the metabolic shift from fermentative pathways towards normal cellular process as well as formation of less cytotoxic by-products of glycolysis that act as a key factor in promoting the soybean growth under flooding stress.

With Al_2O_3 NPs, differentially changed proteins among control, flooding-stressed, and flooding-stressed soybean treated with Al_2O_3 NPs were mainly related to energy

metabolism and cell wall synthesis. Hierarchical clustering highlighted the proteins related to glycolysis exhibiting the greatest changes in abundance. Energy metabolism was decreased with Al_2O_3 NPs-treated compared to flooding-treated soybean. The Al_2O_3 NPs-responsive proteins were mainly related to protein synthesis/degradation, glycolysis, and lipid metabolism. These results suggest that Al_2O_3 NPs ameliorated the soybean growth under flooding stress by compensating the energy demand under flooding stress conditions.

Both Ag and Al_2O_3 NPs mediated the energy metabolism under flooding stress thereby facilitating the soybean growth. Furthermore, the proteomic analysis of soybean under Ag (2, 15, and 50-80 nm) and Al_2O_3 (5, 30-60, and 135 nm) was carried out to examine whether this growth ameliorating effect is dependent on the size or concentration of NPs. This proteomic analysis revealed the proteins related to tricarboxylic acid cycle, redox, and mitochondrial electron transport chain were mainly affected under the varying sizes of the Ag and Al_2O_3 NPs. These results suggest that the different sizes of the NPs affected the mitochondria under flooding stress.

The proteomic results indicate that the abundances of glycolysis- and fermentation-related proteins were increased under flooding stress; however, they were decreased with the application of NPs. These results suggest that energy demand of plant is increased as a strategy to combat the unfavorable conditions under flooding stress. This energy demand is compensated by the Al_2O_3 and Ag NPs acting as key factors for better growth performance of NPs-treated soybeans under flooding stress.

ACKNOWLEDGMENTS

Firstly, I would like to express my deep gratitude to my supervisor, Prof. Setsuko Komatsu, in the National Institute of Crop Science at National Agriculture and Food Research Organization and in Graduate School of Life and Environmental Science at University of Tsukuba, for her dexterous and impetious guidance throughout my research work. I am also thankful to her for providing me all the facilities regarding this research work.

I owe my thanks and appreciation to Prof. Hiroshi Matsumoto, in Graduate School of Life and Environmental Science at University of Tsukuba, for his thought provoking guidance and support as member of my supervisory committee.

I am greatful to the members of my supervisory committee Prof. Hiroshi Takatsuji and Dr. Yukari Sunohara in Graduate School of Life and Environmental Science at University of Tsukuba, for their worthy suggestions to improve this manuscript.

I am also thankful to Dr. Zahed Hossain in the University of Kalyani, India for his valuable suggestions and guidance during my research. I would like to take this opportunity to convey my cordial thanks to Prof. Katsumi Sakata in the Department of Life Sciences and Informatics at Maebashi Institute of Technology for his support to analyze data.

I owe my special thanks to Dr. Yohei Nanjo for his great help and support for MS analysis during my research at National Institute of Crop Science. I wish to express my gratitude to Dr. Keito Nishizawa and Dr. Susumu Hiraga for their valuable comments and advices.

I am thankful to my colleagues Mr. Xiaojian Yin, Ms. Xin Wang, and Ms. Myeong Won Oh for their supportive behavior during my research work. This dissertation would not have been possible without the help of so many people in so many ways. It is difficult to say thanks individually. I am thankful to every person who helped me to fullfil this task.

I gratefully acknowledge the National Institute of Crop Science for providing me all the facilities to complete this research in the specified time frame.

REFERENCES

Aghajani, Z., Pourmeidani, A., Ekhtiyari, R. (2013) Effect of nanoAg on stages of plant growth and yield and composition of essential oil of *Thymus kotschyanus* Boiss. & Hohen. African Journal of Agricultural Research 8, 707-710.

Ahsan, N., Lee, D. G., Lee, S. H., Kang, K. Y., Bahk, J. D., Choi, M. S., Lee, I. J., Renaut, J., Lee, B. H. (2007) A comparative proteomic analysis of tomato leaves in response to waterlogging stress. Physiologia Plantarum 131, 555-570.

Andrianopoulos, A., Kourambas, S., Sharp, J. A., Davis, M. A., Hynes, M. J. (1998) Characterization of the *Aspergillus nidulans* nmrA gene involved in nitrogen metabolite repression. Journal of Bacteriology 180, 1973-1977.

Armstrong, W. (1979) Aeration in higher plants. In: Woolhouse, H. W. W. (Ed.). Advances in Botanical Research, Academic Press, London, UK, Vol-7, pp. 225-332.

Arshad, R. R., Shafi, S. (2010) Pakistan Floods 2010: Preliminary damage and needs assessment. Asian Development Bank and World Bank, Islamabad, Pakistan.

Asharani, P.V., Lian Wu, Y., Gong, Z., Valiyaveettil, S. (2008) Toxicity of silver nanoparticles in zebrafish models. Nanotechnology 19, 255102.

Ashraf, M. A. (2012) Waterlogging stress in plants: A review. African Journal of Agricultural Research 7, 1976-1981.

Aslani, F., Bagheri, S., Muhd Julkapli, N., Juraimi, A. S., Hashemi, F. S., Baghdadi, A. (2014) Effects of engineered nanomaterials on plants growth: an overview. The Scientific World Journal 2014, 641759.

Bailey-Serres, J., Fukao, T., Gibbs, D. J., Holdsworth, M. J., Lee, S. C., Licausi, F., Perata, P., Voesenek, L. A., van Dongen, J. T. (2012) Making sense of low oxygen sensing. Trends in Plant Science 17, 129-138.

Bailey-Serres, J., Voesenek, L. A. C. J. (2008) Flooding stress: acclimations and genetic diversity. Annual Review of Plant Biology 59, 313-339.

Banti, V., Giuntoli, B., Gonzali, S., Loreti, E., Magneschi, L., Novi, G., Paparelli, E., Parlanti, S., Pucciariello, C., Santaniello, A., Perata, P. (2013) Low oxygen response mechanism in green organisms. International Journal of Molecular Sciences 14, 4734-4761.

Beck, E. H., Fettig, S., Knake, C., Hartig, K., Bhattarai, T. (2007) Specific and unspecific responses of plants to cold and drought stress. Journal of Bioscience 32, 501-510.

Beck, E. H., Heim, R., Hansen, J. (2004) Plant resistance to cold stress: Mechanisms and environmental signals triggering frost hardening and dehardening. Journal of Bioscience 29, 449-459.

Benn, T. M., Westerhoff, P. (2008) Nanoparticle silver released into water from commercially available sock fabrics. Environmental Science and Technology 42, 4133-4139.

Bhalla, D., Mukhopadhyay, S. S. (2010) Eutrophication: Can nanophosphorous control this menace?- A preview. Journal of Crop and Weed 6, 13-16.

Bita, C. E., Gerats, T. (2013) Plant tolerance to high temperature in a changing environment: scientific fundamentals and production of heat stress-tolerant crops. Frontiers in Plant Science 4, 273.

Boehm, A. L., Martinon, I., Zerrouk, R., Rump, E., Fessi, H. (2003) Nanoprecipitation technique for the encapsulation of agrochemical active ingredients. Journal of Microencapsulation 20, 433-441.

Bologa, K. L., Fernie, A. R., Leisse, A., Loureiro, M. E., Geigenberger, P. (2003) A bypass of sucrose synthase leads to low internal oxygen and impaired metabolic performance in growing potato tubers. Plant Physiology 132, 2058-2072.

Boyer, J. S. (1982) Plant productivity and environment. Science 218, 443-448.

Bradford, M. M. (1976) A rapid and sensitive method for the quantitation of microgram quantities of protein utilizing the principle of protein-dye binding. Analytical Biochemistry 72, 248-254.

Brosch, M., Yu, L., Hubbard, T., Choudhary, J. (2009) Accurate and sensitive peptide identification with mascot percolator. Journal of Proteome Research 8, 3176-3181.

Brunner, T. J., Wick, P., Manser, P., Spohn, P., Grass, R. N., Limbach, L. K., Bruinink, A., Stark, W. J. (2006) In vitro cytotoxicity of oxide nanoparticles: comparison to asbestos, silica, and the effect of particle solubility. Environmental Science Technology 40, 4374-4381.

Burklew, C. E., Ashlock, J., Winfrey, W. B., Zhang, B. (2012) Effects of aluminum

oxide nanoparticles on the growth, development, and microRNA expression of tobacco (*Nicotiana tabacum*). PLoS ONE 7, e34783.

Buzea, C., Pacheco, I. I., Robbie, K. (2007) Nanomaterials and nanoparticles: sources and toxicity. Biointerphases 2, MR17-MR71.

Carpenter, J. R. and Mitchell, C. A. (1980) Root respiration characteristics of flood-tolerant and intolerant tree species. Journal of the American Society for Horticultural Science 105, 684-687.

Chen, J. Y., Dai, X. F. (2010) Cloning and characterization of the *Gossypium hirsutum* major latex protein gene and functional analysis in *Arabidopsis thaliana*. Planta 231, 861-873.

Choi, O., Hu, Z. (2008) Size dependent and reactive oxygen species related nanosilver toxicity to nitrifying bacteria. Environmental Science Technology 42, 4583-4588.

Colmer, T.D. (2003) Long-distance transport of gases in plants: a perspective on internal aeration and radial oxygen loss from roots. Plant Cell and Environment 26, 17-36.

Dat, J. F., Capelli, N., Folzer, H., Bourgeade, P., Badot, P. M. (2004) Sensing and signaling during plant flooding. Plant Physiology and Biochemistry 42, 273-282.

Deller, S., Macheroux, P., Sollner, S. (2008) Flavin-dependent quinone reductases. Cellular and Molecular Life Sciences 65, 141-160.

Devanathan, S., Erban, A., Jr. Perez-Torres, R., Kopka, J., Makaroff, C. A. (2014) *Arabidopsis thaliana* glyoxalase 2-1 is required during abiotic stress but is not essential under normal plant growth. PLoS One 9, e95971.

Dietz, K. J., Herth, S. (2011) Plant nanotoxicology. Trends in Plant Science 16, 582-589.

Domash, V. I., Sharpio, T. P., Zabreĭko, S. A., Sosnovskaia, T. F. (2008) Proteolytic enzymes and trypsin inhibitors of higher plants under stress conditions. Bioorganicheskaya Khimiya (in Russian) 34, 353-357.

Duran, N., Marcarto, P. D., De Souza, G. I. H., Alves, O. L., Esposito, E. (2007) Antibacterial effects of silver nanoparticles produced by fungal process on textile fabrics and their effluent treatment. Journal of Biomedical Nanotechnology 3, 203-208.

Eapen, S., D'Souza, S. F. (2005) Prospects of genetic engineering of plants for

phytoremediation of toxic metals. Biotechnology Advances 23, 97-114.

Ehsanpour, A. A., Nejati, Z. (2013) Effect of nanosilver on potato plant growth and protoplast viability. Biological Letters 50, 35-43.

Eigenbrod, F., Gonzalez, P., Dash, J., Steyl, I. (2015) Vulnerability of ecosystems to climate change moderated by habitat intactness. Global Change Biology 21, 275-86.

Espartero, J., Sánchez-Aguayo, I., Pardo, J. M. (1995) Molecular characterization of glyoxalase-1 from a higher plant; upregulation by stress. Plant Molecular Biology 29, 1223-1233.

Feichtmeier, N. S., Walther, P., Leopold, K. (2015) Uptake, effects, and regeneration of barley plants exposed to gold nanoparticles. Environmental Science and Pollution Research International 22, 8549-8558.

Fukao, T., Bailey-Serres, J. (2004) Plant responses to hypoxia-is survival a balancing act? Trends In Plant Science 9, 449-456.

Geigenberger, P., Fernie, A. R., Gibon, Y., Christ, M., Stitt, M. (2000) Metabolic activity decreases as an adaptive response to low internal oxygen in growing potato tubers. Biological Chemistry 381, 723-740.

Gibbs, J., Greenway, H. (2003) Review: Mechanisms of anoxia tolerance in plants. I. Growth, survival and anaerobic catabolism. Functional Plant Biology 30, 1-47.

Githiri, S. M., Watanabe, S., Harada, K., Takahashi, R. (2006) QTL analysis of flooding tolerance in soybean at an early vegetative growth stage. Plant Breeding 125, 613-618.

Gornall, J., Betts, R., Burke, E., Clark, R., Camp, J., Willett, K., Wiltshire, A. (2010) Implications of climate change for agricultural productivity in the early twenty-first century. Philosophical Transactions of the Royal Scoeity B 365, 2973-2989.

Green, J. M., Beestman, G. B. (2007) Recently patented and commercialized formulation and adjuvant technology. Crop Protection 26, 320-327.

Greenshields, D. L., Liu, G., Selvaraj, G., Wei, Y. (2005) Differential regulation of wheat quinone reductases in response to powdery mildew infection. Planta 222, 867-875.

Gubbins, E. J., Batty, L. C., Lead, J. R. (2011) Phytotoxicity of silver nanoparticles to Lemna minor L. Environmental Pollution 159, 1551-1559.

Guzmán, K. A., Taylor, M. R., Banfield, J. F. (2006) Environmental risks of nanotechnology: National Nanotechnology Initiative funding, 2000-2004. Environmental Science Technology 40, 1401-1407.

Hao, X. Y., Han, X., Ju, H., Lin, E. D. (2010) Impact of climatic change on soybean production: a review. Ying Yong Sheng Tai Xue Bao 21, 2697-2706.

Hashiguchi, A., Ahsan, N., Komatsu, S. (2010) Proteomics application of crops in the context of climatic changes. Food Research International 43, 1803-1813.

Hashiguchi, A., Sakata, K., Komatsu, S. (2009) Proteome analysis of early-stage soybean seedlings under flooding stress. Journal of Proteome Research 8, 2058-2069.

Hashimoto, M., Kisseleva, L., Sawa, S., Furukawa, T., Komatsu, S., Koshiba, T. (2004) A novel rice PR10 protein, RSOsPR10, specifically induced in roots by biotic and abiotic stresses, possibly via the jasmonic acid signaling pathway. Plant and Cell Physiology 45, 550-559.

He, C. J., Morgan, P. W., Drew, M. C. (2000) Transduction of an ethylene signal is required for cell death and lysis in the root cortex of maize during aerenchyma formation induced by hypoxia. Plant Physiology 112, 463-472.

Helaly, M. N., El-Metwally, M. A., El-Hoseiny, H., Omar, S. A., El-Sheery, N. I. (2014) Effect of nano- particles on biological contamination of in vitro cultures and organogenic regeneration of banana. Australian Journal of Crop Science 8, 612-624.

Heyno, E., Alkan, N., Fluhr, R. (2013) A dual role for plant quinone reductases in host-fungus interaction. Physiologia Plantarum 149, 340-353.

Hossain, Z., Khatoon, A., Komatsu, S. (2013) Soybean proteomics for unraveling abiotic stress response mechanism. Journal of Proteome Research 12, 4670-4684.

Hossain, Z., Lopez-Climent, M. F., Arbona, V., Perez-Clemente, R. M., Gomez-Cadenas, A. (2009) Modulation of the antioxidant system in citrus under waterlogging and subsequent drainage. Journal of Plant Physiology 166, 1391-1404.

Hossain, Z., Mustafa, G., Sakata, K., Komatsu, S. (2015) Insights into the proteomic response of soybean towards Al_2O_3, ZnO, and Ag nanoparticles stress. Journal of Hazardous Materials 304, 291-305.

Hou, F. F., Thseng, F. S. (1991) Studies on the flooding tolerance of soybean seed:

varietal differences. Euphytica 57, 169-173.

Huang, S., Colmer, T. D., Millar, A. H. (2008) Does anoxia tolerance involve altering the energy currency towards PPi? Trands Plant Science 13, 221-227.

Huang, S., Greenway, H., Colmer, T. D., Millar, A. H. (2005) Protein synthesis by rice coleoptiles during prolonged anoxia: implications for glycolysis, growth and energy utilization. Annals of Botany 96, 661-668.

Irsch, T., Krauth-Siegel, R. L. (2004) Glyoxalase II of African trypanosomes is trypanothione-dependent. The Journal of Biological Chemistry 279, 22209-22217.

Ismond, K. P., Dolferus, R., de Pauw, M., Dennis, E. S., Good, A. G. (2003) Enhanced low oxygen survival in *Arabidopsis* through increased metabolic flux in the fermentative pathway. Plant Physiology 132, 1292-1302.

Jackson, M. B., Colmer, T. D. (2005) Response and adaptation by plants to flooding stress. Annals of Botany 96, 501-505.

Jefferson, D. A. (2000) The surface activity of ultrafine particles, Philosophical Transactions of the Royal Society of London, Series A: 358, 2683-2692.

Jiang, H. S., Li, M., Chang, F. Y., Li, W., Yin, L. Y. (2012) Physiological analysis of silver nanoparticles and $AgNO_3$ toxicity to *Spirodela polyrrhiza*. Environmental Toxicology and Chemistry 31, 1880-1886.

Jiang, Y., Yang, B., Harris, N. S., Deyholos, M. K. (2007) Comparative proteomic analysis of NaCl stress-responsive proteins in *Arabidopsis* roots. Journal of Experimental Botany 58, 3591-3607.

Joseph, P., Jaiswal, A. K. (1994) NAD (P)H: quinone oxidoreductase1 (DT diaphorase) specifically prevents the formation of benzo[a]pyrene quinone-DNA adducts generated by cytochrome P4501A1 and P450 reductase. Proceedings of the National Academy of Sciences of the United States of America 91, 8413-8417.

Kaveh, R., Li, Y. S., Ranjbar, S., Tehrani, R., Brueck, C. L., Van Aken, B. (2013) Changes in *Arabidopsis thaliana* gene expression in response to silver nanoparticles and silver ions. Environmental Science and Technology 47, 10637-10644.

Khan, M. N., Sakata, K., Hiraga, S., Komatsu, S. (2014) Quantitative proteomics reveals that peroxidases play key roles in post-flooding recovery in soybean roots. Journal of Proteome Research 13, 5812-5828.

Kim, S., Choi, J. E., Choi, J., Chung, K. H., Park, K., Yi, J., Ryu, D. Y. (2009) Oxidative stress-dependent toxicity of silver nanoparticles in human hepatoma cells. Toxicology In Vitro 23, 1076-1084.

Kochian, L. V., Hoekenga, O. A., Pineros, M. A. (2004) How do crop plants tolerate acid soils? Mechanisms of aluminum tolerance and phosphorous efficiency. Annual Review of Plant Biology 55, 459-493.

Komatsu, S., Deschamps, T., Hiraga, S., Kato, M., Chiba, M., Hashiguchi, A., Tougou, M., Shimamura, S., Yasue, H. (2011a) Characterization of a novel flooding stress-responsive alcohol dehydrogenase expressed in soybean roots. Plant Molecular Biology 77, 309-322.

Komatsu, S., Yamamoto, A., Nakamura, T., Nouri, M. Z., Nanjo, Y., Nishizawa, K., Furukawa, K. (2011b) Comprehensive analysis of mitochondria in roots and hypocotyls of soybean under flooding stress using proteomics and metabolomics techniques. Journal of Proteome Research 10, 3993-4004.

Komatsu, S., Han, C., Nanjo, Y., Altaf-Un-Nahar, M., Wang, K., He, D., Yang, P. (2013b) Label-free quantitative proteomic analysis of abscisic acid effect in early-stage soybean under flooding. Journal of Proteome Research 12, 4769-4784.

Komatsu, S., Nakamura, T., Sugimoto, Y., Sakamoto, K. (2014) Proteomic and metabolomics analysis of soybean root tips under flooding stress. Protein and Peptide Letters 21, 865-884.

Komatsu, S., Nanjo, Y., Nishimura, M. (2013a) Proteomic analysis of flooding tolerance mechanism in mutant soybean. Journal of Proteomics 79, 231-250.

Komatsu, S., Tougou, M., Nanjo, Y. (2015) Proteomic Techniques and Management of Flooding Tolerance in Soybean. Journal of Proteome Research 14, 3768-3778.

Komatsu, S., Yamamoto, R., Nanjo, Y., Mikami, Y., Yunokawa, H., Sakata, K. (2009) A comprehensive analysis of the soybean genes and proteins expressed under flooding stress using transcriptome and proteome techniques. Journal of Proteome Research 8, 4766-4778.

Kong, F. J., Oyanagi, A., Komatsu, S. (2010) Cell wall proteome of wheat roots under flooding stress using gel-based and LC MS/MS-based proteomics approaches. Biochimica et Biophysica Acta 1804, 124-136.

Kreuzwieser, J., Gessler, A. (2010) Global climate change and tree nutrition: influence of water availability. Tree Physiology 30, 1221-1234.

Kumari, M., Mukherjee, A., Chandrasekaran, N. (2009) Genotoxicity of silver nanoparticles in *Allium cepa*. Science and Total Environment 407, 5243-5246.

Lamb, H. K., Leslie, K., Dodds, A. L., Nutley, M., Cooper, A., Johnson, C., Thompson, P., Stammers, D. K., Hawkins, A. R. (2003) The negative transcriptional regulator NmrA discriminates between oxidized and reduced dinucleotides. Journal of Biological Chemistry 278, 32107-32114.

Laohavisit, A., Shang, Z., Rubio, L., Cuin, T. A., Very, A. A., Wang, A., Mortimer, J. C., Macpherson, N., Coxon, K. M., Battery, N. H., Brownlee, C., Park, O. K., Sentenac, H., Shabala, S., Webb, A. A., Davies, J. M. (2012) *Arabidopsis* annexin1 medicates the radical-activated plasma membrane Ca^{2+}- and K^{+} -permeable conductance in root cells. Plant Cell 24, 1522-1533.

Laskowski, M. J., Dreher, K. A., Gehring, M. A., Abel, S., Gensler, A. L., Sussex, I. M. (2002) FQR1, a novel primary auxin-response gene, encodes a flavin mononucleotide-binding quinone reductase. Plant Physiology 128, 578-590.

Lee, C. W., Mahendra, S., Zodrow, K., Li, D., Tsai YC, Braam J, Alvarez PJ. (2010) Developmental phytotoxicity of metal oxide nanoparticles to *Arabidopsis thaliana*. Environmental Toxicology and Chemistry 29, 669-675.

Lee, S., Lee, E. J., Yang, E. J., Lee, J. E., Park, A. R., Song, W. H., Park, O. K. (2004) Proteomic identification of annexins, calcium-dependent membrane binding proteins that mediate osmotic stress and abscisic acid signal transduction in *Arabidopsis*. Plant Cell 16, 1378-1391.

Liao, C. T., Lin, C. H. (2001) Physiological adaptation of crop plants to flooding stress. Proceedings of the National Science Council Republic of China, Part B, Life Sciences 25, 148-157.

Lin, D., Xing, B. (2007) Phytotoxicity of nanoparticles: Inhibition of seed germination and root growth. Environmental Pollution 20, 1-8.

Liu, J. X., Howell, S. H. (2010) Endoplasmic reticulum protein quality control and its relationship to environmental stress in plants. Plant Cell 22, 2930-2942.

López-Moreno, M. L., de la Rosa, G., Hernández-Viezcas, J. A., Castillo-Michel, H.,

Botez, C. E., Peralta-Videa, J. R., Gardea-Torresdey, J. L. (2010) Evidence of the differential biotransformation and genotoxicity of ZnO and CeO_2 nanoparticles on soybean (*Glycine max*) plants. Environmental Science and Technology 44, 7315-7320.

Lu, C. M., Zhang, C. Y., Wen, J. Q., Wu, G. R., Tao, M. X. (2002) Research of the effect of nanometer materials on germination and growth enhancement of *Glycine max* and its mechanism. Soybean Science (in Chinese) 21, 168-172.

Luoma, N. S. (2008) Silver nanotechnologies and the environment: Old problems or new challenges? The Project on Emerging Nanotechnologies. Vol. 15. September 2008.

Ma, J. F. (2000) Role of organic acids in detoxification of aluminium in higher plants. Plant and Cell Physiology 41, 383-390.

Ma, J. F., Furukawa, J. (2003) Recent progress in the research of external Al detoxification in higher plants: a minireview. Journal of Inorganic Biochemistry 97, 46-51.

Ma, X., Geisler-Lee, J., Deng, Y., Kolmakov, A. (2010) Interactions between engineered nanoparticles (ENPs) and plants: phytotoxicity, uptake and accumulation. The Science of the Total Environment 408, 3053-3061.

Manavalan, L. P., Guttikonda, S. K., Tran, L. S., Nguyen, H. T. (2009) Physiological and molecular approaches to improve drought resistance in soybean. Plant and Cell Physiology 50, 1260-1276.

Manke, A., Wang, L., Rojanasakul, Y. (2013) Mechanisms of nanoparticle-induced oxidative stress and toxicity. BioMed Research International 2013, 942916.

Marmstål, E., Aronsson, A. C., Mannervik, B. (1979) Comparison of glyoxalase I purified from yeast (*Saccharomyces cerevisiae*) with the enzyme from mammalian sources. The Biochemical Journal 183, 23-30.

Matsumura, Y., Yoshikata, K., Kunisaki, S., Tsuchido, T. (2003) Mode of bactericidal action of silver zeolite and its comparison with that of silver nitrate. Applied and Environmental Microbiology 69, 4278-4281.

Maysinger, D. (2007) Nanoparticles and cells: good companions and doomed partnerships. Organic and Biomolecular Chemistry 5, 2335-2342.

McShan, D., Ray, P. C., Yu, H. (2014) Molecular toxicity mechanism of nanosilver. Journal of Food and Drug Analysis 22, 116-127.

Medic, J., Atkinson, C., Jr Hurburgh, C. R. (2014) Current knowledge in soybean composition. Journal of the American Oil Chemists' Society 91, 363-384.

Miao, A. J., Schwehr, K. A., Xu, C., Zhang, S. J., Luo, Z., Quigg, A., Santschi, P. H. (2009) The algal toxicity of silver engineered nanoparticles and detoxification by exopolymeric substances. Environmental Pollution 157, 3034-3041.

Millar, A. H., Heazlewood, J. L., Kristensen, B. K., Braun, H. P., Møller, I. M. (2005) The plant mitochondrial proteome. Trends in Plant Science 10, 36-43.

Mirzajani, F., Askari, H., Hamzelou, S., Schober, Y., Römpp, A., Ghassempour, A., Spengler, B. (2014) Proteomics analysis of silver nanoparticles toxicity on *Bacillus thuringiensis*. Ecotoxicology and Environmental Safety 100, 120-130.

Nair, P. M., Chung, I. M. (2014) A mechanistic study on the toxic effect of copper oxide nanoparticles in soybean (*Glycine max* L.) root development and lignification of root cells. Biological Trace Element Research 162, 342-352.

Nakayama, N., Hashmoto, S., Shimada, S., Takahashi, M., Kim, Y. H., Oya, T., Arihara, J. (2004) The effect of flooding stress at the germination stage on the growth of soybean in relation to initialseed moisture content. Journal of Crop Science 73, 323-329.

Nanjo, Y., Jang, H. Y., Kim, H. S., Hiraga, S., Woo, S. H., Komatsu, S. (2014) Analyses of flooding tolerance of soybean varieties at emergence and varietal differences in their proteomes. Phytochemistry 106, 25-36.

Nanjo, Y., Nakamura, T., Komatsu, S. (2013) Identification of indicator proteins associated with flooding injury in soybean seedlings using label-free quantitative proteomics. Journal of Proteome Research 12, 4785-4798.

Nanjo, Y., Skultety, L., Ashraf, Y., Komatsu, S. (2010) Comparative proteomic analysis of early-stage soybean seedlings responses to flooding by using gel and gel-free techniques. Journal of Proteome Research 9, 3989-4002.

Nanjo, Y., Skultety, L., Uváčková, L., Klubicová, K., Hajduch, M., Komatsu, S. (2012) Mass spectrometry-based analysis of proteomic changes in the root tips of flooded soybean seedlings. Journal of Proteome Research 11, 372-385.

Navarro, E., Baun, A., Behra, R., Hartmann, N.B., Filser, J., Miao, A.J., Quigg, A., Santschi, P.H., Sigg, L. (2008) Environmental behavior and ecotoxicity of engineered nanoparticles to algae, plants, and fungi. Ecotoxicology 17, 372-386.

Navrot, N., Collin, V., Gualberto, J., Gelhaye, E., Hirasawa, M., Rey, P., Knaff, D. B., Issakidis, E., Jacquot, J. P., Rouhier, N. (2006) Plant glutathione peroxidases are functional peroxiredoxins distributed in several subcellular compartments and regulated during biotic and abiotic stresses. Plant Physiology 142, 1364-1379.

Nel, A., Xia, T., Mädler, L., Li, N. (2006) Toxic potential of materials at the nanolevel. Science 311, 622-627.

Nessler, C. L., Allen, R. D., Galewsky, S. (1985) Identification and characterization of latex-specific proteins in opium poppy. Plant Physiology 79, 499-504.

Normile, D. (2008) Agricultural research. Reinventing rice to feed the world. Science 321, 330-333.

Novrotsky, A. (2003) Energetics of nanoparticles oxides: interplay between surface energy and polymorphism. Genochemical Transactions 4, 34-37.

Nowack, B., Bucheli, T. D. (2007) Occurrence, behavior and effects of nanoparticles in the environment. Environmental Pollution 150, 5-22.

Nowack, B., Krug, H. F., Height, M. (2011) 120 years of nanosilver history: implications for policy makers. Environmental Science and Technology 45, 1177-1183.

Oberdörster, G., Oberdörste,r E., Oberdörster, J. (2005) Nanotoxicology: an emerging discipline evolving from studies of ultrafine particles. Environmental Health Perspectives 113, 823-839.

Oh, M. W., Nanjo, Y., Komatsu, S. (2014) Analysis of soybean root proteins affected by gibberellic acid treatment under flooding stress. Protein and Peptide Letters 21, 911-947.

Olesen, J. E., Trnka, M., Kersebaum, K. C., Skjelvåg, A. O., Seguin, B., Peltonen-Sainio, P., Rossi, F., Kozyra, J., Micale, F. (2011) Impacts and adaptation of European crop production systems to climate change. European Journal of Agronomy 34, 96-112.

Olsen, J. V., de Godoy, L. M., Li, G., Macek, B., Mortensen, P., Pesch, R., Makarov, A.,

Lange, O., Horning, S., Mann, M. (2005) Parts per million mass accuracy on an Orbitrap mass spectrometer via lock mass injection into a C-trap. Molecular and Cellular Proteomics 4, 2010-2021.

Oukarroum, A., Barhoumi, L., Samadani, M., Dewez, D. (2015) Toxic effects of nickel oxide bulk and nanoparticles on the aquatic plant *Lemna gibba* L. Biomedical Research International 2015, 501326.

Owen, R., Handy, R. (2007) Formulating the problems for environmental risk assessment of nanomaterials. Environmental Science and Technology 41, 582-588.

Pan, B., Xing, B. (2010) Manufactured nanoparticles and their sorption of organic chemicals. Advances in Agronomy 108, 137-181.

Parvaiz, A., Satyawati, S. (2008) Salt stress and phyto biochemical responses of plants. Plant Soil Journal 54, 89-99.

Pedrazzini, F. R., McKee, K. L. (1984) Effect of flooding on activities of soil dehydrogenases and alcohol dehydrogenase in rice (*Oryza sativa* L.) roots. Soil Science and Plant Nutrition 30, 359-366.

Pérez-de-Luque, A., Rubiales, D. (2009) Nanotechnology for parasitic plant control. Pest Managment Science 65, 540-545.

Poborilova, Z., Opatrilova, R., Babula, P. (2013) Toxicity of aluminium oxide nanoparticles demonstrated using a BY-2 plant cell suspension culture model. Environmental and Experimental Botany 91, 1-11.

Poschenrieder, C., Gunsé, B., Corrales, I., Barceló, J. (2008) A glance into aluminum toxicity and resistance in plants. The Science of the Total Environment 400, 356-368.

Prasad, T. N. V. K. V., Sudhakar, P., Sreenivasulu, Y., Latha, P., Munaswamy, V., Raja Reddy, K., Sreeprasad, T. S., Sajanlal, P. R., Pradeep, T. (2012) Effect of nanoscale zinc oxide particles on the germination, growth and yield of peanut. Journal of Plant Nutrition 35, 905-927.

Radauer, C., Lackner, P., Breiteneder, H. (2008) The Bet v 1 fold: an ancient, versatile scaffold for binding of large, hydroponic ligands. BMC Evolutionary Biology 8, 286.

Radziun, E., Dudkiewicz, Wilczyńska, J., Książek, I., Nowak, K., Anuszewska, E. L.,

Kunicki, A., Olszyna, A., Ząbkowski, T. (2011) Assessment of the cytotoxicity of aluminium oxide nanoparticles on selected mammalian cells. Toxicology in Vitro 25, 1694-700.

Rajeshwari, A., Kavitha, S., Alex, S. A., Kumar, D., Mukherjee, A., Chandrasekaran, N., Mukherjee, A. (2015) Cytotoxicity of aluminum oxide nanoparticles on Allium cepa root tip--effects of oxidative stress generation and biouptake. Environmental Science and Pollution Research International 22, 11057-11066.

Ramesh, M., Palanisamy, K., Babu, K., Sharma, N. K. (2014) Effects of bulk and nano-titanium dioxide and zinc oxide on physio-morphological changes in *Triticum aestivum* Linn. Journal of Global Biosciences 3, 415-422.

Raskar, S.V., Laware, S.L. (2014) Effect of zinc oxide nanoparticles on cytology and seed germination in onion. International Journal of Current Microbiology and Applied Sciences 3, 467-473.

Reidy, B., Haase A., Luch A., Dawson K.A. Lynch, I. (2013) Mechanisms of silver nanoparticle release, transformation and toxicity: a critical review of current knowledge and recommendations for future studies and applications. Materials 6, 2295-2350.

Rezvani, N., Sorooshzadeh, A., Farhadi, N. (2012) Effect of nano-silver on growth of saffron in flooding stress. World Academy of Science, Engineering and Technology 6, 519-524.

Rhee, H., Murata, K., Kimura, A. (1986) Purification and characterization of glyoxalase I from *Pseudomonas putida*. Biochemical and Biophysical Research Communications 141, 993-209.

Riahi-Madvar, A., Rezaee, F., Jalili, V. (2012) Effects of alumina nanoparticles on morphological properties and antioxidant system of *Triticum aestivum*. Iranian Journal of Plant Physiology 3, 595-603.

Rico, C. M., Majumdar, S., Duarte-Gardea, M., Peralta-Videa, J. R., Gardea-Torresdey, J. L. (2011) Interaction of nanoparticles with edible plants and their possible implications in the food chain. Journal of Agricultural and Food Chemistry 59, 3485-3498.

Rivoal, J., Thind, S., Pradet, A., Ricard, B. (1997) Differential induction of pyruvate

decarboxylase subunits and transcripts in anoxic rice seedlings. Plant Physiology 114, 1021-1029.

Ruperti, B., Bonghi, C., Ziliotto, F., Pagni, S., Rasori, A., Varotto, S., Tonutti, P., Giovannoni, J. J., Ramina, A. (2002) Characterization of a major latex protein (MLP) gene down-regulated by ethylene during peach fruitlet abscission. Plant Science 163, 265-272.

Russel, D. A., Wong, D. M. L., Sachs, M. M. (1990) The anaerobic response of soybean. Plant Physiology 92, 401-407.

Russell, A. D., Hugo, W. B. (1994) Antimicrobial activity and action of silver. Progress in Medicinal Chemistry 31, 351-370.

Saglio, P., Drew, M. C., Pradet, A. (1988) Metabolic acclimation to anoxia induced by low (2-4 kPa partial pressure) oxygen pre-treatment (hypoxia) in root tips of *Zea mays*. Plant Physiology 8, 61-66.

Sairam, R. K., Dharmar, K., Chinnusamy, V., Meena, R. C. (2009) Waterlogging-induced increase in sugar mobilization, fermentation, and related gene expression in the roots of mung bean (*Vigna radiata*). Journal of Plant Physiology 166, 602-6016.

Salama, H. M. H. (2012) Effects of silver nanoparticles in some crop plants, common bean (*Phaseolus vulgaris* L.) and corn (*Zea mays* L.). International Research Journal Biotechnology 3, 190-197.

Sanford J., El-Badawy, A. Feldhake, D., Venkatapathy, R. (2010) State of the science literature review: everything nanosilver and more. Washington, DC: USEPA 221.

Santoro, C. M., Duchsherer, N. L., Grainger, D. W. (2007) Antimicrobial efficacy and ocular cell toxicity from silver nanoparticles. Nanobiotechnology 3, 55-65.

Sauter, M. (2013) Root responses to flooding. Current Opinion in Plant Biology 16, 282-286.

Schmutz, J., Cannon, S. B., Schlueter, J., Ma, J., Mitros, T., Nelson, W., Hyten, D. L., Song, Q., Thelen, J. J., Cheng, J., Xu, D., Hellsten, U., May, G. D., Yu, Y., Sakurai, T., Umezawa, T., Bhattacharyya, T. U., Sandhu, D., Valliyodan, B., Lindquist, E., Peto, M., Grant, D., Shu, S., Goodstein, D., Barry, K., Futrell-Griggs, M., Abemathy, B., Du, J., Tian, Z., Zhu, L., Gill, N., Joshi, T., Libault, M., Sethuraman, A., Zhang, X. C., Shinozaki, K., Nguyen, H. T., Wing, R. A., Cregan, P., Specht, J.,

Grimwood, J., Rokhsar, D., Shoemaker, R. C., Jackson, S. A. (2010) Genome sequence of the palaeopolyploid soybean. Nature 463, 178-183.

Schopfer, P., Heyno, E., Drepper, F., Krieger-Liszkay, A. (2008) Naphthoquinone-dependent generation of superoxide radicals by quinone reductase isolated from the plasma membrane of soybean. Plant Physiology 147, 864-878.

Scrinis, G., Lyons, K. (2007) The emerging nano-corporate paradigm: nanotechnology and the transformation of nature, food and agri-food systems. International Journal of Sociology of Food and Agriculture 15, 22-44.

Sedghi, M. Hadi, M. Toluie S.G. (2013) Effect of nano zinc oxide on the germination of soybean seeds under drought stress. Annals of West University of Timişoara, ser. Biology XVI 2, 73-78.

Sharma, P., Bhatt, D., Zaidi, M. G., Saradhi, P. P., Khanna, P. K., Arora, S. (2012) Silver naoparticle-mediated enhancement in growth and antioxidant status of *Brassica juncea*. Applied Biochemistry and Biotechnology 167, 2225-2233.

Sharma, V. K. (2013) Stability and toxicity of silver nanoparticles in aquatic environment: a review. In: Sustainable nanotechnology and the environment: advances and achievements. Shamim, N., Sharma, V. K. editors. ACS symposium series, Washington, DC: American Chemical Society 1124, 165-179.

Stadler, T., Buteler, M., Weaver, D. K. (2011) Novel use of nanostructured alumina as an insecticide. Pest Management Science 66, 577-579.

Stammers, D. K., Ren, J., Leslie, K., Nichols, C. E., Lamb, H. K., Cocklin, S., Dodds, A., Hawkins, A. R. (2001) The structure of the negative transcriptional regulator NmrA reveals a structural superfamily which includes the short-chain dehydrogenase/reductases. EMBO Journal 20, 6619-6626.

Stampoulis, D., Sinha, S. K., White, J. C. (2009) Assay-dependent phytotoxicity of nanoparticles to plants. Environmental Science and Technology 43, 9473-9479.

Steffens, B., Sauter, M. (2010) G proteins as regulators in ethylene-mediated hypoxia signaling. Plant Signaling and Behavior 5, 375-378.

Stott, P. A., Tett, S. P. B., Jones, G. S., Allen, M. R., Ingram, W. J., Mitchell, J. F. B. (2010) Attribution of twentieth sentury temperature change to natural and anthropogenic causes. Climate Dynamics 17, 1-21.

Strömvik, M. V., Sundararaman, V. P., Vodkin, L. O. (1999) A novel promoter from soybean that is active in a complex developmental pattern with and without its proximal 650 base pairs. Plant Molecular Biology 412, 217-231.

Sturn, A., Quackenbush, J., Trajanoski, Z. (2002) Genesis: cluster analysis of microarray data. Bioinformatics 18, 207-208.

Su, M., Liu, H., Liu, C., Qu, C., Zheng, L., Hong, F. (2009) Promotion of nano-anatase $TiO_{(2)}$ on the spectral responses and photochemical activities of D1/D2/Cyt b559 complex of spinach. Spectrochimica Acta Part A, Molecular and Biomolecular Spectroscopy 72, 1112-1116.

Subbaiah, C. C., Sachs, M. M. (2003) Molecular and cellular adaptations of maize to flooding stress. Annals of Botany 90, 119-127.

Sweetlove, L. J., Taylor, N. L., Leaver, C. J. (2007) Isolation of intact, functional mitochondria from the model plant *Arabidopsis thaliana*. Methods in Molecular Biology 372, 125-136.

Syu, Y. Y., Hung, J. H., Chen, J. C., Chuang, H. W. (2014) Impact of size and shape of silver nanoparticles on *Arabidopsis* plant growth and gene expression. Plant Physiology and Biochemistry 83, 57-64.

Tanaka, N., Mitsui, S., Nobori, H., Yanagi, K., Komatsu, S. (2005) Expression and function of proteins during development of the basal region in rice seedlings. Molecular and Cellular Proteomics 4, 796-808.

Tanz, S. K., Castleden, I., Hooper, C. M., Vacher, M., Small, I., Millar, H. A. (2013) SUBA3: a database for integrating experimentation and prediction to define the SUBcellular location of proteins in *Arabidopsis*. Nucleic Acids Res. 41(Database issue):D1185-1191.

Thornalley, P. J. (1990) The glyoxalaxe system: new developments towards functional characterization of a metabolic pathways fundamental to biological life. Biochemical Journal 269, 1-11.

Tougou, M., Hashiguchi, A., Yukawa, K., Nanjo, Y., Hiraga, S., Nakamura, T., Nishizawa, K., Komatsu, S. (2012) Response to flooding stress in soybean seedlings with the alcohol dehydrogenase transgene. Plant Biotechnology 29, 301-305.

Tsukuda, S., Gomi, K., Yamamoto, H., Akimitsu, K. (2006) Characterization of cDNAs

encoding two distinct miraculin-like proteins and stress-related modulation of the corresponding mRNAs in *Citrus jambhiri* lush. Plant Molecular Biology 60, 125-136.

Usadel, B., Nagel, A., Thimm, O., Redestig, H., Blaesing, O. E., Palacios-Rofas, N., Selbig, J., Hannemann, J., Piques, M. C., Steinhauser, D., Scheible, W. R., Gibon, Y., Morcuende, R., Weicht, D., Meyer, S., Stitt, M. (2005) Extension of the visualization tool MapMan to allow statistical analysis of arrays, display of corresponding genes, and comparison with known responses. Plant Physiology 138, 1195-1204.

Usadel, B., Poree, F., Nagel, A., Lohse, M., Czedik-Eysenberg, A., Stitt, M. (2009) A guide to using MapMan to visualize and compare Omics data in plants: a case study in the crop species, Maize. Plant Cell and Environment 32, 1211-1229.

Valle, S. R., Carrasco, J., Pinochet, D., Calderini, D. F. (2009) Grain yield, above-ground and root biomass of Al-tolerant and Al-sensitive wheat cultivars under different soil aluminum concentrations at field conditions. Plant and Soil 318, 299-310.

van der Zande, M., Vandebriel, R. J., Van Doren, E., Kramer, E., Herrera Rivera, Z., Serrano-Rojero, C. S., Gremmer, E. R., Mast, J., Peters, R. J., Hollman, P. C., Hendriksen, P. J., Marvin, H. J., Peijnenburg, A. A., Bouwmeester, H. (2012) Distribution, elimination, and toxicity of silver nanoparticles and ions ions in rats after 28-day oral exposure. ACS Nano 28, 7427-7442.

van Dongen, J. T., Roeb, G. W., Dautzenberg, M., Froehlich, A., Vigeolas, H., Minchin, P. E., Geigenberger, P. (2004) Phloem import and storage metabolism are highly coordinated by the low oxygen concentrations within developing wheat seeds. Plant Physiology 135, 269-80.

Vannini, C., Domingo, G., Onelli, E., De Mattia, F., Bruni, I., Marsoni, M., Bracale, M. (2014) Phytotoxic and genotoxic effects of silver nanoparticles exposure on germinating wheat seedlings. Journal of Plant Physiology 171, 1142-1148.

Vannini, C., Domingo, G., Onelli, E., Prinsi, B., Marsoni, M., Espen, L., Bracale, M. (2013) Morphological and proteomic responses of *Eruca sativa* exposed to silver nanoparticles or silver nitrate. PLoS One 8, e68752.

Vantoai, T. T., Fausey, N. R., Jr Mcdonald, M. B. (1987) Anaerobic metabolism enzymes as markers of flooding stress in maiz seeds. Plant and Soil 102, 33-39.

Verano-Braga, T., Miethling-Graff, R., Wojdyla, K., Rogowska-Wrzesinska, A. (2014) Insights into the cellular response triggered by silver nanoparticles using quantitative proteomics. ACS nano 8, 2161-2175

Vernikov, V. M., Arianova, E. A., Gmoshinskii, I. V., Khotimchenko, S. A., Tutelian, V. A. (2009) Nanotechnology in food production: advances and problems. Voprost Pitaniia (In Russian) 78, 4-17.

Vizcaíno, J. A., Côté, R. G., Csordas, A., Dianes, J. A., Fabregat, A., Foster, J. M., Griss, J., Alpi, E., Birim, M., Contell, J., O'Kelly, G., Schoenegger, A., Ovelleiro, D., Pérez-Riverol, Y., Reisinger, F., Ríos, D., Wang, R., Hermjakob, H. (2013) The PRoteomics IDEntifications (PRIDE) database and associated tools: Status in 2013. Nucleic Acids Research 41, D1063-D1069.

Voesenek, L. A., Bailey-Serres, J. (2013) Flooding tolerance: O2 sensing and survival strategies. Current Opinion in Plant Biology 16, 647-653.

Voesenek, L. A., Colmer, T. D., Pierik, R., Millenaar, F. F., Peeters, A. J. (2006) How plants cope with complete submergence. New Phytologist 170, 213-226.

Voit, E. O. (2000) Computational analysis of biochemical systems. Cambridge, UK: Cambridge University Press.

von Uexküll, H. R., Mutert, E. (1995) Global extent, development and economic impact of acid soils. Plant and Soil 171, 1-15.

Wijnhoven, S. W. P., Peijnenburg, W. J. G. M., Herberts, C. A., Hagens, W. I., Oomen, A. G., Heugens, E. H.W., Roszek, B., Bisschops, J., Gosens, I., Van De Meent, D., Dekkers, S., De Jong, W. H., van Zijverden, M., Sips, A. J. A. M., Geertsma, R. E. (2009) Nano-silver-a review of available data and knowledge gaps in human and environmental risk assessment. Nanotoxicology 3, 109-138.

Xiong, L., Ishitani, M., Zhu, J. K. (1999) Interaction of osmotic stress, temperature, and abscisic acid in the regulation of gene expression in *Arabidopsis*. Plant Physiology 119, 205-212.

Yadav, S.K., Singla-Pareek, S. L., Reddy, M. K., Sopory, S. K. (2005) Transgenic tobacco plants overexpressing glyoxalase enzymes resist an increase in

methylglyoxal and maintain higher reduced glutathione levels under salinity stress. FEBS Letters 579, 6265-6271.

Yang, L., Watts, D. J. (2005) Particle surface characteristics may play an important role in phytotoxicity of alumina nanoparticles. Toxicology Letters 158, 122-132.

Yasur, J., Rani, P. U. (2013) Environmental effects of nanosilver: impact on castor seed germination, seedling growth, and plant physiology. Environmental Science and Pollution Research International 20, 8636-8648.

Yin, L., Colman, B. P., McGill, B. M., Wright, J. P., Bernhardt, E. S. (2012) Effects of silver nanoparticle exposure on germination and early growth of eleven wetland plants. PLoS One 7, e47674.

Yin, W., Zhou, L., Ma, Y., Tian, G., Zhao, J., Yan, L., Zheng, X., Zhang, P., Yu, J., Gu, Z., Zhao, Y. (2015) Phytotoxicity, translocation, and biotransformation of NaYF4 upconversion nanoparticles in a soybean plant. Small (Weinheim and der Bergstrasse, Germany) 11, 4774-4784.

Yin, X., Sakata, K., Nanjo, Y., Komatsu, S. (2014) Analysis of initial changes in the proteins of soybean root tip under flooding stress using gel-free and gel-based proteomic techniques. Journal of Proteomics 106, 1-16.

Zhang, Y., Wen, Z., Washburn, M. P., Florens, L. (2009) Effect of dynamic exclusion duration on spectral count based quantitative proteomics. Analytical Chemistry 81, 6317-6326.